BIANCA DEL BIANCO SAHM

MODULAÇÃO DO FATOR DE TRANSCRIÇÃO TBX2 COMO NOVA ESTRATÉGIA ANTICÂNCER: ESTUDO BASEADO NA ATIVIDADE BIOLÓGICA DE CROMOMICINA A_5 EM CÉLULAS DE MELANOMA.

São Paulo
2020

BIANCA DEL BIANCO SAHM

MODULAÇÃO DO FATOR DE TRANSCRIÇÃO TBX2 COMO NOVA ESTRATÉGIA ANTICÂNCER: ESTUDO BASEADO NA ATIVIDADE BIOLÓGICA DE CROMOMICINA A_5 EM CÉLULAS DE MELANOMA

Tese apresentada ao programa de Pós-graduação em Farmacologia ao Instituto de Ciências Biomédicas da Universidade de São de Paulo para obtenção do título de doutora em Ciências

Área de concentração: Farmacologia
Orientadora: Profa. Dra. Leticia Veras Costa Lotufo
Versão original

São Paulo
2020

CATALOGAÇÃO NA PUBLICAÇÃO (CIP)
Serviço de Biblioteca e informação Biomédica
do Instituto de Ciências Biomédicas da Universidade de São Paulo

Ficha Catalográfica elaborada pelo(a) autor(a)

Del Bianco Sahm, Bianca
Modulação do fator de transcrição TBX2 como nova abordagem anticâncer: estudo baseado na atividade biológica de cromomicina A5 em células de melanoma / Bianca Del Bianco Sahm; orientadora Leticia Veras Costa Lotufo. -- São Paulo, 2020.
113 p.

Tese (Doutorado)) -- Universidade de São Paulo, Instituto de Ciências Biomédicas.

1. Descoberta de novas drogas. 2. Terapia alvo-direcionada. 3. Produtos Naturais Marinhos. 4. Anticâncer. 5. Melanoma. I. Veras Costa Lotufo, Leticia, orientador. II. Título.

BIANCA DEL BIANCO SAHM

MODULATION OF TBX2 TRANSCRIPTION FACTOR AS A NEW ANTICANCER STRATEGY: A STUDY BASED ON THE BIOLOGICAL ACTIVITY OF CHROMOMYCIN A_5 IN MELANOMA CELLS

Thesis presented to the post-graduate program in Pharmacology at the Institute of Biomedical Sciences of the University of São Paulo to obtain the title of PhD in Science.

Area of concentration: Pharmacology
Supervisor: Prof. Leticia Veras Costa Lotufo, PhD
Original version

São Paulo
2020

UNIVERSIDADE DE SÃO PAULO
INSTITUTO DE CIÊNCIAS BIOMÉDICAS

Candidata: Bianca Del Bianco Sahm

Titulo da Tese: **Modulação do fator de transcrição TBX2 como nova abordagem anticâncer: estudo baseado na atividade biológica de cromomicina A_5 em células de melanoma.**

Orientadora: Profa. Dra. Leticia Veras Costa Lotufo

A Comissão Julgadora dos trabalhos de Defesa da Dissertação de Mestrado/Tese de Doutorado, em sessão publica realizada a **...../...../.....**, considerou a candidata:

( ) Aprovado(a) ( ) Reprovado(a)

Examinador(a): Assinatura: .....
Nome: .....
Instituição: .....

Examinador(a): Assinatura: .....
Nome: .....
Instituição: .....

Examinador(a): Assinatura: .....
Nome: .....
Instituição: .....

Presidente: Assinatura: .....
Nome: .....
Instituição: .....

To all the teachers who brought me here,
and especially to my dearest supervisor,
Leticia V. Costa Lotufo

“If you had an idea that was going to outrage society,
would you keep it to yourself?”
Charles Darwin

Acknowledgments

Firstly, I would like to thank my supervisors, brave women and scientists who inspire me every day: Prof. Leticia Veras Costa Lotufo, Prof. Paula Cristine Jimenez and Prof. Sharon Prince. Thank you for entrusting me with this very special project, which has marked the beginning of this beautiful collaboration. I hope that you are all satisfied with the final result.

I am grateful to the development agencies that financed this work: CAPES (Coordenação de Aperfeiçoamento de Nível Superior, Government of Brazil - Finance code 001) PDSE (Programa de Doutorado Sanduíche no Exterior - CAPES - Process no: 88881.186974/2018-01), CNPq (Conselho Nacional de Desenvolvimento Científico e Tecnológico, Government of Brazil - Process no: 141508/2017-5), FAPESP (Fundação de Amparo à Pesquisa do Estado de São Paulo - Process no: 2015/17177-6). Investing in research is to guarantee internal development and the future of the next generations. I am grateful for the opportunity to contribute to the generation of knowledge, which is fundamental for the solution of problems in all sectors of society.

Thanks to the Department of Pharmacology, Institute of Biomedical Sciences (ICB) and to the University of São Paulo (USP), for the infrastructure and reception. To the secretaries Mônica Nunes da Silva and Camila Gonçalvez Trindade for helping me with all the doubts and bureaucratic questions, you were really important. I also thank the neighboring professors and laboratories for sharing their spaces, materials and intellectual contributions in carrying out the experiments. To Prof. João Agostinho Machado Neto, for always being available and interested in discussing experiments and results. To Helori Vanny Domingos, and Simone Aparecida Teixeira for the technical assistance. To the National Laboratory of Biosciences (LNBIO-CNPEM, Campinas, São Paulo) for use of their facilities. And I also acknowledge Dr. Daniel Maturana for valuable technical assistance, for his help to perform experiments and to interpret results.

To my colleagues from the marine pharmacology laboratory (LAFARMAR ICB-USP): Paola Branco, Cristine Pontes, Amanda Hirata, Paula Rezende, Darwin Carvalho, Jaime Matheus, Vanessa Franco, Ives Charlie, Larissa Machado, Luciana Furtado, Karen Velasco, Catarina Sofia, and Lucas Ariel; and to my colleagues from

the T-Box Lab (University of Cape Town - South Africa): Abid Ali, Ana Popovic, Alexis Neumann, Hapiloe Maranyane, Jade Peres, Saif Khan, Vuyo Mlaza, Rehana Omar, Mohsin Khan, Victoria Damerell, Luqmaan Mohamed, Suparna Chakraborty, Athi Welsh, Thulisa Mkatazo, Thato Medupe, Michelle Du Toit, Desiree Bowers, Claire Bellis and Arul Jothi for all their contributions, help with experiments and for being supportive.

Finally, I need to thank some people who indirectly contributed to this work through their support, understanding and encouragement: My dear parents, Marise and José Alfredo, my sister Giulia, my family in general, my friends Larissa Guimarães, Renan Daku Saes, Juliana Gaeta, Julia Portela, Nathalia Pedrassoli and Mariana Raymundi. To the Brazilian Capetonian family: Nath Dellabianca, Marcos Santiago, Juliana Mota, Antonio, Mariana Bolzan, and Dinesh Trevi. I am very grateful to my dear friend Linda Eggertsen for all the conversations, advices, affection and friendship to face this challenge, and also for helping with thesis translation. And last but not least, I thank my partner Sandro Giuliano for always being around, for his encouragement, love and admiration.

Modulação do fator de transcrição TBX2 como nova estratégia anticâncer: estudo baseado na atividade biológica de cromomicina A_5 em células de melanoma. Autora: Bianca Del Bianco Sahm. Orientadora: Leticia Veras Costa Lotufo. Programa de pós-graduação em Farmacologia, ICB-USP.

Resumo

O melanoma é uma neoplasia derivada de melanócitos, que apresenta alta taxa de heterogeneidade, reduzindo a eficácia do tratamento disponível para essa doença. Assim sendo, a busca por novos tratamentos que atuem em alvo moleculares distintos, ainda é necessária na terapia do melanoma. Estudos demonstraram que o fator de transcrição TBX2, conhecido por suas funções na embriogênese, favorece a proliferação e imortalidade de células de melanoma através do escape da senescência, e ainda confere resistência ao tratamento com agentes alquilantes de DNA, sendo considerado um novo alvo anticâncer. Os produtos naturais marinhos compreendem um grande arsenal de moléculas únicas com diversas atividades biológicas, sendo uma importante fonte de compostos com atividade anticâncer. Assim, o presente estudo se propôs a identificar compostos naturais de origem marinha com potencial de ligação ao fator de transcrição TBX2. Nossa estratégia de prospecção foi a utilização de um procedimento de afinidade reversa, no qual a proteína recombinante de TBX2 foi utilizada como isca. No presente estudo nós exploramos a capacidade de bactérias marinhas em produzir compostos bioativos a partir da descrição do isolamento e caracterização de moléculas pertencente à classe das cromomicinas. Posteriormente, as cromomicinas foram testadas frente ao seu potencial de ligação com TBX2. Os resultados evidenciam que cromomicina A_5 (CA_5) potencialmente se liga a este alvo. CA_5 também apresentou forte atividade citotóxica contra uma linhagem de melanoma metastático dependente de TBX2 (IC_{50} 0.8 nM). Ainda, usando modelos geneticamente modificados, onde a expressão de TBX2 foi aumentada ou diminuída, observou-se que a presença deste fator de transcrição altera o perfil de citotoxicidade de CA_5 nestas células. Estudos seguintes de caracterização da atividade anticâncer sugerem que a modulação da transcrição de TBX2 pode ter participação nos efeitos citotóxicos de CA_5 em células de melanoma. Por fim, nós discutimos o atual cenário de diferentes estratégias que

objetivam a modulação de fatores de transcrição como uma importante abordagem na terapia anticâncer.

Palavras-chave: Anticâncer; terapia alvo-direcionada; TBX2; produtos naturais marinhos; melanoma

Modulation of TBX2 transcription factor as a new anticancer strategy: a study based on the biological activity of chromomycin A5 in melanoma cells. Author: Bianca Del Bianco Sahm. Supervisor: Leticia Veras Costa Lotufo. Graduation program in Pharmacology, ICB-USP.

Abstract

Melanoma is a neoplasm derived from melanocytes, with a high rate of heterogeneity that hinders the effectiveness of the treatment currently available for this disease. Therefore, the search for new treatments that act on different molecular targets is still necessary in melanoma therapy. Studies have shown that the transcription factor TBX2, known for its functions in embryogenesis, favors the proliferation and immortality of melanoma cells through the escape of senescence, and still confers resistance to treatment with DNA-alkylating agents, being considered a new anticancer target. Marine natural products represent a large arsenal of unique molecules with diverse biological activities, being an important source of compounds with anticancer activity. Thus, the present study aimed to identify natural compounds of marine origin with potential for binding to the TBX2 transcription factor. Our prospecting strategy was to use a reverse affinity procedure where the TBX2 recombinant protein was used as bait. In the present study we explored the ability of marine bacteria in producing bioactive compounds and describe the isolation and characterization of molecules belonging to the class of chromomycins. Subsequently, chromomycins were tested for their potential to bind with TBX2. The results show that chromomycin A_5 (CA_5) potentially binds to this target. CA_5 also showed strong cytotoxic activity against a TBX2-driven metastatic melanoma cell line (IC_{50} 0.8 nM). Still, using genetically modified models, where the expression of TBX2 was increased or depleted, revealed that the presence of this transcription factor alters the cytotoxicity profile of CA_5 in these cells. Further studies of anticancer characterization suggest that modulation of TBX2 transcription properties may play a role in the cytotoxic effects of CA5 in melanoma cells. Finally, we discuss the current scenario of different strategies that aim the modulation of transcription factors as an important approach in anticancer therapy.

Keywords: Anti-cancer; target-directed therapy; TBX2; Marine natural products; melanoma.

Contents

Resumo **10**

Abstract **12**

1. Introduction **14**

1.1 Melanoma *14*

1.2 TBX2 transcription factor *22*

1.3 Melanoma Therapy *27*

1.4 Marine Natural Products and cancer *30*

1.5 Prospection strategy - Bio-affinity chromatography *34*

2. Relevance and justification **37**

3. Objectives **38**

3.1 General objective *38*

3.2 Specific objectives *38*

4. Study rational **39**

5. Chapter 1 - Dextrorotatory chromomycins from the marine *Streptomyces sp.* associated to *Palythoa caribaeorum* **41**

6. Chapter 2 - Targeting the oncogenic TBX2 transcription factor with chromomycins. **53**

7. Chapter 3 - Antitumor characterization of chromomycin A_5 in TBX2-driven melanoma cells **63**

8. FINAL CONSIDERATIONS **92**

9. REFERENCES **96**

Attachment I - Ethics commiitee exempition certificate **112**

Supplementary figure 1 (Fig. S1) **113**

1. Introduction

1.1 Melanoma

Cancer is the name given to a group of more than 100 diseases that have in common the uncontrolled growth of cells that invade tissues and organs. Dividing rapidly, these cells tend to be very aggressive, leading to the formation of malignant tumors that can spread to other parts of the body (INCA, 2018). Risk factors related to the onset of cancer are, in general, linked to harmful disorders to the genetic material, which can occur endogenously (eg aging, genetic predisposition and heredity) or exogenous (eg smoking, viral infections or exposure to ultraviolet radiation - UVR) (WHO, 2018). With the world population on the rise and older, cancer has been highlighted as one of the most important diseases of the 21st century, with an estimated 18.1 million new cases and 9.6 million deaths caused by the disease in 2018 (FERLAY et al., 2019).

Derived from genetic instability, the development of cancer is complex and heterogeneous. Revealing itself as a model analogous to evolutionary Darwinism, where pro-tumor genes (oncogenes) gain dominant function and tumor suppressor genes become recessive, normal cells begin to express carcinogenic characteristics that, in turn, are transmitted by cell replication (HANAHAN; WEINBERG, 2000). Each type of cancer has a "signature", depending on the type of organ or tissue in which it develops, however, Hanahan and Weinberg (2000 e 2011) reviewed a series of biological capabilities acquired by tumor cells that are common to all neoplasms, in order to rationalize the complexity of this disease.

Briefly, and without necessarily following an order, cancer cells exhibit some or all of the following acquired characteristics: (i) sustaining proliferative signals; (ii) evasion of cell growth suppressors; (iii) resistance to cell death; (iv) capacity for replicative immortality; (v) angiogenesis induction; (vi) invasion and metastasis activation; (vii) reprogramming of energy metabolism; (viii) avoidance of autoimmune destruction. The authors also argue that such acquired capacities are orchestrated by genetic instability (occurrence of genetic mutations is necessary), by the inflammatory condition (which helps in the promotion of multiple capacities) and by

the tumor microenvironment (recruitment of normal cells that contribute to the acquisition of capabilities) (HANAHAN; WEINBERG, 2000; 2011).

Among the various types of cancer, the melanoma, derived from melanocytes (melanin-producing cells located in the basal layer of the epidermis, in the central nervous system and in the ocular retina), represents an important public health problem due to its high rate of lethality and resistance to treatment (CURTIN et al., 2005; PRADO; SVOBODA; RIGEL, 2019). Cutaneous melanoma, developed from skin epidermal melanocytes, is the most common type that often appears in regions of high exposure to sunlight, such as arms, hands, neck and face. This kind of melanoma can be subdivided according to its morphological appearance in superficial spreading melanoma, nodular, acral lentiginous melanoma, lentigo maligna, and desmoplastic nevoid. Other less frequent types, called non-cutaneous melanoma, can develop in the choroidal layer of the eye, in the meninges, in the genitourinary mucous membranes or in organs from the respiratory or gastrointestinal systems (TSAO et al., 2012).

The main risk factor for the development of cutaneous melanoma is exposure to ultraviolet radiation (UV-R) emitted by the sun or in tanning chambers. Still, some individual characteristics have been described as favorable for the appearance of this cancer, such as having fair skin, tendency to sunburn, inability to tan, family history, age (> 60 years) and immunosuppression (GILCHREST et al., 1999; KHAN; TRAVERS; KEMP, 2018). This type of skin cancer mainly affects the caucasian population inhabiting regions of the tropics, where its incidence is becoming increasingly common with the number of new cases tripled in the last four decades (SIEGEL; MILLER; JEMAL, 2017; OLSEN et al., 2019).

In 2016, cutaneous melanoma was counted as one of the five most prevalent cancers for the population of the United States, where it is stipulated that one out of 24 Americans is at risk to develop the disease during their lifetime (MILLER et al., 2016; PRADO; SVOBODA; RIGEL, 2019). In Australia, despite the advance of prevention programs, melanoma still ranks third place among the most common and deadly cancers in the country (MAHUMUD et al., 2019). Melanoma also significantly affects the European population, which showed an increase in the incidence rate of both invasive and *in situ* disease (SACCHETTO et al, 2018). The lowest incidence rates, however, are found in African or South American countries, where the population is predominantly composed of racial groups with darker pigmentation

(SANTOS; SOUZA, 2019). In Brazil, although the incidence is considered low, its rate almost doubled in 15 years (from 2.52 to 4.84/100,000 men and from 1.93 to 3.22/100,000 women), where melanoma was responsible for about 1800 deaths in 2015 (INCA, 2018; MELO et al., 2018). Early diagnosis and excision of melanomas results in a survival rate of more than 5 years in 99% of cases, but inefficient treatment for more advanced cases of the disease is responsible for 80% of skin cancer-related deaths (PITT et al., 2016; WELSH et al., 2016).

Melanocytes play an important photoprotective function against ultraviolet radiation (UVR). These cells, contained in the basal layer of the epidermis, have dendritic extensions which establish contact with several epithelial keratinocytes. The prolongations are important for transfer of the melanin pigment, which is produced by melanocytes as a product of genetic regulation at the cellular and tissue level or by environmental stimulus, such as exposure to UVR (CICHOREK et al., 2013).

UVR is electromagnetic radiation with wavelengths (λ) ranging from 100 - 400 nm. The main source of this type of radiation is the light emitted by the sun that reaches the Earth's atmosphere. It can be subdivided into UVA (λ = 320 - 400 nm), UVB (λ = 280 - 320 nm) and UVC (λ = 100 - 280 nm), and all types are considered carcinogenic in humans (WHO, 2019). The UVR is absorbed by the cells present in the epidermis, reaching deep levels like proteins and DNA. Its carcinogenic ability is mainly due to genetic damage caused in DNA sequences, either directly (damaging the molecular structure) or indirectly (generation of free radicals and modulation of the cellular response to genomic damage - repair system) (KHAN; TRAVERS; KEMP, 2018). Interestingly, the melanin produced by melanocytes is capable of absorbing and dispersing UVR, making it less harmful to epithelial cells. In addition, melanin promotes the elimination of free radicals coupled with oxidative-reduction reactions, promoting photoprotection by increasing degenerative resistance and neutralizing oxidative stress (ORTONNE, 2002; GHOSH; GHOSH, 2017). That said, it is evident that the lack or deficiency in melanin pigment production raises the risk for development of skin cancers, including melanoma.

Indeed, genomic DNA sequences extracted from melanoma samples have revealed a multitude of genetic mutations typically derived from UVR (REF). Typically, UVR induces the formation of photoproducts in genomic DNA, such as cyclobutane pyrimidine dimers (CPDs), which forms cyclobutane rings in the bond between two pyrimidine bases. Cytosine bases, one of the amino acids that compose

the base class of pyrimidines (along with thymine and uracil), are commonly stable and rarely undergo spontaneous removal, which would result in possible genetic mutations (FREDERICO; KUNKEL; SHAW, 1990). However, cytosines surrounded by CPDs are much less stable, resulting in an increased frequency of spontaneous removals (BURGER et al., 2003). Absent cytosines are replaced by uracil which, if not repaired, are copied by DNA polymerase resulting in fixing the transitions C□T/G□A in DNA sequences. Such transitions characterize the "UV signature" of mutations in the genetic code. The large number of "UV signature" mutations found in cutaneous melanomas shows the relevance of UVR as an important trigger for the appearance and development of this type of cancer (KHAN; TRAVERS; KEMP, 2018).

The melanoma development stages are well defined and orchestrated by genetic changes that characterize the progression to malignant (metastatic) melanoma (Figure 2) (PALMIERI et al., 2018; JACKETT; SCOLYER, 2019). Characteristically, the loss of density-dependent regulation in melanocytes results in the appearance of benign nevi, which is small proliferations with low mutation rate that remain stable due to the functionalization of tumor suppressor genes. However, the acquisition of subsequent genetic changes drives the neoplasm to more aggressive stages. Malignant melanoma can be divided into three distinct phases: radial growth phase (RGP), where the tumor is confined to the epidermis, followed by vertical growth phase (VGP), in which cells invade the lower layer of the dermis, and, finally, the metastatic phase, when the tumor cells spread to other organs (MILLER; MIHN, 2006; SHAIN et al, 2015; JACKETT; SCOLYER, 2019). In general, the success of each stage is related to proliferative efficiency and escape from cellular senescence.

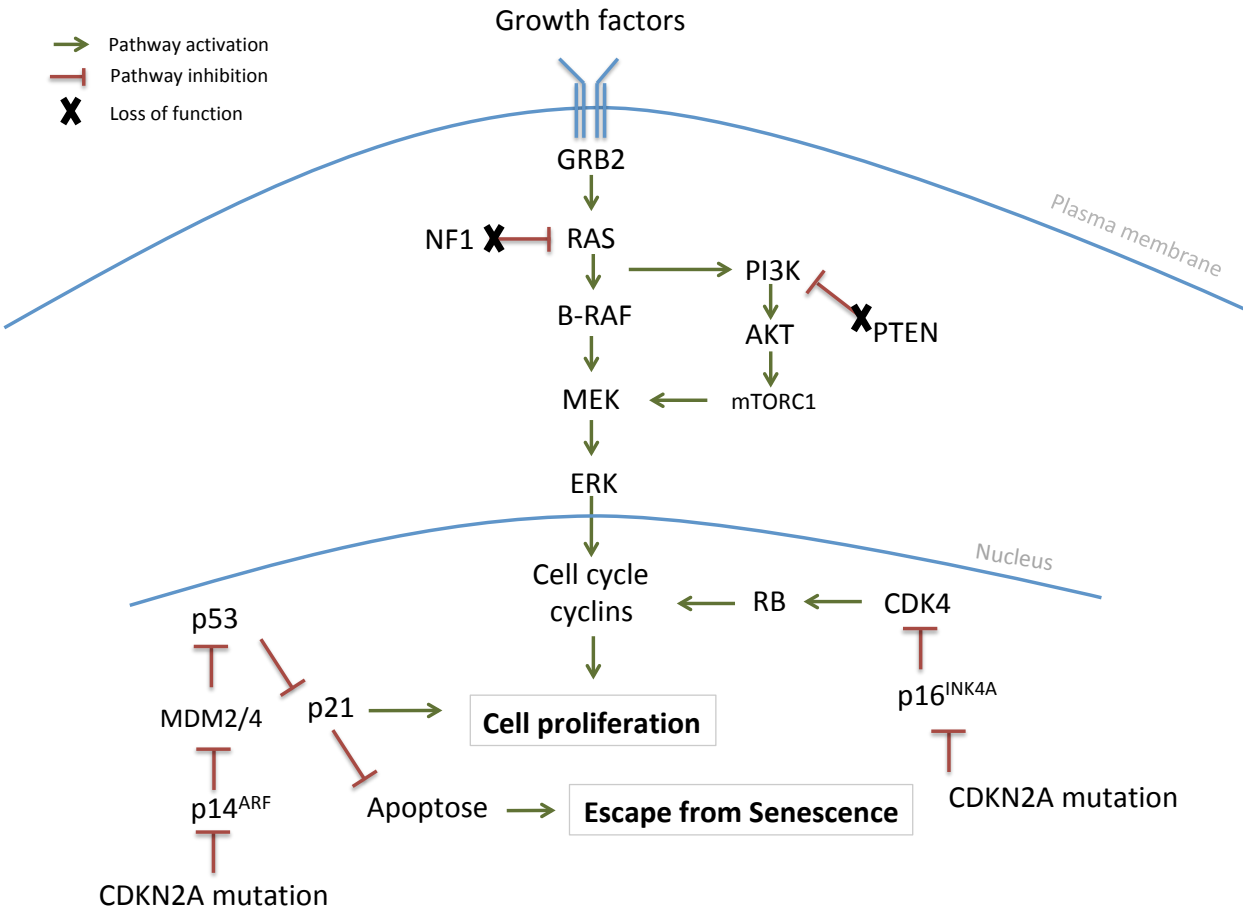
The molecular events associated with the development of melanoma are widely studied and characterized (CURTIN et al., 2005, ALONSO et al., 2004; SHAIN, et al., 2015; PALMIERI et al., 2018; JACKETT; SCOLYER, 2019). Figure 1 below illustrates the most common signaling pathways involved in melanomagenesis. The cancer genetics research network has divided melanoma into 4 subtypes based on the presence of mutations in the BRAF, RAS (N / K / H), NF1 and triple-negative genes (when none of the mutations exist) (TCGA, 2015). More recently, Palmieri et al. (2018) proposed the division into three subtypes: $BRAF^{mut}$, RAS^{mut} and non-

$BRAF^{mut}$/non-RAS^{mut}, since they found that the coexistence of mutations in BRAF and RAS is quite uncommon in the same melanoma (PALMIERI et al., 2018).

Usually, the proliferative phenotype occurs due to a gain of function of RAF or RAS kinases, whereas $BRAF^{V600E}$ (substitution of the amino acid valine for glutamic acid in the region of codon 600) and NRAS (mutations in codon Q61) are described as the most frequent mutations (DAVIES et al., 2002). BRAF is active in around 50% of melanoma tumors, and NRAS mutations in approximately 30% (MILLER; MIHN, 2006; PALMIERI et al., 2018). Both operate the RAS - RAF - MEK1/2 - ERK1/2 pathway, known as MAPK (Mitogen-Activated Protein Kinase), which plays an important role in terms of cell growth, proliferation and survival in melanomas (DAI; MARTINKA; LI, 2005; DAVIES et al., 2002; HAYASHI et al., 2008; LAVOIE; THERRIEN, 2015; MILLER; MIHN, 2006; TSAO et al., 2012). When active, BRAF and NRAS stimulate the constitutive activation of MAPK, which leads to the appearance of proliferative anomalies.

BRAF mutations have been characterized as an important precursor for the appearance of melanoma. Is commonly found in benign nevus, where its oncogenic activation is necessary but not sufficient for the development of malignant disease (PATTON et al., 2005). Moreover, other pathways can also contribute to the pathogenesis and/or resistance to BRAF and MEK inhibition, such as the loss of NF1 (Neurofibromin 1) and activation of the PI3K (Phosphatidylinositol-3-OH kinase) pathway. NF1 is a tumor suppressor that negatively regulates RAS and the loss of its function is found in high mutation burden melanomas, characterized as an UV mutational signature (PHILPOTT et al, 2017; CIRENAJWIS et al., 2017). Constitutive activation of the PI3K pathway occurs in approximately 70% of sporadic melanomas, resulting in loss of function of the tumor suppressor gene PTEN (Phosphatase and Tensin homolog) and/or amplification of AKT3 (serine/threonine kinase 3), which leads to reactivation of MAPK through mTORC1 (CHIAPPETTA et al., 2015; DHAWAN et al., 2002; STAHL et al., 2004; SULLIVAN; FLAHERTY, 2013; TCGA, 2015; VREDEVELD et al., 2012).

Figure 1 - Schematic diagram showing the most common signaling pathways involved in melanomagenesis.



Adapted from John; Cowey, (2015); Cosgaria et al, (2017); Palmieri et al, (2018).

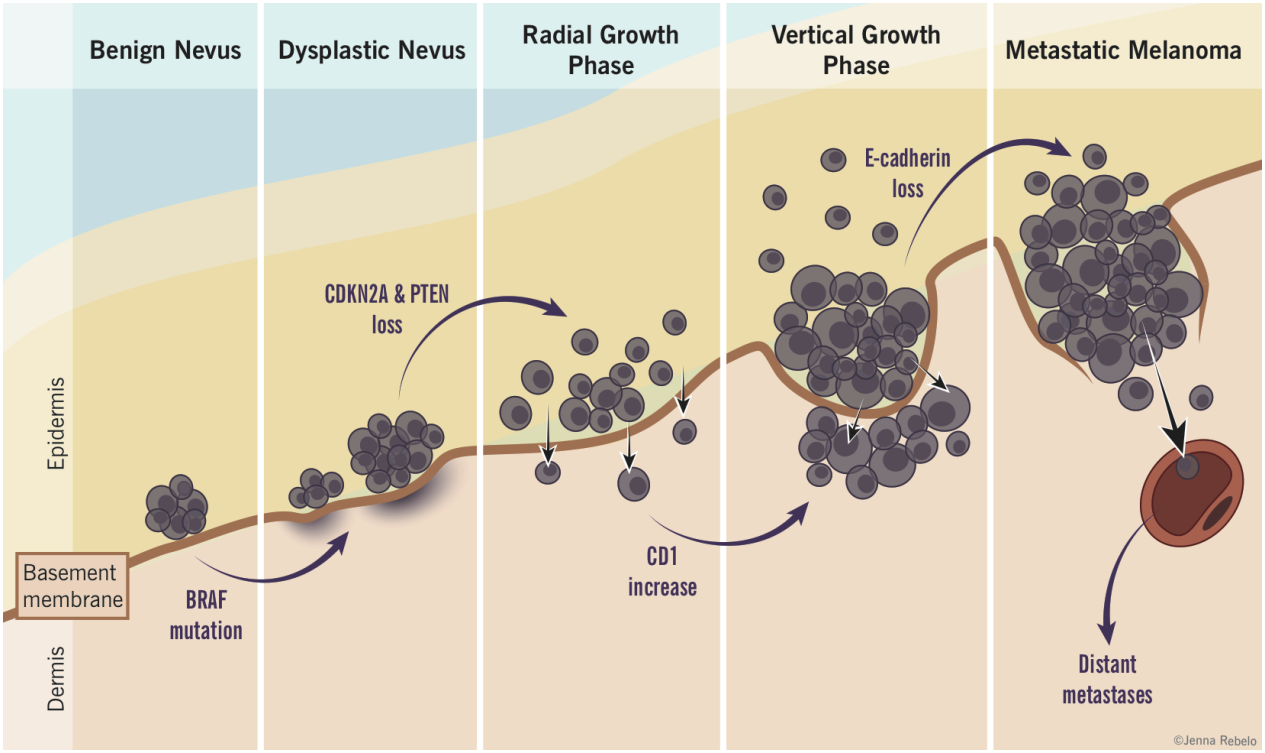
In addition to mutations that promote uncontrolled cell proliferation, another important point acquired by melanoma cells refers to the escape from senescence. Senescence is a term used to define a physiological program of irreversible disruption of cell growth, being an important barrier to malignancy as it prevents the formation of immortal cells (HA; MERLINO; SVIDERSKAYA, 2008; LIU; SHARPLESS, 2012). Cellular senescence can be triggered by telomere shortening, as a consequence of cell division (replicative senescence), or by cellular stress (oncogene-induced senescence). In general, the most important signaling pathways for senescence are $p14^{ARF}$–p53–p21 and $p16^{INK4A}$–RB (ZHANG, 2007). While $p14^{ARF}$ positively regulates the levels of p53 protein (responsible for suppressing DNA replication and activating repair mechanisms or driving the cell to apoptosis) through

the inhibition of ubiquitin ligase MDM2, $p16^{INK4A}$ inhibits CDK4, which directs cell cycle progression through phosphorylation of retinoblastoma protein (RB1), leading, in turn, to the activation of cyclin transcription factors (cell cycle regulation) and thus the expression of S phase genes for cell division (TERZI; IZMIRLI; GOGEBAKAN, 2016). Interferences in any point of the pathways results in cellular escape from DNA repair and senescence.

The loss of tumor suppressor genes is characterized as an important step in the malignant melanoma progression. Mutations in the CDKN2A gene, which encodes the tumor suppressor proteins $p16^{INK4A}$ and $p14^{ARF}$, occur in approximately 40% of familial melanomas (BERWICK et al., 2006; HARLAND et al., 2014; LEACHMAN et al., 2009), followed by mutations in CDK4 (TCGA, 2015). Furthermore, the increase in the expression of the CCND1 gene that encodes CD1 (Cyclin D1), is also an important mutation in the development of melanoma, which when combined with CDK4/6, promotes the positive regulation of cell proliferation through the activation of RB1 (YOUNG et al., 2014; YADAV et al., 2015). Amplifications of TERT (Telomerase Reverse Transcriptase) are also commonly found in melanomas, usually in association with constitutive MAPK activation (BAI et al., 2017). TERT allows the maintenance of telomeres homeostasis by decreasing their progressive shortening during mitosis (HEIDENREICH; KUMAR, 2017).

The transition to the final stage of the disease (invasive metastatic melanoma) also presents important mutational transitions that favor the motility and spread of tumor cells through lymphatic and vascular channels (JACKETT; SCOLYER, 2019). Such events are facilitated by the epithelial-mesenchymal transition (EMT, Epithelial-Mesenchymal Transition), a dynamic and reversible process in which epithelial cells acquire mesenchymal phenotypes, such as increased invasive and migratory capacities (KALLURI; WEINBERG, 2009; LAMOULLI; XU; DERYNCK, 2014). The loss of E-cadherin function, a transmembrane protein that mediate the junction of cell-cell adhesion, is perhaps the critical point for the activation of EMT and transformation of metastatic melanoma (THIERY; SLEEMAN, 2006; KELLER et al, 2013; SUN et al., 2018). The metastatic form adds several mutations that are difficult to control, characterizing it as the terminal phase of the disease, lacking effective treatments available to date. Metastatic cutaneous melanomas tend to colonize lungs, liver, brain and bones (JACKETT; SCOLYER, 2019).

Figure 2 - Illustrative scheme showing the different stages of melanoma development and the main genetic mutations involved for each phase.



BRAF mutations are determinant for the initial proliferative effect leading to the formation of benign nevus. The subsequent loss of tumor suppressor genes, such as CDKN2A and PTEN, favors the transformation from benign to malignant forms. Malignant melanoma then enters the first stage of its development, called the radial growth phase, while remaining retained in the epidermal compartment. In the vertical growth phase, the tumor increases its proliferative capacity, usually by increasing CD1, and initiates colonization of the dermis. The loss of E-cadherin signals the initiation of EMT, which facilitates the metastasis of melanoma to other tissues and organs. Image available at: http://www.pathophys.org/melanoma/melanoma-progression/

There are many molecular processes involved in melanomagenesis, which despite having made great progress in its characterization, there is still much to be unveiled. Several transcription factors have been described as acting directly or assisting tumor capacities acquired in all stages of melanoma (BESCH; BERKING, 2014; ASNAGHI et al., 2015; SEBERG; OTTERLOO; CORNELL, 2017; COHEN-

SOLAL; KAUFMAN; LASFAR, 2018), including T-box transcription factors (WANSLEBEN et al., 2014; PERES; MOWLA; PRINCE, 2015; CHANG et al., 2016).

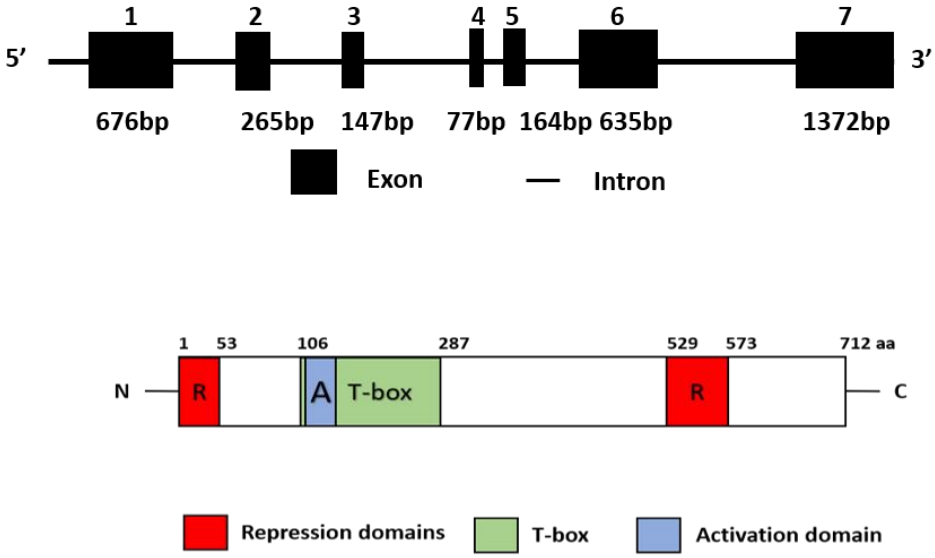
1.2 TBX2 transcription factor

Transcription factors are at the center of the regulatory network that drives gene expression programs in order to promote different biological responses (SPITZ; FURLONG, 2012). The genes belonging to the T-box transcription factors family are important regulators of embryonic development. They are present in all metazoans and are highly conserved along the phylogenetic scale. Based on phylogenetic and expression studies, this family is divided into 5 subfamilies namely: T, Tbx1, Tbx2, Tbx6 and T-brain. All T-box transcription factors are characterized by having a highly conserved DNA binding domain comprised of 180 – 200 amino acid residues (the T-box domain) which recognizes and binds to the core sequence 5'-GGTGTGA-3' (T-element) (SEBĒ-PEDROS & RUIZ- TRILO, 2017), acting as activators or repressors of gene transcription (KAVKA; GREEN, 1997; NAICHE et al., 2005). Because they were initially recognized for their crucial role in embryogenesis, their functions during this process are well described in literature, especially with regard to cell differentiation, proliferation, migration and survival (DOUGLAS; PAPAIOANNOU, 2013; NAICHE et al., 2005).

TBX2 is a member of the subfamily Tbx2, together with TBX4, TBX5 and its closely related homolog TBX3 (AGULNIK et al, 1996). It is encoded by chromosome 17q23, functioning as either a transcriptional activator or repressor. The TBX2 protein is composed by an activation domain prior to the conserved T-box DNA binding domain, and two repression domains, one in the N-terminal with 52 aa residues and the second located in the C-terminal with 529-573 aa residues (figure 3) (CARREIRA, LIU, CODING, 1998; PAXTON et al., 2001; ABRAHAMS et al., 2010; SAKABE et al., 2012). During embryogenesis, the expression of TBX2 is related to the development of heart, kidneys, limb, mammary glands, eyes and lungs (ABRAHAMS, PARKER, PRINCE; 2010; PAPAIOANNOU, 2014; SHEEBA; LOGAN, 2017; WOJAHN et al., 2019). The importance of TBX2 to the embryonic development is highlighted by the fact that disturbances of its expression during embryogenesis can result in abnormal formations. Microdeletions in chromosome 17q23,

encompassing the region of TBX2 and TBX4, is described to be related with an unclassified syndrome regarding developmental disorders such as limb abnormalities, congenital microcephaly, heart defects, pulmonary hypertension, thyroid duct cyst, sensorineural hearing loss and skeletal deformities (BALLIF et al., 2010; NIMMAKAYALU et al., 2011; LAURELL et al., 2013; LIU et al., 2018). Moreover, Tbx2 homozygous mutation in mice results in embryonic death whereas the heterozygous mutant remains viable (WAKKER et al., 2010).

Figure 3 - Schematic representation of TBX2 mRNA and protein.



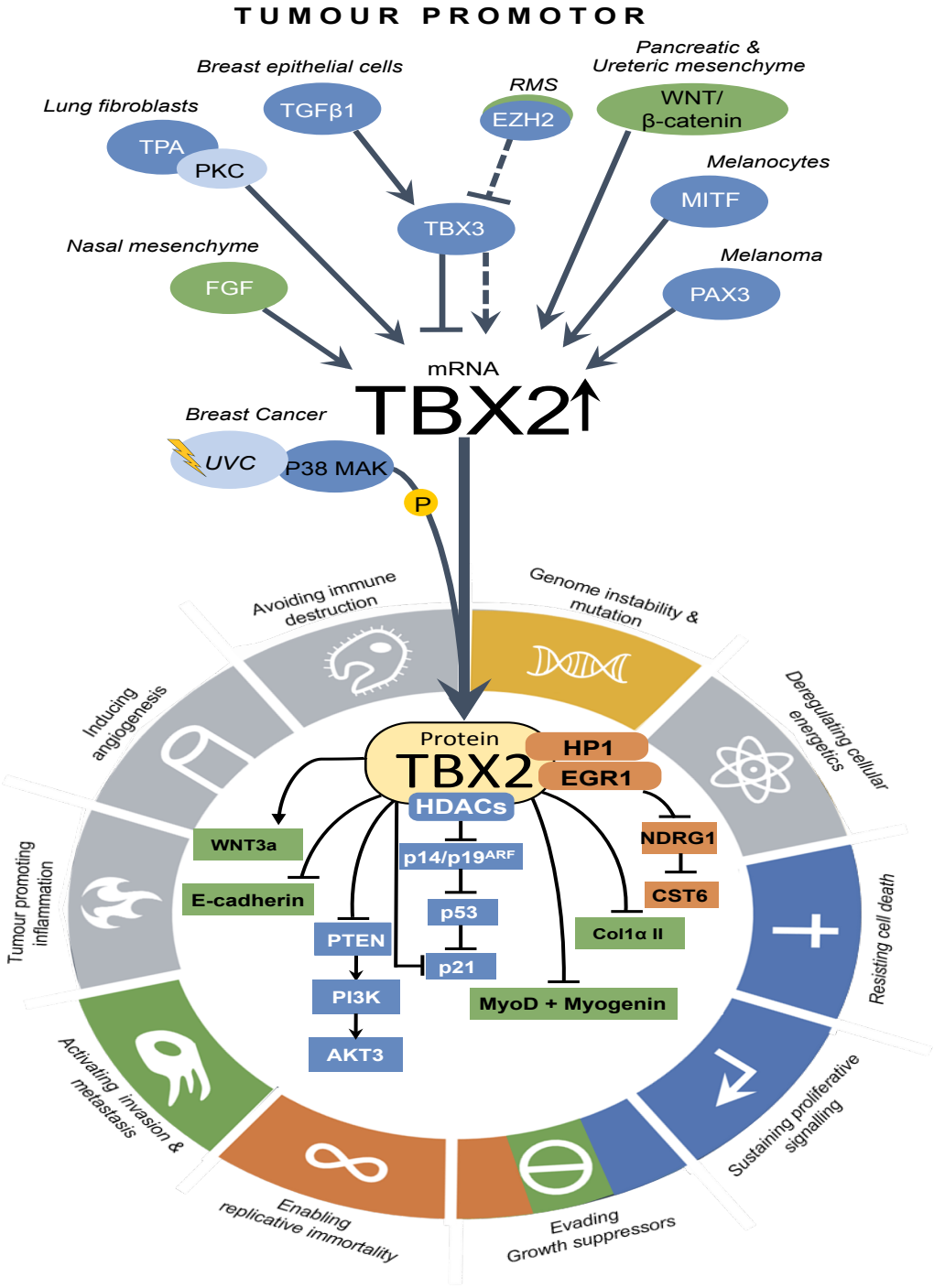
(A) TBX2 mRNA showing seven exons and their respective size. (B) TBX2 protein showing the activation domain (blue), the repression domains (red) and the T-box DNA binding domain (green).

The carcinogenesis process shares some characteristics similar to those that occur during embryonic development such as phenotypic plasticity, proliferative capacity and invasion. Thus said, it is expected that important developmental regulators, including members of the T-box family, are involved in carcinogenesis (BEN-PORATH et al., 2008; BRIEGEL, 2006). In fact, several T-box factors have been described to play a role in tumor promotion or tumor suppression functions (PAPAIOANNOU, 2014; WANSLEBEN et al., 2014; CHANG et al., 2016), with the main collected evidences referring mainly to TBX2 and TBX3 (LINGBEEK; JACOBS;

LOHUIZEN, 2002; LU et al., 2010; PERES et al, 2010; DOUGLAS; PAPAIOANNOU., 2013; KHAN et al., 2019).

There is strong evidence to suggest that TBX2 is implicated in key carcinogenesis processes such as tumor cell immortality and proliferation, tumorigenesis, invasion and metastasis through EMT process, and resistance to anticancer chemotherapeutics (JACOBS et al., 2000; PRINCE et al 2004; DAVIS et al., 2008; ABRAHAMS et al., 2010; WANSLEBEN et al., 2013; CHANG et al., 2016). Figure 4 below summarizes the signaling pathways involved in TBX2-driven carcinogenesis processes disclosed so far (Figure 4). It should be noted that different signaling pathways are describe for each type of cancer, and this is not surprising if we consider the high rate of heterogeneity involved in carcinogenesis. Nevertheless, TBX2 seems to be triggered in order to execute its suppression/activation functions over important tumor regulators, adding advantages for tumor progression. The overexpression of TBX2 was initially detected in breast tumors (JACOBS et al., 2000; REDMOND et al., 2010), where its high expression is correlated with a poor prognosis (WANG et al 2012). Currently, TBX2 is known to be overexpressed with tumorigenic functions in a set of cancers including breast (JACOBS et al., 2000; REDMOND et al., 2010) and prostate cancer (DU et al., 2017; NANDANA et al., 2017), nasopharyngeal carcinomas (LV et al., 2017), rhabdomyosarcomas (ZHU et al., 2014), gastric cancer (YU et al., 2015), pancreatic cancer (DUO et al., 2009) and colorectal cancer (HAN et al., 2013).

Figure 4 - Illustrative scheme showing the main signaling pathways described for TBX2 in different cancer cells as tumor promoter.



Scheme elaborated and gently provided by Msc. Mihlali Mlaza, UCT, South Africa.

TBX2 also occurs in several subtypes of melanomas (CARREIRA; LIU; GODING, 2000; VANCE et al., 2005), and a microarray study revealed that the

average expression of TBX2 is significantly higher in melanomas than in other types of tumors (WANG et al., 2004). Moreover, a meta-analysis using data provided by Badal and collaborators (2017), where the transcriptome changes in benign states and late-stages of melanoma tumors were examined, revealing that TBX2 expression is significantly higher in samples from melanoma malignant stages (BADAL et al., 2017) (figure S1 - Supplementary material).

The occurrence of overexpressed TBX2 in melanoma subtypes raised the question of how this gene can contribute to melanomagenesis through promoting the cell's escape from senescence. Studies have shown that TBX2 functions as an anti-senescence factor in human and rodent melanoma cell lines (PRINCE et al., 2004; VANCE et al., 2005; PERES et al., 2010). Previously, Prince et al. (2004) and Vance et al. (2005) demonstrated that Tbx2 in cells of murine melanoma of the B16 lineage, led to the suppression of senescence by direct binding and repressing the $p21^{WAF1}$ cyclin-dependent kinase inhibitor gene, through recruitment of HDAC1 (Histone Deacetylase 1) for the p21 promoter (PRINCE et al., 2004; VANCE et al, 2005). Later, a sequential study carried out by the same group, showed that RB1, when activated, binds to Tbx2 and increases its repression on p21 (VANCE et al., 2010). Following the previous results, Peres et al. (2010) demonstrated that silencing the TBX2 gene in VGP melanoma cells induced several senescence characteristics as well as reduced its proliferation. In a metastatic melanoma cell line, knocking down TBX2 diminished the proliferation rate, but it did not appear to interfere with cell migration abilities (PERES et al., 2010).

Another important function assigned to TBX2 concerns its role in resistance to DNA-alkylating chemotherapeutic agents. It was first demonstrated that the ectopic expression of TBX2 resulted in genetically unstable polyploidy cells with increased resistance to cisplatin treatment (DAVIS et al., 2008). In 2009, a study found that the expression of TBX2 in SW13 adrenocortical carcinoma cells promotes doxorubicin and UV irradiation resistance (ISMAIL; BATEMAN, 2009). More recently, Tasaka et al (2018) reported the inverse association of TBX2 expression levels with platinum-sensitivity in patients with ovarian serous carcinoma (TASAKA et al., 2018).

In an attempt to identify whether the endogenous TBX2 overexpression is associated with DNA-damaging chemotherapeutics resistance, Wansleben et al. (2013) silenced TBX2 in cisplatin-resistant breast carcinoma and melanoma cell

lines. It was demonstrated that the lack of TBX2 sensitized the cells to cisplatin by disrupting the ATM-CHK2-p53 signaling pathway, and that it switched the increased S-phase cell cycle arrest, first found for cisplatin resistance condition, to robust G2/M arrest. The authors concluded that knocking down TBX2 prevented the DNA repair cascade ATM-CHK2-p53 to operate, which results in the TBX2-deficient cells undergoing mitotic catastrophe after entering mitosis with damaged DNA (WANSLEBEN et al., 2013).

Genomic instability is one of the key features of a transformed cell that often culminates in mitotic defects as a result of failure in execution of a proper cell division. Bypassing relevant cell cycle checkpoints, which could interrupt the replication of such mitotic defects, and investing efficient DNA repair systems, are somatic key features found in tumorigenic cells (NIGG, 2001; DAVIS et al., 2008). The effective response of certain anti-cancer chemotherapeutics can be compromised by these modified systems found in cancer cells. To conclude, the findings mentioned above clearly indicate that TBX2 plays important anti-senescence and pro-proliferative roles during melanomagenesis, and that its expression is also important for DNA-damaging resistance in this type of cancer. That said, the inhibition of TBX2 functions could result in diminishing the proliferation of melanoma cells, in addition to increasing sensibility of the malignant cell to the action of DNA alkylating agents, which configures TBX2 as a new anticancer-target for the treatment of melanoma (LU et., 2010; WANSLEBEN et al., 2013).

1.3 Melanoma Therapy

Until a few years ago, typical treatments for melanomas included alkylates drugs such as dacarbazine and temozolomide, which had low efficacy and no improvement in patient overall survival (JOHN; COWEY, 2015). Additionally, immunotherapy-using cytokines such as interferon and interleukin-2 (IL-2) have not respond as expected with high levels of toxicity (ATKINS et al., 1999). In this therapeutic scenario, the average survival rate for patients with metastatic melanoma was between 6 to 8 months after diagnosis, and no new agent had been able to improve this outlook in subsequent clinical trials (MANOLA et al., 2000).

It was from 2011 that a new generation of chemotherapeutics for metastatic melanoma has emerged, with 8 new agents approved by the FDA-USA (Agency for Food and Drug Administration in the USA) in the following 4 years (KNACKSTEDT et al., 2018; MISHRA et al., 2018). The new therapeutic options have had positive impacts in the response rate and improvement in survival for patients with all stages of melanoma (Table 1). Two main strands were developed: target-driven treatments (COSGAREA et al., 2017) and immunotherapy (RODRÍGUEZ-CERDEIRA et al., 2017).

Vemurafenib and dabrafenib represents the first in the class of drugs for targeted-therapy in the treatment of melanomas, being potent $BRAF^{V600E}$ inhibitors (DAVIES et al., 2002; MENZIES; LONG; MURALI, 2012). The first results of therapy with $BRAF^{V600E}$ inhibitors revealed a rapid response in around 80% of treated patients, increasing the average survival of patients in up to 20 months (HAUSCHILD et al., 2012; MCARTHUR et al., 2014). Despite being promising, soon severe adverse effects such as the appearance of keratoacanthomas and squamous cell carcinoma, in addition to the high rate of recurrence of the disease, limited the use of BRAF inhibitors as monotherapy.

In general, resistance to target-driven treatment involves the re-activation of MAPK pathway through other pathways, resulting in renewed cell proliferation and tumor growth of previously suppressed metastases (JOHANNESSEN et al., 2010). Currently, some combinatorial therapies have been applied in order to circumvent the mechanisms of resistance for target-directed treatment in melanomas, such as the synergistic use of MEK (Mitogen-activated protein Kinase) inhibitors trametinib and cobimetinib (COSGAREA et al., 2017; KAROULIA; GAVATHIOTIS; POULIKAKOS, 2017), however, the definitive success of the therapy has not yet been achieved.

Agents targeting the immune system have also been actively investigated within the aim of improving efficacy and reducing toxicity in melanoma treatments. The greatest advances in this field have been achieved using drugs that block the inhibitory control machinery responsible for the regulation of the immune system, such as PD-1 (Programmed Death 1), and CTLA-4 (Cytotoxic T-Limphocyte-Associeated protein 4). The strategy applied by this therapy involves the inactivation of receptors for cytotoxic activation of T lymphocyte cells, ensuring that they are triggered against the tumor, which, in turns, result in increased patient antitumor immunity (SHARMA; ALLISON, 2015). Denominated as *immune checkpoint*

inhibitors, ipilimumab (anti-CTLA-4), nivolumab and pembrolizumab (both anti-PD-1), were approved as monotherapy or combinatorial therapy for the treatment of advanced melanoma due to the good results regarding the survival rate.

Table 1. Therapeutic agents approved by the FDA / ANVISA, from 2011, for the treatment of melanoma.

Agent *(comercial name)*	**Class**	**Mechanism of action**	**Approved year (FDA/ANVISA)**
Vemurafenib *(Zelboraf®)*	Target-driven molecule	$BRAF^{V600E}$ inhibitor	2011/2012
Dabrafenib *(Tafinlar®)*		$BRAF^{V600E/K}$ inhibitor	2013/2016
Trametinib *(Meknist®)*		MEK inhibitor	2013/2016
Cobimetinib *(Cotellic®)*		MEK inhibitor	2015/2016
Ipilimumab *(Yervoy®)*	Immune system checkpoint inhibitors	Anti-CTLA-4	2011/2012
Pembrolizumab *(Keytruda®)*		Anti-PD-1	2014/2016
Nivolumab *(Opdivo®)*		Anti-PD-1	2014/2016

Adapted from (KAROULIA; GAVATHIOTIS; POULIKAKOS, 2017; SHARMA; ALLISON, 2015; KNACKSTEDT et al., 2018; MISHRA et al., 2018).

In addition, topical immunotherapy for cutaneous melanoma is currently being explored. Imiquimod is an agonist of toll-like receptors (TLR) 7 and 8 and. This immunomodulatory drug upregulates the release of cytokines (e.g. IL-6, IFN-α and TNF-α) and the nitric oxide secretion from macrophages (KAMATHY et al., 2018), stimulating the immune system cancer attack. There are good evidences showing that imiquimod is effective as adjuvant therapy after surgical excision in first-stages melanoma, but its action in metastatic stages is still not satisfactory (KNACKSTEDT et al., 2018). A more recent approach for the immunological treatment of melanomas is the intratumoral injection of oncolytic viruses. Despite being yet poorly developed,

in 2015 the FDA approved the Talimogene laherparepvec (T-VEC) for the treatment of unresectable melanoma, evidencing improved median overall survival of patients with intermediate melanoma stages (ANDTBACKA et al., 2015; KNACKSTEDT et al., 2018). T-VEC is a *Herpes simplex* virus type-1 designed to selective replicate within tumors and deliver oncolytic immunotherapy by producing granulocyte macrophage colony-stimulating factor (GM-CSF) to enhance systemic antitumor immune response (ANDTBACKA et al., 2015).

Despite the actual existence of different options, the search for effective treatment against metastatic melanoma continues. Different approaches such as the combination of other immunotherapies, development of new formulations using nanoparticles and the elucidation of new molecular targets therapeutically relevant to the disease can further expand these results (JOHN; COWEY, 2015; MISHRA et al., 2018).

1.4 Marine Natural Products and cancer

Natural products play a fundamental role in the discovery of new drugs as they comprise a diversity of chemical structures, sometimes highly complex, with relevant biological activities which have found therapeutic application for several diseases (CARLSON, 2010; HARVEY, 2008). The great value of natural compounds in the field of new drugs discovery is particularly evident in the case of anti-cancer agents, where, of the more than 170 molecules that came into clinical use between years 1940 and 2014, 75% are classified as non-synthetic, and approximately 50% are extrinsic natural products or directly derived from them (CRAGG; NEWMAN, 2016).

In addition to the classic terrestrial sources for natural products, such as plants, bacteria and fungi, a field that is gaining prominence is the research evolving natural products from marine origin (MOLINSKI et al., 2009; NEWMAN; CRAGG, 2016). Seas and oceans occupy more than 2/3 of the Earth's surface, where diverse and extreme ecosystems are inserted. Moreover, the marine environment host 34 of the 36 phyla representing living organisms, including some strictly marine phyla (ARRIETA; ARNAUD-HAOND; DUARTE, 2010; FENICAL, 2006; RAMIREZ-LLODRA et al., 2010). In this scenario, for at least 60 years researchers have been exploring the pharmacological potential of secondary metabolites from marine organisms, motivated by the size of the oceans and the still unknown level of

biodiversity in this environment (GLASER; MAYER, 2009). Nowadays, it is well established that the marine environment is a valuable source of natural products that presents great variability of chemical structures with promising bioactivities useful as therapeutic agents (BLUNT et al., 2018; JIMENEZ; WILKE; LOTUFO, 2018; SHINDE et al., 2019)

To date, 10 marine-based pharmaceuticals have been approved for clinical use and there are a considerable number of substances undergoing pre-clinical and clinical tests for the treatment of various diseases (https://www.midwestern.edu/departments/marinepharmacology/clinical-pipeline.xml). Also, the great number of new marine molecules patents, filed between 2015 and 2018, clearly highlights the value of these chemicals as sources of new therapeutic agents (SHINDE et al., 2019). Among those marine-derived drugs in the clinical field, seven of them are prescribed for cancer treatment: cytarabine (Cytosar®), trabectedin (Yondelis®), eribulin mesylate (Halaven®), plitidepsin (Aplidin®) and the antibodies conjugates (ADC): brentuximab vedotin (Acentris®), enfortumab vedotin-ejfv (PADCEV™) and Polatuzumamu vedotin (Polivy™) (JIMENEZ et al., 2020; https://www.midwestern.edu/departments/marinepharmacology/clinical-pipeline.xml).

Cytarabine (Cytosar®) was the first approved for clinical use in 1969. This molecule is a synthetic arabinose-nucleoside, which was inspired by previously isolated natural products derived from the caribbean marine sponge *Tectithethya crypta* (BERGMANN; FEENEY, 1951; MURPHY; YEE, 2017). Since this molecule mimics the cytosine nucleotide, its mechanism of action involves the incorporation of cytarabine, into the DNA, in the place of cytosine. The presence of arabinose coupled to cytarabine, instead of deoxyribose, prevents the elongation of DNA strains, thus blocking the process of DNA synthesis (NEWMANN; CRAGG, 2014; 2016). This drug inaugurated the concept of antimetabolites in cancer Therapy. Eribulin mesylate (Halaven®) is a mesylate salt analog to halichondrin B, a macrocyclic polyether natural molecule previously isolated from another marine sponge *Halicondriha okadai*. It is a potent antimitotic compound that acts as an inhibitor of microtubule dynamics by targeting and immobilizing the globular protein tubulin. The result is an irreversible mitosis blockage which leads to cell death by apoptosis (JORDAN et al., 2005; JIMENEZ; WILKE; COSTA-LOTUFO, 2018).

Presumably, the most interesting marine compound is trabectedin (Yondelis®), which has been shown to play an unique and multivariate anticancer mechanism of action. Trabectedin is a natural product previously isolated from the ascidian tunicate marine invertebrate *Ecteinascia turbinata* (CUEVAS; FRANCESCH, 2009), currently produced in a semi-synthetic form, and was approved in 2015 for the treatment of advanced liposarcomas and leiomyosarcomas (BARONE et al., 2017; GORDON et al., 2016). This molecule exerts its antitumor functions through binding to the minor groove of the DNA double helix, which can causes structural and genomic machinery damages, but it also able to operate by a direct interaction of the compound with specific factors involved in DNA transcription and repair (LARSEN; GALMARINI; D'INCALCI, 2016).

Trabectedin attachment to DNA strands cause the inhibition of the DNA separation during the transcription process and the blockage of DNA repair systems, that leads to the generation of double-strand breaks in its structure. It also exerts the inhibition of active transcription by blocking and triggering the degradation of RNA polymerase II. Lastly, and perhaps the most important of all effects, trabectedin is able to displace oncogenic transcription factors from its target promoters, which leads to reverse of cell differentiation and other cancerous features (MINUZZO, 2005; SVEJSTRUP, 2007; D'INCALCI; GALMARINI, 2010; CHARYTONOWICZ et al., 2012; DI GIANDOMENICO et al., 2013). The effects of trabectedin on transcription factors and transcriptional activity is considered unique and opens up to new possibilities for anticancer drugs that bind to DNA.

Plitidepsin is another tunicate compound that was recently approved by Australian regulatory agency for clinical treatment of multiple myeloma in combination with dexamethasone for patients that relapse after three lines of treatment (www.ebs.tga.gov.au). The proposed mechanism of action for this compound is very unique with the inhibition of the elongation factor eEF1A2, resulting in the accumulation of misfolded toxic proteins in cancer cells, triggering apoptosis (for review see Jimenez et al., 2020).

Another very innovative concept is the use of antibody conjugates that enable the delivering of toxic molecules to specific tumor cells expressing the desired antigen. These systems included a monoclonal antibody that will guide the ADC to target cells, a potent cytotoxic compound and a linker that will be accountable for releasing the cytotoxic compounds inside target cells (Senter & Sievers, 2012;

Jimenez et al., 2020). Adcetris was the first the first approved drug using this formulation in 2011 for the treatment of Hodgkin's lymphoma and systemic anaplastic large cell lymphoma, but the concept have been largely applied to different targets resulting in dozens of ADC in clinical trials and the recent approval of enfortumab vedotin-ejfv (PADCEV™) and Polatuzumamu vedotin (Polivy™) for the treatment of metastatic urothelial cancer and non-Hodgkin lymphoma (and other hematological cancers), respectively (https://www.midwestern.edu/departments/marinepharmacology/clinical-pipeline.xml).

Reiterated by all these stimulants examples, marine organisms are recognized as prolific sources of molecules with unique mechanism of action. Even more promising, the obtention of natural products from marine microorganisms figures as an interesting alternative considering the issues of biotechnological versatility, material supply and the sustainability of the process (MANIVASAGAN et al., 2013) (FENICAL; JENSEN, 2006).

Salinosporamide A is a β-lactone isolated from the marine-restricted actinomycete bateria *Salinispora tropica*, and it in phase II of clinical tests for myelomas treatment (POTTS et al., 2011). Its mechanisms of action involve the linkage with the catalytic subunit 20S of the proteasome, which results in the inhibition of its functions and, consequently, inhibition of proteolysis regulation and cellular apoptosis activation (BORISSENKO; GROLL, 2007). It entered into clinical trials in record time - only 2 years after its discovery - and all tests were carried out with the natural product obtained from fermentations of *S. tropica* (FENICAL et al., 2008).

More recently, a new natural product isolated from the marine bacterium belonging to the genus *Serinicoccus*, the seriniquinone, demonstrated potent activity on several tumor cell lines, with particular selectivity for the Malme-3M melanoma cell line (TRZOSS et al., 2014). Using an immunoprecipitation strategy, researchers identified that seriniquinone targets to dermcidin protein in order to promote its cytotoxicity roles. In addition, high levels of dermcidin expression was found in the Malme-3M, which directly correlates the selectivity of seriniquinone for these cells.

Notably, natural products isolated from marine microorganisms appear as a rich source of new compounds with interesting activities. For more than 15 years, the research group conduct by Professor Leticia V. Costa Lotufo aims to investigate the

pharmacological potential of marine species inhabiting the Brazilian coast. In this sense, bioactive molecules from marine invertebrates were isolated as lipid amino acids from the zoanthid *Palythoa grandiflora* (WILKE et al., 2009, 2010) and derivatives of 7-oxo-staurosporine from ascidia *Eudistoma vannamei* (JIMENEZ et al., 2012), among others (FERREIRA et al., 2011; TAKEARA et al., 2008). In 2009, studies on the biotechnological potential of marine bacteria were initiated, aiming the prospection of associated microbiota of marine invertebrates and sediments. Other bioactive molecules were obtained from this source (ARTHAUD et al., 2012; GUIMARÃES et al., 2014; JIMENEZ et al., 2013; RODRIGUES et al., 2015; SAHM, 2014; SOUSA et al., 2012), highlighting the biotechnological richness of the huge microbial biodiversity present in Brazilian coast.

1.5 Prospection strategy - Bio-affinity chromatography

One of the biggest obstacles to the development of drugs from natural products is the long period required for their development (MARTINS et al., 2014). Despite this, the peculiar biological activity inserted in natural products continues to achieve this source as unique, not only for the development of new therapies but also as important tools in biological research (CARLSON, 2010). While new compounds with great potential are discovered in the marine environment, the development of methods that accelerate the connection between isolation and biological characterization are necessary, in order to reduce the time and costs inserted in the research.

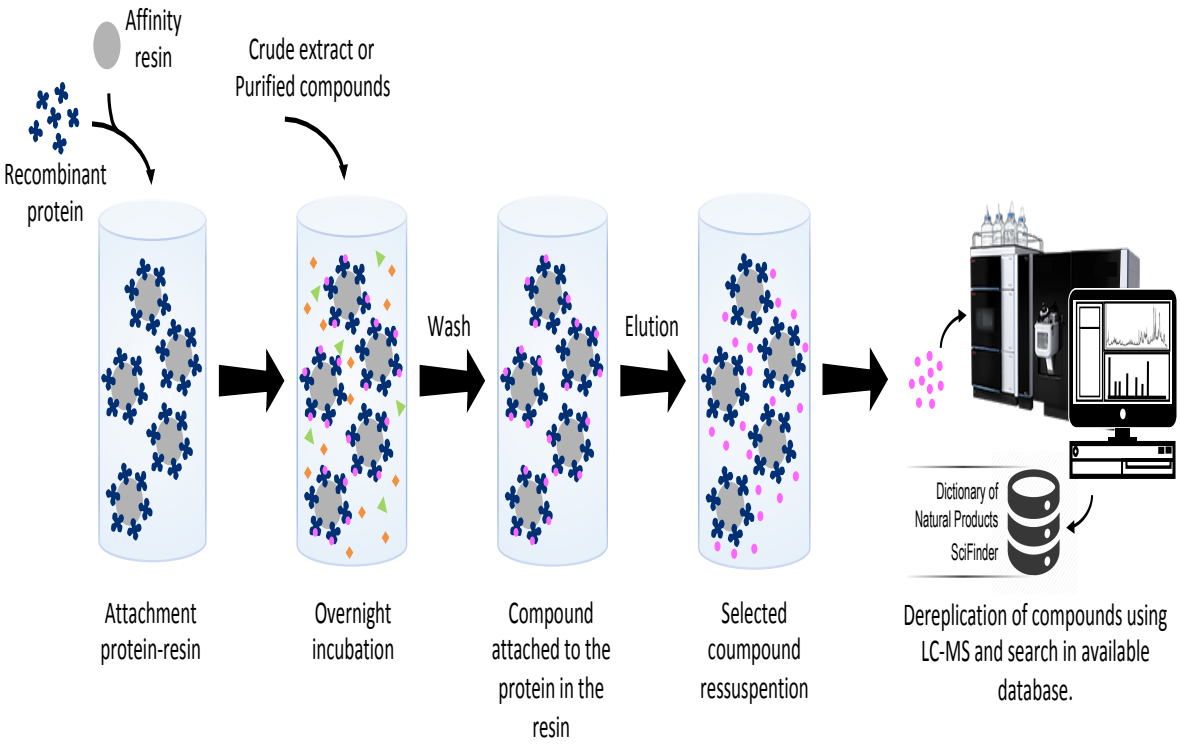
Traditionally, studies with natural products are carried out based on the observation of biological activity in organic extracts. From this point onwards, the active molecule is isolated and identified, guided by its activity. Posterior studies are then necessary to elucidate the mechanism of action responsible for the biological activity. Such studies are carried out through the evaluation in different biological tests, often without pointing to a specific target, making several steps necessary until the pathway by which the substance performs its functions is defined (HUGHES et al., 2011; AGARWAL et al., 2014).

In most recent years, the integration of DNA technologies into pharmaceutical research, opened up to a revolution of new strategies in the field of drug discovery and development. A molecular target-oriented approach quickly spread through the

labs. In this strategy, which is called target-drug discovery (TDD), the molecular target important to the disease biology is firstly identified and its complementary DNA (cDNA) is used to express recombinant protein for purification, or to generate genetic engineering cell lines that overexpress the target. TDD assays relies on measuring the activity of recombinant molecular target of interest. Additional experimental studies that link the specific target to a disease model or condition is the bedrock for TDD strategies, a process that is denominated "target validation" (HUGHES et al., 2011; LEE; BERG, 2013). In general, phenotypic assays are frequently used as "next step" experiments in TDD workflows, which shows that traditional and most-modern approaches are essential and complementary in drug discovery programs.

Aiming to reduce the number of steps of traditional procedures, and to optimize the isolation of substances that act on specific molecular targets, Lau and collaborators (2015) developed the method called functional (bioaffinity) chromatography, a reverse affinity procedure exemplified in figure 5 (LAU et al., 2015). The technique was built along the lines of a TDD prospecting approach, where a recombinant protein (biological target) is attached in an affinity resin following incubation a crude extract or a purified compound. Functioning as a fishery, where the fish is selectively attracted by the bait, this procedure aim the isolation of compounds with binding specificities with the molecular target. After separation, the identification of the compound or compounds of interest is done quickly by well-developed and highly sensitive chemical methods, such as nuclear magnetic resonance and mass spectrometry, enabling the detection of compounds in small quantities and precise structural determination.

Figure 5. Schematic exemplification of the reverse affinity technique (Bioaffinity chromatography) developed by Lau et al., (2015).



Firstly, the recombinant protein is attached to the affinity resin following by crude extract or purified compound overnight incubation. After washed procedures, the selected compounds are eluted from the affinity column next proceeding to chemical identification by LC-MS analysis. Scheme gently provided by Prof. Larissa Alves Guimarães.

2. Relevance and justification

We're going through a unique moment for clinical research with new techniques of molecular precision that enable a better understanding of drug-target interactions. All new agents approved for the treatment of melanoma act independently and show a significant improvement in the survival rate of patients with advanced disease. However, despite the excellent results found, some gaps still need to be filled regarding the efficiency, scope and resistance of therapy against melanomas. Studies have shown that TBX2 transcription factor play an important role as anti-senescence, favoring the proliferation during melanomagenesis, and promoting resistance to DNA-damaging drugs, which configures the inhibition of its functions as a new target for the development of new anticancer drugs.

Natural products are still the main source for the discovery of new bioactive substances, giving emphasis on natural products from marine origin and its unique structures linked to potent biological activities. Even more promising is the biotechnological versatility coupled the biosynthesis of natural compounds by marine microorganisms, which guarantee the material supply. Moreover, the prospect of natural products has been improving on methods to ensure the efficiency of compounds isolation with reduced cost and time invested. The use of the bioaffinity chromatography technique, together with chemical and biophysical tools already established, figures as a highly effective strategy in prospecting marine natural products aiming the discovery of anticancer strands.

Recognizing all the facts mentioned above, the present PhD thesis expresses the interest in isolating and studying the potential of new substances from marine microorganisms, through bioaffinity chromatography, with potential to act as modulators of TBX2 pathway in melanoma cell lines and exploring its potential mechanisms of action.

3. Objectives

3.1 General objective

To identify natural molecules with affinity to TBX2 transcription factor and understand the possible modulation of its function in melanoma cell lines.

3.2 Specific objectives

1. Study the anticancer activity of natural products isolated from marine microorganisms;

2. Validate the bioaffinity chromatography technique using the recombinant TBX2 protein as bait;

3. Study and determine the binding affinity between chromomycin A5 and TBX2 protein;

4. Evaluate the cytotoxicity of chromomycin A5 in cells genetically engineering with TBX2 overexpression and knocked down;

5. Characterize the anticancer potential of chromomycin A5 in a TBX2-driven melanoma cell line.

4. Study rational

The present PhD thesis was elaborated into three chapters in order to facilitate the understanding of the developed work during the last four years.

The chapter 1 describe the isolation and identification of four dextrorotatory chromomycins found in an extract produced by the marine actinobacteria *Streptomyces sp*. BRA-384. The characterization, production and isolation of such molecules is considered fundamental in this work since the compounds became the center of our investigations. Chromomycins are potent anticancer molecules already known, but here we describe the isolation of rare chromomycins, including two new ones, that were poorly study regarding its biological activity. This part of the work was conducted in collaboration with Dr. Otila Pessoa's group at the Federal University of Ceará, specialized in chemical studies with marine microorganisms. This first section was published in 2019 at the Journal of Brazilian Chemical Society (PINTO et al., 2019).

In the chapter 2 we test and evaluate the binding potential of two chromomycins A_5 (CA_5) and A_6 (CA_6) isolated as described in chapter 1 with the TBX2 DNA-binding domain recombinant protein. This part of our study was based in a first screening using a bio-affinity chromatography technique, where we uncovered CA_5 as a potential ligand to TBX2. The screening was followed by the measurement of the binding interactions using microscale thermophoresis in order to quantify the affinity (K_D). In this section we also compare the activity of CA_5 in different TBX2-driven cancer cells, including those from melanoma, sarcoma and breast carcinoma. In addition, studies with a melanoma cell line (501mel) genetic engineering to knock down or overexpress TBX2. These results were recently accepted for publication in the Frontiers in Chemistry (SAHM et al., 2020).

In the chapter 3, we performed additional assays in order to characterize the anticancer profile of CA_5 in a TBX2-driven melanoma cell line compared to doxorubicin and CA_6. We also investigate the effects of these drugs in the signaling pathways for DNA-damage and TBX2 modulation, in an attempt to better understand the involvement of TBX2 in the mechanisms of action. The protein and mRNA levels expression of TBX2 target genes were also measured. It is worth mentioning that this study is a part of an ambitious project developed in collaboration of Prof. Sharon

Prince's group from University of Cape Town in South Africa, where the author spent a year of internship during her PhD.

The whole work showed very exciting results that certainly uncovered CA_5 as a possible modulator of TBX2, that should be further studied to contribute for advances in the field of cancer treatment.

5. Chapter 1

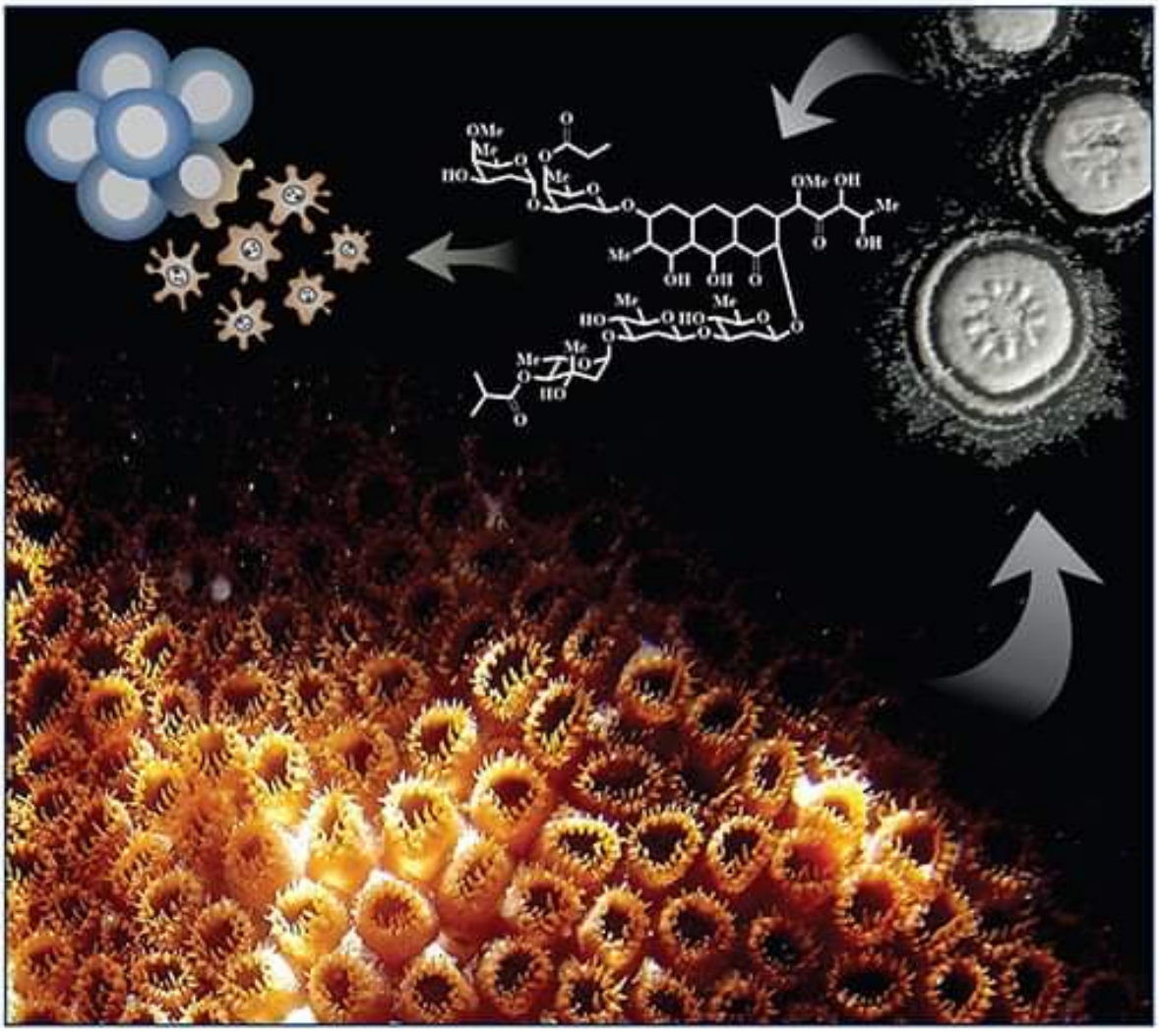
Dextrorotatory chromomycins from the marine *Streptomyces sp.* associated to *Palythoa caribaeorum*

Journal of the Brazilian Chemical Society

JBCS

Vol. 31, No. 1
January, 2020

ISSN 0103-5053
ISSN online 1678-4790



Dextrorotatory Chromomycins from the Marine *Streptomyces* sp. Associated to *Palythoa caribaeorum*

Francisco C. L. Pinto, Edilberto R. Silveira, Ana Caroline L. Vasconcelos, Katharine G. D. Florêncio, Francisca A. S. Oliveira, Bianca B. Sahm, Letícia V. Costa-Lotufo, Anelize Bauermeister, Norberto P. Lopes, Diego V. Wilke and Otília D. L. Pessoa

http://dx.doi.org/10.21577/0103-5053.20190144

J. Braz. Chem. Soc., Vol. 00, No. 00, 1-10, 2019
Printed in Brazil - ©2019 Sociedade Brasileira de Química

Article

Dextrorotatory Chromomycins from the Marine *Streptomyces* sp. Associated to *Palythoa caribaeorum*

*Francisco C. L. Pinto,[a] Edilberto R. Silveira,[a] Ana Caroline L. Vasconcelos,[b] Katharine G. D. Florêncio,[b] Francisca A. S. Oliveira,[b] Bianca B. Sahm,[c] Letícia V. Costa-Lotufo,[c] Anelize Bauermeister,[c,d] Norberto P. Lopes,[d] Diego V. Wilke**,[b] and Otília D. L. Pessoa**,[a]

[a]Departamento de Química Orgânica e Inorgânica, Universidade Federal do Ceará, 60021-970 Fortaleza-CE, Brazil

[b]Núcleo de Pesquisa e Desenvolvimento de Medicamentos, Departamento de Fisiologia e Farmacologia, Universidade Federal do Ceará, 60430-275 Fortaleza-CE, Brazil

[c]Departamento de Farmacologia, Instituto de Ciências Biomédicas, Universidade de São Paulo, 05508-900 São Paulo-SP, Brazil

[d]Departamento de Física e Química, Faculdade de Ciências Farmacêuticas de Ribeirão Preto, Universidade de São Paulo, 14040-903 Ribeirão Preto-SP, Brazil

A *Streptomyces* sp. (BRA-384) was selected among nine strains of bacteria isolated from the zoanthids *Palythoa caribaeorum* due to the high cytotoxic activity presented by its EtOAc extract (inhibitory concentration mean (IC_{50}) of 2 ng mL^{-1}) against colon cancer cell line. From the EtOAc extract of BRA-384 three new chemical entities (A_6, A_7 and A_8) and one dextrorotatory chromomycin (A_5), a promising class of anticancer compounds, were identified. The cytotoxicity of chromomycins A_5 to A_8 was tested against five tumor cell lines (HCT 116 (human colon adenocarcinoma), MCF-7 (human breast carcinoma), PC-3M (human metastatic prostate cancer), 501-mel (human metastatic melanoma) and MM200 (metastatic melanoma)). All chromomycins were highly potent showing IC_{50} values from 0.2 to 133 nM. Chromomycin A_5 was consistently the most potent over all tested cells (IC_{50} values from 0.2 in MM200 to 7.9 nM in PC-3M), inclusive when compared to the standard chemotherapeutic agent doxorubicin, that presented IC_{50} values ranging from 147 to 568 nM against MM200 and MCF-7, respectively.

Keywords: *Palythoa caribaeorum*, chromomycins, cytotoxic activity

Introduction

Marine microorganisms have emerged as an immensurable resource of bioactive compounds. Among the microbial sources, the actinomycetes, filamentous Gram-positive bacteria, have been highlighted as producers of a great number of active secondary metabolites. In fact, there is evidence that ca. 10,000 active compounds have been discovered from actinomycetes, representing 43% of all bioactive microbial metabolites.[1,2] Among the actinomycetes, the genus *Streptomyces* (family: Streptomycetaceae, order: Actinomycetales) has been considered as the major producer of active compounds, contributing significantly to cancer treatments.[3,4] Several antitumor compounds currently used in human chemotherapy are produced by *Streptomyces* species, and includes the actinomycin, mitomycin, anthracycline, bleomycin, pentostatin, resistomycin and aureolic acid families.[1,5]

Chromomycins are tricyclic glycosylated polyketides, produced by terrestrial and marine bacteria of the genus *Streptomyces* belonging to the aureolic acid family.[4,6-8] Initially, the interest in chromomycins was due to their antimicrobial properties,[9] but, nowadays, the main goal of studying chromomycins is related to their anticancer activity and antiproliferative properties.[4,10,11] These molecules bind to the deoxyribonucleic acid (DNA) minor grove, causing DNA damage of treated cells, enhancing the expression

*e-mail: diegowilke@gmail.com; otilialoiola@gmail.com

of apoptosis related genes.[12,13] Most of this knowledge is related to chromomycin A_3 effects, but it is assumed to be true for the whole family of compounds. Previously, we reported[14] autophagy induction on melanoma cells by chromomycin A_2 isolated from *Streptomyces* sp. recovered from marine sediment.

As part of a program on marine natural products bioprospection, we have devoted our attention to the study of the zoanthids *Palythoa caribaeorum* and *Palythoa variabilis*, two abundant zoanthids in the Brazilian coast.[15] Recently, we have extended the scope of our research investigating the chemical and microbiological profiles of these species from the Brazilian coast through an omics approach which revealed a great chemical and biosynthetic gene clusters diversity.[15] In this paper, we present the isolation and structure elucidation of four dextrorotatory chromomycins from a cytotoxic extract produced by a *Streptomyces* bacteria strain recovered from the zoanthid *P. caribaeorum*, collected at Pedra Rachada Beach, located on the west coast of Ceará State, including the previously described chromomycin A_5.[10] The cytotoxic activity of the isolated compounds was evaluated in a panel of five tumor cell lines, including melanoma, breast, colon and prostate carcinomas.

Results and Discussion

A total of nine bacterial strains were isolated from the zoanthids *P. caribaeorum* and *P. variabilis* collected at Taíba and Pedra Rachada beaches (Ceará State) in the northeastern Brazil coast. The bacteria were cultured, and their crude EtOAc extracts were evaluated against the human HCT 116 colon cancer cells. The most active extract, from the BRA-384 strain, showed an inhibitory concentration mean (IC_{50}) value equal to 2 ng mL^{-1}, and therefore, it was selected to be further investigated. BRA-384 was identified as *Streptomyces* sp. based on the 16S rRNA sequencing by comparison to the sequences present at NCBI[16] using basic local alignment search tool (BLAST) followed by phylogenetic analysis (Figure S1, Supplementary Information (SI) section).

In this study, the time-course of the production of chromomycins (**1** to **4**) by BRA-384 was investigated (Figure 1a). Firstly, the chromatographic conditions to the identification of each peak of the chromomycins were established (see Figure S2, SI section). Once the aureolic acid is the common chromophore of all these molecules,[4] a positive correlation of the peak areas with the quantity of chromomycin was expected. The peaks of compound **1** increased, while **3** diminished progressively from 1 h to 9 days. On the other hand, compound **2** depicted larger peaks at days 5 and 7. Compound **4** detection was always much lower than compounds **1**-**3**. Additionally, when the BRA-384 strain was removed from the culture broth, by filtration (0.22 μm), the extracts kept the same profile until day 9 (see Figure S3, SI section). These data suggested that the variation in the relative amounts of chromomycins were made by the bacteria itself, once all the culture conditions were the same, except by the bacteria removal. The biomass and organic extract yielding increased markedly on A1 culture broth with BRA-384 until day 7. The growth inhibition of HCT 116 cells was sustained above 80% by all the organic extracts tested at 50 μg mL^{-1} (data not shown). Once the cytotoxicity potency of chromomycins is well known, this high growth inhibition was expected. Based on these observations, we performed BRA-384 extractions at day 6 aiming to achieve both favorable yield and optimized amounts of chromomycins as well.

Liquid chromatography (LC) analysis of the crude extract exhibited an UV profile (λ_{max} 410, 320, 280 and 235 nm), which is characteristic of members of the aureolic acid family.[4,10] The compounds associated with main peaks observed in the high-pressure liquid chromatography (HPLC) were isolated and the chemical structures were characterized by high resolution mass spectra (HRMS), and nuclear magnetic resonance (NMR). A preliminary analysis by ^{1}H NMR spectra (see Table 1) of the isolated compounds from the BRA-384 exhibited signals for two benzene protons (δ_H 6.63-6.77), five anomeric protons (δ_H 4.61-5.23), two methoxyls (δ_H 3.51-3.61), seven methyl groups (δ_H 1.18-2.19), and *O*-acylated groups (δ_H 2.15-2.19), again typical of the aureolic acid family (chromomycin, mithramycin, olivomycin and durhamycin).[6,8] Those compounds are structurally characterized by a tetrahydro antracenone substituted at C-3 and C-7 by aliphatic chains, and at C-2 and C-6 by oligosaccharide chains constituted by oliose (sugars A and B), olivose (sugars C and D) and chromose (sugar E), which can be acetylated and/or *O*-methylated.[6,8,9] Despite the common structural aspects, each member has a peculiar characteristic which enables its identification even in mixtures, for instance: while the chromomycins and mithramycins display a characteristic methyl at C-7, the durhamycins have a *sec*-butyl at the same position. On the other hand, olivomycins in turn, are not substituted in this position.[4,7,10,17] Although both chromomycins and mithramycins present the same aglycones, they differ in the stereochemistry of the sugar units. In chromomycins, the disaccharide at C-2 is β-A(3→1)-α-B and the trisaccharide at C-6 is β-C(3→1)-β-D-(3→1)-α-E, whereas in mithramycins, all units glycosides have β-*c*onfiguration at the anomeric carbons.[10] These main differences are easily observed by NMR data.

Compound **1**, a yellow amorphous powder, had its molecular formula $C_{57}H_{82}O_{26}$ determined by high resolution electrospray ionization mass spectrometry (HRESIMS) from the deprotonated molecular ion $[M - H]^-$ at *m/z* 1181.4999 (calcd. 1181.5022; 1.9 ppm error). Its ^{1}H NMR spectrum (see Table 1) displayed two chelated

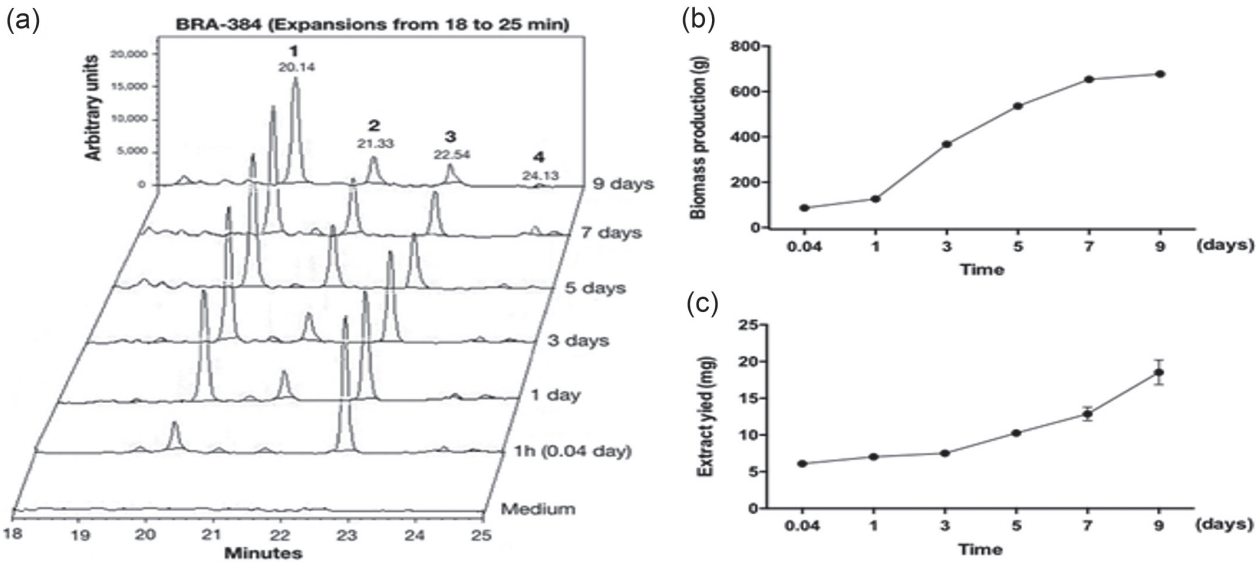


Figure 1. (a) Representative chromatograms expansion of the EtOAc extracts highlighting the chromomycins **1** to **4** production by *Streptomyces* sp. (BRA-384 strain) cultured in A1 broth monitored up to 9 days; (b) biomass production; (c) EtOAc extract yield of A1 broth of BRA-384 strain. The data are depicted as mean and standard deviation of experiments performed in triplicate.

Table 1. ^{1}H (500 MHz) and ^{13}C (75 MHz) NMR data assignments for **1**-**4** in $CDCl_3$

Position	**1**		**2**		**3**		**4**
	δ_C	δ_H (*J* in Hz)	δ_C	δ_H (*J* in Hz)	δ_C[a]	δ_H (*J* in Hz)	δ_H (*J* in Hz)
Aglycon moiety							
1	202.3		202.0		202.3		
2	76.2	4.73, d (12.0)	75.9	4.73, d (11.5)	76.1	4.73, d (11.2)	4.73, d (11.4)
3	43.9	2.58, m	43.7	2.58, m	43.8	2.58, m	2.58, m
4	27.1	3.10, d (12.8)	27.3	3.10, d (12.3)	27.1	3.10, d (12.3)	3.10, d (12.8)
		2.69, m		2.69, m		2.69, m	2.69, m
5	101.1	6.65, s	100.9	6.67, s	100.9	6.63, s	6.65, s
6	159.9		159.5		159.8		
7	111.9		111.7		111.8		
8	156.4		156.3		156.2		
9	165.5		165.5		165.4		
10	117.2	6.76, s	116.8	6.77, s	117.2	6.75, s	6.75, s
4a	134.8		134.4		134.7		
8a	108.3		108.1		108.2		
9a	108.3		108.4		108.2		
10a	138.6		138.9		138.5		
7-Me	8.4	2.19, s	8.5	2.19, s	8.4	2.18, s	2.18, s
8-OH		9.83, s		9.83, s		9.82, s	9.83, s
9-OH		15.71, s		15.71, s		15.71, s	15.71, s
1’	82.0	4.72, d (1.5)	81.8	4.72, d (1.5)	82.1	4.72, d (1.5)	4.70, d (1.4)
2’	211.5		211.3		211.5		
3’	78.4	4.23, br s	78.2	4.23, br s	78.4	4.23, br s	4.21, br s
4’	68.1	4.37, br q (6.7)	67.9	4.37, br q (6.5)	68.0	4.37, br q (6.4)	4.37, br q (6.7)
5’	20.8	1.37, d (6.7)	20.9	1.37, d (6.5)	20.6	1.37, d (6.4)	1.37, d (6.7)
1’-OMe	59.9	3.53, s	59.6	3.53, s	59.8	3.53, s	3.51, s

Table 1. ^{1}H (500 MHz) and ^{13}C (75 MHz) NMR data assignments for **1**-**4** in $CDCl_3$ (cont.)

Position	**1**		**2**		**3**		**4**
	δ_C	δ_H (*J* in Hz)	δ_C	δ_H (*J* in Hz)	δ_C[a]	δ_H (*J* in Hz)	δ_H (*J* in Hz)
Sugar A							
A1	97.6	5.22, dd (10.8, 2.9)	97.4	5.23, dd (9.9, 2.0)	97.6	5.22, dd (9.9, 2.4)	5.23, dd (9.9, 2.4)
A2	33.1	2.21, m	32.9	2.21, m	33.2	2.21, m	2.21, m
		2.06, m		2.07, m		2.06, m	2.06, m
A3	70.2	4.00, m	69.9	4.00, m	70.0	4.00, m	3.99, m
A4	67.5	5.18, d (2.6)	67.0	5.18, d (2.8)	67.4	5.18, d (2.4)	5.18, d (2.1)
A5	69.9	3.83, br q (6.5)	69.7	3.83, br q (6.5)	69.9	3.82, br q (6.2)	3.81, br q (6.2)
A6	17.0	1.29, d (6.5)	16.9	1.29, d (6.5)	16.9	1.29, d (6.2)	1.29, d (6.2)
A4-O-	acetyl		acetyl		acetyl		propionyl
1”	171.1		170.8		171.1		
2”	21.0	2.18, s	20.9	2.18, s	21.0	2.19, s	2.45, q (7.1)
3”							1.20, t (7.1)
Sugar B							
B1	95.4	5.13, br s	95.1	5.12, br s	95.3	5.13, br s	5.11, br s
B2	33.7	1.77, m	33.5	1.77, m	33.6	1.77, m	1.77, m
		1.75, m		1.75, m		1.75, m	1.75, m
B3	66.1	4.00, m	66.3	4.00, m	66.0	4.00, m	3.99, m
B4	81.7	3.23, d (2.6)	81.5	3.23, d (3.0)	81.7	3.23, d (2.7)	3.23, d (1.8)
B5	66.9	3.88, br q (6.5)	66.9	3.88, br q (6.8)	66.8	3.88, br q (6.5)	3.88, br q (6.7)
B6	17.5	1.30, d (6.5)	17.2	1.30, d (6.8)	17.4	1.30, d (6.5)	1.30, d (6.7)
B4-OMe	62.6	3.61, s	62.3	3.61, s	62.5	3.61, s	3.59, s
Sugar C							
C1	100.5	5.10, dd (9.0, 2.0)	100.2	5.10, dd (9.8, 1.8)	100.5	5.10, dd (9.8, 2.1)	5.08, dd (9.7, 2.1)
C2	37.7	2.50, m	37.6	2.50, m	37.6	2.50, m	2.49, m
		1.72, m		1.72, m		1.72, m	1.72, m
C3	82.5	3.59, m	82.2	3.59, m	82.5	3.59, m	3.59, m
C4	75.3	3.14, d (8.0)	75.2	3.14, d (8.6)	75.3	3.14, d (7.7)	3.12, d (8.9)
C5	72.4	3.32, dq (8.0, 6.9)	72.3	3.32, dq (8.6, 6.9)	72.3	3.32, dq (7.7, 6.9)	3.32, dq (8.9, 6.0)
C6	18.2	1.38, d (6.9)	18.1	1.38, d (6.9)	18.2	1.38, d (6.9)	1.38, d (6.0)
Sugar D							
D1	99.9	4.63, d (9.5)	99.7	4.63, d (9.6)	99.9	4.61, d (9.5)	4.61, d (9.4)
D2	37.3	2.28, dd (12.9, 3.3)	37.2	2.28, dd (12.9, 5.5)	37.2	2.28, dd (12.1, 4.0)	2.28, dd (12.5, 6.5)
		1.68, m		1.68, m		1.68, m	1.68, m
D3	80.9	3.50, m	80.7	3.50, m	80.7	3.50, m	3.49, m
D4	75.5	3.14, d (8.0)	75.2	3.14, d (8.6)	75.4	3.12, d (8.5)	3.11, d (8.1)
D5	72.5	3.39, dq (8.0, 6.8)	72.2	3.40, dq (8.6, 6.8)	72.4	3.40, dq (8.5, 6.0)	3.39, dq (8.1, 6.0)
D6	18.0	1.39, d (6.8)	17.9	1.39, d (6.8)	18.0	1.39, d (6.0)	1.39, d (6.0)
Sugar E							
E1	97.3	5.03, dd (4.5, 1.8)	97.1	5.03, dd (4.3, 2.0)	97.2	5.03, dd (4.8, 2.4)	5.01, dd (3.5, 1.7)
E2	43.9	2.06, m	43.9	2.07, m	43.9	2.07, m	2.05, m
		2.00, m		2.02, m		2.00, m	2.00, m
E3	70.8		70.5		70.8		
E4	79.8	4.61, d (9.0)	79.6	4.61, d (9.0)	79.5	4.61, d (9.5)	4.61, d (9.4)
E5	67.2	4.00, m	67.0	4.00, m	67.2	4.00, m	3.99, m
E6	18.0	1.24, d (6.3)	18.0	1.24, d (6.5)	18.0	1.24, d (6.5)	1.24, d (6.5)
E3-Me	23.2	1.37, s	23.2	1.36, s	23.1	1.36, s	1.36, s
E4-O-	acetyl		propionyl		isobutyryl		isobutyryl
1”’	171.5		175.3		177.7		
2”’	21.0	2.15, s	27.8	2.44, q (7.5)	34.4	2.65, m	2.62, m
3”’			9.3	1.19, t (7.5)	19.1	1.21, d (7.0)	1.18, t (7.1)
4”’					19.1	1.21, d (7.0)	1.18, t (7.1)

[a]Signals ^{13}C NMR for the down-field were obtained by $^{1}H \times {}^{13}C$ correlations of HSQC and HMBC.

phenol protons at δ_H 15.71 (9-OH) and 9.83 (8-OH), two singlets for benzene protons at δ_H 6.76 (H-10) and 6.65 (H-5), five anomeric protons at δ_H 5.22 (d, *J* 10.8, 2.9 Hz, A1), 5.13 (br s, B1), 5.10 (d, *J* 9.0, 2.0 Hz, C1), 5.03 (dd, *J* 4.5, 1.8 Hz, E1) and 4.63 (d, *J* 9.5 Hz, D1), and two methoxyl groups at δ_H 3.61 (s, MeO-B4) and 3.58 (s, MeO-1'). In addition, the ^{1}H NMR spectrum showed signals to twelve methyl groups, including those at δ_H 2.19 (s, Me-7), 2.18 (MeCO-A4) and 2.15 (MeCO-E4). The ^{13}C NMR and heteronuclear single quantum correlation (HSQC) spectra displayed signals to 57 carbon atoms (see Table 1), assignable to the twelve methyl groups as observed in the ^{1}H NMR spectrum including those corresponding to two methoxyls and two acetyl groups, six methylenes, and twenty-four methines, including the anomeric carbons. Comparatively, 13 non-hydrogenated carbons, including two ketone carbonyls [δ_C 211.5 (C-2') and 202.3 (C-1)] and two acetyl carboxyls [δ_C 171.5 (MeCO-E4) and 171.1 (MeCO-A4)] what is in accordance with the ^{1}H NMR spectrum that showed two methyls of acetyl esters. Comparison of the ^{1}H and ^{13}C NMR data of **1** with those previously reported to chromomycin A_3 $[\alpha]_D^{20}$ −42.0° (*c* 1.0, EtOH) indicated remarkable similarities,[18] since no significant differences in the chemical shifts (larger difference $\Delta\delta_C$ 0.4 ppm and $\Delta\delta_H$ 0.09 ppm) were observed (see Table S1, SI section). Nevertheless, the dextrorotatory specific rotation of $[\alpha]_D^{20}$ +48.2° (*c* 0.1, MeOH) observed for **1**, indicated that these compounds are, indeed, stereoisomers. The complete ^{1}H and ^{13}C NMR assignments of **1** were made by a combination of ^{1}H and ^{13}C NMR, correlation spectroscopy (COSY), HSQC and heteronuclear multiple bond correlation (HMBC) experiments (see Figures S4-S10, SI section). Based on the above data **1** is a new member of aureolic acid family and following the denotation adopted for the five chromomycins already reported, it was assigned as chromomycin A_6.

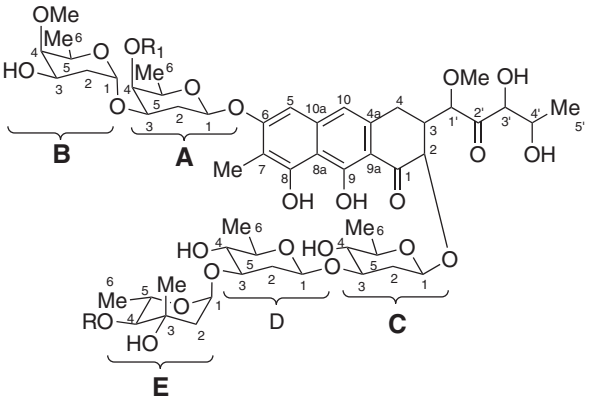
Compound **2** was also isolated as a yellow amorphous powder. Its molecular formula was established as $C_{58}H_{84}O_{26}$ based on the $[M - H]^-$ ion peak observed by HRESIMS for the deprotonated molecular ion at *m/z* 1195.5169 (calcd. 1195.5178, 0.8 ppm error). A detailed analysis of the 1D and 2D NMR spectra revealed that **2** shared high structural similarity to **1** being the difference related to the presence of a propionyl moiety as established by the ^{1}H and ^{13}C NMR data (δ_C/δ_H 175.3 (C=O), 27.8/2.44 (q, *J* 7.9 Hz, CH_2) and 9.3/1.18 (t, *J* 7.9 Hz, CH_3)) instead an acetyl group (see Table 1). The unequivocal positioning of the propionyl moiety at C-E4 (δ_C 79.6) was confirmed by the HMBC correlation of the proton signal at δ_H 4.61 (d, *J* 9.0 Hz, H-E4) with the ester carbonyl at δ_C 175.3 (CH_3CH_2CO-E4), 70.5 (C-E3), 67.0 (C-E5) and 18.0 (C-E6). The above data support a structure similar to that of chromomycin A_p (patent number 64967-61-9),[19] which was previously isolated from a *Streptomyces griseus* strain. Although the authors of the patent have stated that they have used NMR data, we were not able to find them, making it impossible to do any comparative analysis. However, the optical rotation described of $[\alpha]_D^{20}$ −56.0° (*c* 0.1, EtOH)[19] had the opposite sign to that found for **2** $[\alpha]_D^{20}$ +18.4° (*c* 0.1, MeOH), suggesting that these compounds are indeed stereoisomers. However, the lack of NMR data for chromomycin A_p does not permit to conclude whether they are diastereomers or enantiomers. Thus, compound **2** was assigned as the new chromomycin A_7.

Compound **3**, also isolated as a yellow amorphous powder, had its molecular formula described as $C_{59}H_{86}O_{26}$ based on the deprotonated molecular $[M - H]^-$ ion peak at *m/z* 1209.5274 (calcd. 1209.5308, 2.8 ppm error) as observed in the HRESIMS. The ^{1}H and ^{13}C NMR spectra also showed typical signals for a chromomycin nucleus. From a detailed analysis of their 1D and 2D NMR data it was obvious that **3** had a structure similar to **1** and **2** only differing in the replacement of the acetyl (MeCO-A4) in **1** or the propionyl (CH_3CH_2CO-E4) in **2** by an isobutyryl moiety as evidenced by the chemical shifts at δ_C/δ_H 177.7 (C=O), 34.4/2.65 (m, CH), 19.1/1.21 (d, *J* 7.0 Hz, CH_3) and 19.1/1.21 (d, *J* 7.0 Hz, CH_3) in the ^{1}H and ^{13}C NMR spectra (see Table 1). The unequivocal position of the isobutyryl group at C-E4 (δ_C 79.5) was confirmed by the HMBC correlation of the H-E4 at δ_H 4.61 (d, *J* 9.6 Hz) with the ester carboxyl at δ_C 177.7 (C=O). Analysis of ^{1}H and ^{13}C NMR data allowed to suggest an identical structure to those of chromomycin A_5 $[\alpha]_D^{24}$ +57.6° (*c* 0.035, EtOH)[10] or chromomycin A_2 $[\alpha]_D^{24}$ −61.4° (*c* 1.0, EtOH)[19] since the subtle differences in the NMR data are not enough to differentiate one from each other (see Tables S2 and S3, SI section). Nevertheless, the positive optical rotation $[\alpha]_D^{20}$ +48.8° (*c* 0.1, MeOH) observed for **3**, led to the conclusion that **3** was indeed chromomycin A_5. This compound was firstly obtained from a microorganism identified as *Streptomyces* sp. recovered from sedimentary specimen collected on the Beaufort Sea coast of Alaska by Pettit *et al.*,[10] who described chromomycin A_5 as a stereoisomer of chromomycin A_2 at C-2 and/or C-3.

Compound **4**, a yellow amorphous powder, also exhibited a dextrorotatory specific rotation $[\alpha]_D^{20}$ +8.1° (*c* 0.1, MeOH). Its molecular formula of $C_{60}H_{88}O_{26}$ was determined by HRESIMS which exhibited a $[M - H]^-$ ion peak at *m/z* 1223.5455 (calcd. 1223.5491, 2.9 ppm error) indicating 14 a.m.u. higher than compound **3**. Its ^{1}H NMR data were similar to those of **3** (see Table 1) only differing by

an extra methylene signal consistent with the replacement of the acetyl group in **3** by a propionyl moiety [δ_H 2.44 (q, *J* 7.1 Hz) and 1.20 (d, *J* 7.1 Hz)] corroborating with the molecular formula. Although some chemical shifts were missing in the 2D NMR experiments, the signals related to the propionyl moiety were clearly observed in the HSQC spectrum (δ_H 2.44/δ_C 27.0 and 1.20/δ_C 9.0) as well as in the HMBC spectrum which displayed correlations for both the methylene (δ_H 2.44) and the methyl (δ_H 1.20) protons with the carboxyl ester at δ_C 174.5 (C=O) supporting the suggested structure. Moreover, the mass fragmentation of **4** {*m/z* 917.38 $[M + Na]^+$-G_{AB} glycoside moiety (calcd. for $C_{44}H_{62}O_{19}Na$), *m/z* 773.27 $[M + Na]^+$-G_{CDE} glycoside moiety (calcd. for $C_{37}H_{50}O_{16}Na$) and *m/z* 497.19 $[G_{CDE} + Na]^+$-$C_{37}H_{50}O_{16}$ (calcd. for $C_{23}H_{38}O_{10}Na$)} provided by LC-MS/MS gave additional argumentation to confirm the propionyl moiety at C-A4 as shown in Figures 2 and S36 (SI section). Interestingly, Oki *et al.*[20] isolated from a culture of *Streptomyces* sp. a chromomycin (codified as SR1768A) bearing a propionyl group at the same position. To the best of our knowledge, this was the only report on the isolation of this compound, but its NMR data and the optical rotation were not reported, which did not permit any comparison. Thus, we believe that chromomycin **4** is a new dextrorotatory entity of this family, and then, designated chromomycin A_8.

Chromomycins, as well as other aureolic acids, are type II polyketides and their biosynthetic clusters include the genes for polyketide biosynthesis and modifications, deoxysugar biosynthesis or sugar transfer, pathway regulation and resistance.[6-8] Genome mining can be used to increase the production yield and also to obtain modified chromomycins.[6-8] The compounds **1**-**4** share the same aglycone moiety showing only minor differences at C-A4 or C-E4 of the saccharide side chains (Figure 2). Concerning to the latter dissimilarities, the activity of CmmA acetyltransferase, an enzyme located in the cell membrane of *Streptomyces* which accepts several acyl-CoA substrates, could explain the acylation diversity of **1** to **4**,[7] corroborating the data from time-course experiments, where the presence of the bacteria strain is responsible for the appearance of compounds **1**-**4** in the culture media.



	R =	R_1 =	Name
1	$COCH_3$	$COCH_3$	A_6
2	$COCH_2CH_3$	$COCH_3$	A_7
3	$COCH(CH_3)_2$	$COCH_3$	A_5
4	$COCH(CH_3)_2$	$COCH_2CH_3$	A_8

Figure 2. Molecular structures of chromomycins **1**-**4** isolated from *Streptomyces* sp.

The cytotoxicity of the compounds **1**-**4** was further evaluated against five human cell lines including the human tumor cell lines MCF-7 (breast carcinoma), HCT 116 (colon adenocarcinoma), PC-3M (metastatic prostate cancer), 501-mel (metastatic melanoma) and MM200 (metastatic melanoma). Chromomycins **1**-**4** were highly potent against tumor cells showing IC_{50} values ranging from 0.2 nM for compound **3**, over MM200 cells, to 133 nM for compound **2** over MCF-7 cells. In fact, compound **3** was consistently more active throughout all tested cell lines. Doxorubicin, used as positive control, was far less active than compounds **1**-**4**, being the biggest difference in the sensitivity of doxorubicin and chromomycin A_5 (**3**) over HCT 116 cells, where the positive control was more than one thousand times less active (see Table 2).

Previous studies on the molecular interactions of chromomycin A_3 and DNA revealed that this compound dimerizes, in a process coordinated by the presence of Mg^{2+}, and binds to the minor groove of the DNA duplex.[12] The binding involves the interaction of the chromophore and D, E and F sugar moieties with residues of the minor grove, while A-B sugar moieties and part of the chromophore interact with the phosphate backbone.[12] The C3-side chain is not directly related to the DNA binding properties, thus the influence in the observed cytotoxicity seemed to be secondary to modifications in the sugar moieties and the chromophore. A review in the literature regarding to chromomycins bearing the $CH(OMe)-CO-CH(OH)-CH(OH)-CH_3$ side chain at C-3 shows that only four chromomycins including the chromomycins A_5,[10] DAC-A_3,[4] 02-3G and 02-3D,[21] exhibit positive optical rotation values. Indeed, Pettit *et al.*[10] described chromomycin A_5 as a potent cytotoxic compound as other aureolic acid analogues, showing IC_{50} values ranging from 0.73 ng mL^{-1} against MCF-7 to 4.3 ng mL^{-1} on colon cancer KM20L2 cells. The potency is quite similar to the one observed in the present work.

Table 2. Cytotoxicity of chromomycins **1**-**4** on a panel of cell lines

Cell line	IC_{50} (95%CI) / nM				
	1	**2**	**3**	**4**	Doxorubicin
MCF-7	14.1 (7.9-25.1)	133.0 (84-210.0)	3.7 (2.2-6.3)	10.5 (4.2-26.3)	568.0 (305-1058.0)
HCT 116	3.5 (2.7-4.5)	47.3 (31.4-71.3)	0.4 (0.3-0.6)	1.4 (1.0-2.0)	453.0 (396.0-517.0)
501-mel	2.3 (1.7-2.7)	49.0 (31.3-76.7)	0.8 (0.5-1.0)	1.6 (1.1-2.2)	400.0 (384.0-563.0)
MM200	2.6 (2.1-3.2)	39.1 (33.6-46.6)	0.2 (0.1-0.3)	0.8 (0.5-1.3)	147.0 (122.0-176.0)
PC-3M	67.8 (51.7-88.9)	n.t.	7.9 (6.5-9.5)	88.3 (70.8-110.1)	799.2 (426.3-1499.0)

MCF-7: human breast carcinoma; HCT 116: human colon adenocarcinoma; 501-mel: human metastatic melanoma; MM200: human melanoma; PC-3M: human metastatic prostate cancer. Activity was evaluated using the MTT assay after 72 h incubation. Doxorubicin was used as positive control. The inhibition concentration means (IC_{50}) and confidence interval of 95% (CI95%) values were obtained by nonlinear regression of three independent experiments.

Conclusions

A *Streptomyces* sp. strain recovered from the zoanthid *P. caribaeorum* with presumable ability to biosynthesize only, or mainly, dextrorotatory chromomycins was investigated. The chromomycins A_5, A_6, A_7 and A_8 were highly cytotoxic, exhibiting an exciting profile of this class of compounds for antitumor application.

Experimental

General

Optical rotations were measured with a Jasco P-2000 polarimeter, operating with a tungsten lamp at a wavelength of 589 nm at 20 °C. HRESIMS spectra were acquired using a Shimadzu chromatographic system coupled to a mass spectrometer (Bruker Daltonics) equipped with an electrospray ionization source (ESI^-) and a quadrupole-time-of-flight analyzer. 1D and 2D ^1H, ^{13}C NMR spectra were obtained on a Bruker Avance DRX-500 or DPX-300 MHz spectrometers, using $CDCl_3$ or CD_3OD as solvent. A Shimadzu ultra-fast liquid chromatograph (UFLC) semi-preparative system (equipped with ternary pumps and diode array SPD-M20A UV-Vis detector) was used for high-performance liquid chromatography.

Sampling of zoanthids and isolation of their associated bacterial strains

Colonies of *Palythoa caribaeorum* and *Palythoa variabilis* (ca. 20 g of each colony) were sampled manually on the intertidal zone during the low tide at Pedra Rachada Beach, Paracuru City (3°39'5"S, 39°01'3"W) on the west coast of Ceará State, of the northeastern Brazil. The specimens were sprayed with 70% EtOH/H_2O (v/v) for superficial decontamination, then washed with sterile seawater at the collection sites and kept in ice for 2 h. The license for collection of zoanthids was granted by Biodiversity Authorization and Information System (SISBIO number 48522-2, SisGen number AC0781C). The samples were further processed under sterile conditions: extensively cut colonies of the zoanthids were spread on agar-media plates and incubated at room temperature (approximately 26 °C). From 2 to 6 weeks later, nine apparently different strains were separated from three different media: trace minerals agar (TMA) composed of 18 g agar, 1 g glucose, 1 g yeast extract, 7 g Na_2HPO_4, 1 g KNO_3, 3 g NaCl, 1 g $MgSO_4.7H_2O$, 0.2 g $CaCl_2.2H_2O$, 0.2 g $FeSO_4.7H_2O$, 0.18 g $ZnSO_4.7H_2O$, 0.02 g $MnSO_4.4H_2O$, 0.09 g $CuSO_4.5H_2O$, 0.01 g $CoSO_4.7H_2O$, 0.1 g H_3BO_3 and 0.1 g $(NH_4)6Mo_7O_{24}.4H_2O$ dissolved in 1 L of artificial seawater and supplemented with 0.1 mg mL^{-1} cycloheximide; sea water agar (SWA), composed of 18 g of agar dissolved in 1 L of artificial seawater; and starch casein agar (SCA), composed of 10 g of soluble starch, 1 g powdered casein, 15 g agar dissolved in 1 L of artificial seawater.

Molecular identification of BRA-384 bacterial strain and phylogenetic tree

A molecular based approach was carried out for taxonomic identification of the BRA-384 strain. The genomic DNA of the isolated was extracted as previously described[22] with minor modifications. For DNA extraction the cell pellet from 1.0 mL of the BRA-384 culture was obtained and suspended in 500 µL of cetyltrimethylammonium bromide (CTAB) lysis buffer for three cycles of freezing (−70 °C at 10 min) and thawing (65 °C at 10 min). The DNA was purified by phenol-chloroform-isoamyl alcohol (25:24:1), precipitated with sodium acetate and isopropanol, washed with ethanol and eluted with 10 mM Tris buffer. The sample was subjected to three cycles of freezing (−70 °C for 10 min) and thawing (10 min at 65 °C), and DNA extracted from the lysate by phenol-chloroform extraction and ethanol precipitation.

The gene 16S rRNA was amplified by polymerase chain reaction (PCR) using 27 F (5'AGA GTT TGA TCM TGG CTC AG3')[23] and 1492 R (5'CGG TTA CCT TGT TAC GAC TT3').[24] The PCR amplification was performed in a final volume of 25 µL total containing 5 µL of 5X Green Gotaq (Promega), 0.5 µL of dNTPs (10 mM), 1.0 µL of each primer (10 µM), 0.125 µL *Taq* polymerase (5 U μL^{-1}, GoTaq, Promega), 1.0 µL of template DNA, and water to complete. The PCR cycling was performed under the following conditions: 95 °C for 3 min, followed by 30 cycles of 95 °C for 30 s, 54.8 °C for 30 s, and 72 °C for 1 min, with a final extension at 72 °C for 5 min. The PCR product was analyzed by electrophoresis on a 1% agarose gel stained with SYBR™safe DNA gel stain (Invitrogen) and cleaned with ExoSAP-IT (Affymetrix). The sequencing was conducted at the Laboratório de Genética Molecular Humana (LGMH), Departamento de Genética of Universidade Federal de Pernambuco (UFPE) using Bigdye™ terminator v3.1 cycle sequencing kit (ThermoFisher). Sequences were obtained in both forward and reverse directions. Chromatograms were checked and the sequences edited using Geneious R10 software.[25] The sequence obtained in this study was compared with the NCBI[16] database using the basic local alignment search tool (BLAST) and deposited under the accession number MK163342. For the construction of the phylogenetic tree, some sequences were downloaded from NCBI[16] and the aligned was performed using MAFFT v7.222.[26] The phylogenetic tree was constructed with Geneious R10 software[25] using inference by the neighbor-joining (NJ)[27] method with bootstrap based on 1000 replication and by Tamura-Nei genetic distance model. The tree obtained was visualized using FigTree v1.4.2.[28]

Isolation and purification of chromomycins

Streptomyces sp. (BRA-384) was grown in A1 broth (100 g soluble starch, 40 g yeast extract and 20 g peptone) supplemented with 1 g calcium carbonate, 5 g $Fe_2(SO_4)_3$ and 5 g KBr, dissolved in 1 L of artificial seawater. The culture broth (8 L) was fermented during 6 days under 150 rpm agitation at 28 °C and extracted with EtOAc. The solvent was removed under reduced pressure to yield 230 mg of a crude extract that was purified by semi-preparative HPLC using a C_{18} column, and a gradient solvent system: solvent A [H_2O (CF_3CO_2H acid 0.01%)] and solvent B [MeCN (CF_3CO_2H acid 0.01%)], ranging from 50-100% B in 15 min, monitored in the 280 and 410 nm channels, with rate flow of 4.72 mL min^{-1}, to obtain compounds: **1** (10.0 mg, retention time (t_R) 7.45 min), **2** (4.8 mg, t_R 8.80 min), **3** (5.7 mg, t_R 10.18 min) and **4** (1.1 mg, t_R 11.58 min).

Chromomycin A_6 (**1**)

Yellow amorphous powder; $[\alpha]_D^{20}$ +48.2° (*c* 0.1, MeOH); UV (MeOH) λ / nm 411, 320, 278 and 230; ^{1}H NMR (500 MHz, $CDCl_3$) and ^{13}C NMR (75 MHz, $CDCl_3$) see Table 1; HRESIMS (negative mode) *m/z*, calcd. for $C_{57}H_{82}O_{26}$ $[M - H]^-$: 1181.5022, found: 1181.4999.

Chromomycin A_7 (**2**)

Yellow amorphous powder; $[\alpha]_D^{20}$ +18.4° (*c* 0.1, MeOH); UV (MeOH) λ / nm 412, 320, 280 and 229; ^{1}H NMR (500 MHz, $CDCl_3$) and ^{13}C NMR (75 MHz, $CDCl_3$) see Table 1; HRESIMS (negative mode) *m/z*, calcd. for $C_{58}H_{84}O_{26}$ $[M - H]^-$: 1195.5178, found: 1195.5169.

Chromomycin A_8 (**4**)

Yellow amorphous powder; $[\alpha]_D^{20}$ +8.1° (*c* 0.1, MeOH); UV (MeOH) λ / nm 411, 320, 278 and 230; ^{1}H NMR (500 MHz, $CDCl_3$) see Table 1; HRESIMS (negative mode) *m/z*, calcd. for $C_{60}H_{88}O_{26}$ $[M - H]^-$: 1223.5491, found: 1223.5455.

Investigation of the time influence on the extract yielding, biomass production and chromomycins bioproduction

Triplicates of BRA-384 strain were inoculated in Erlenmeyer flasks containing 250.0 mL of medium A1, kept under constant stirring at 170 rpm. The extractions were performed in the time intervals: 1 h (0.04 day) followed by 1, 3, 5, 7 and 9 days, with 200.0 mL of EtOAc under stirring at 130 rpm for 2 h. Some BRA-384 broths were filtered at day 1 using a 0.22 µm vacuum filtration system (Sarsted). These extractions of the bacteria-free broths were performed on the days 3, 5, 7 and 9. To determine the biomass dry weight, after the extraction process, the biomass-containing the growth medium was filtered on filter paper (Whatman) using a vacuum system and then dried in an oven at 80 °C for 40 min. The weight of the extracts and biomass were measured.

Cell lines, cell culture maintenance and cytotoxic assay

The 501-mel (human metastatic melanoma), MM200 (human melanoma) and HCT 116 (human colon adenocarcinoma) cells were grown in Roswell Park Memorial Institute medium (RPMI), while MCF-7 (human breast carcinoma), PC-3M (human metastatic prostate cancer), were grown in Dulbecco's modified eagle medium (DMEM), both media were supplemented with 10% fetal bovine serum (FBS), 1% penicillin (10,000 IU mL^{-1}) and streptomycin (10,000 µg mL^{-1}) antibiotics. Cells were kept in an incubator with 5% CO_2 at 37 °C and regularly split

to maintain them into exponential growth state. HCT 116 was used for the initial screening of the active extracts and for the bioguided fractionation of BRA-384 extract as well.

The antiproliferative activity was evaluated by the MTT (3-(4,5-dimethylthiazol-2-yl)-2,5-diphenyltetrazolium bromide) assay.[29] The cells were seeded on 96-well plates at a density of 1×10^4 (501-mel, MM200, HCT 116 and MCF-7) or 3×10^4 (PC-3M) *per* well with 200 µL culture medium. After 24 h, extracts and fractions (0.00064 to 50 µg mL^{-1}) or compounds **1**-**4** (0.016 to 1000 nM) were added to the cultures and incubated during 69 h. Dimethyl sulfoxide (DMSO, 0.05%) was used as negative control and the antineoplastic compound doxorubicin (0.64 to 10,000 nM) was used as positive control. After treatment, culture media were replaced by fresh media containing MTT solution (0.5 mg mL^{-1}) and incubated for additionally 3 h. The MTT solution was, then, removed and the plates dried at 35 °C for 30 min. The formazan product was solubilized in 150 µL of DMSO and the absorbance was read at 570 nm. The inhibition concentration means (IC_{50}) values and their 95% confidence intervals (CI 95%) were calculated by nonlinear regression of the normalized absorbance data to percentage of growth inhibition using GraphPad Prism 6.1 software.[30]

Supplementary Information

Supplementary information (experimental, NMR comparison of chromomycin, NMR spectra and HRESIMS of isolated compounds) is available free of charge at http://jbcs.sbq.org.br as PDF file.

Acknowledgments

The authors gratefully acknowledge financial support and fellowships from the National Council for Scientific and Technological Development (CNPq, Conselho Nacional de Desenvolvimento Científico e Tecnológico), grants Nos. 420454/2016-0 and 309060/2016-8, National Institute of Science and Technology (INCTBioNat), grant No. 465637/2014-0 and FAPESP (2015/17177-6, 2017/17648-4 and 2014/50926-0).

References

1. Aftab, U.; Zechel, D. L.; Sajid, I.; *Biol. Res.* **2015**, *48*, DOI 10.1186/s40659-015-0046-3.
2. Ramesh, S.; Aalbersberg, W.; *Microbiol. Res.* **2012**, *167*, 571.
3. Lu, Y.; Xing, Y.; Chen, C.; Lu, J.; Ma, Y.; Xi, T.; *Phytochem. Lett.* **2012**, *5*, 459.
4. Hu, Y.; Espindola, A. P. D. M.; Stewart, N. A.; Wei, S.; Posner, B. A.; MacMillan, J. B.; *Bioorg. Med. Chem.* **2011**, *19*, 5183.
5. Newman, D. J.; Cragg, G. M.; *J. Nat. Prod.* **2016**, *79*, 629.
6. Menéndez, N.; Nur-e-Alam, M.; Fischer, C.; Braña, A. F.; Salas, J.A.; Rohr, J.; Méndez, C.; *Appl. Environ. Microbiol.* **2006**, *72*, 167.
7. Menéndez, N.; Nur-e-Alam, M.; Braña, A. F.; Rohr, J.; Salas, J. A.; Méndez, C.; *Mol. Microbiol.* **2004**, *53*, 903; García, B.; González-Sabín, J.; Menéndez, N.; Braña, A. F.; Núñez, L. E.; Morís, F.; Salas, J. A.; Méndez, C.; *Microb. Biotechnol.* **2011**, *4*, 226.
8. Menéndez, N.; Nur-e-Alam, M.; Braña, A. F.; Rohr, J.; Salas, J. A.; Méndez, C.; *Chem. Biol.* **2004**, *11*, 21.
9. Lombó, F.; Menéndez, N.; Salas, J. A.; Méndez, C.; *Appl. Microbiol. Biotechnol.* **2006**, *73*, 1.
10. Pettit, G. R.; Tan, R.; Pettit, R. K.; Doubek, D. L.; Chapuis, J.-C.; Weber, C. A.; *RSC Adv.* **2015**, *5*, 9116.
11. Sun, L.; Zeng, J.; Cui, P.; Wang, W.; Yu, D.; Zhan, J.; *J. Biol. Eng.* **2018**, *12*, DOI 10.1186/s13036-018-0103-x.
12. Boer, D. R.; Canals, A.; Coll, M.; *Dalton Trans.* **2009**, 399.
13. Zihlif, M.; Catchpoole, D. R.; Stewart, B. W.; Wakelin, L. P. G.; *Cancer Genomics Proteomics* **2010**, *7*, 323.
14. Guimarães, L. A.; Jimenez, P. C.; Sousa, T. S.; Freitas, H. P. S.; Rocha, D. D.; Wilke, D. V.; Martín, J.; Reyes, F.; Pessoa, O. D. L.; Costa-Lotufo, L. V.; *Mar. Drugs* **2014**, *12*, 5839.
15. Pinto, F. C. L.; Almeida, J. G. L.; Silveira, E. R.; Costa, A. M.; Guimarães, L. A.; Wilke, D. V.; Costa-Lotufo, L. V.; Torres, M. C. M.; Pessoa, O. D. L.; *J. Braz. Chem. Soc.* **2017**, *28*, 485; Almeida, J. G. L.; Maia, A. I. V.; Wilke, D. V.; Silveira, E. R.; Braz-Filho, R.; La Clair, J. J.; Costa-Lotufo, L. V.; Pessoa, O. D. L.; *Mar. Drugs* **2012**, *10*, 2846; Wilke, D. V.; Jimenez, P. C.; Pessoa, C.; de Moraes, M. O.; Araujo, R. M.; da Silva, W. M. B.; Silveira, E. R.; Pessoa, O. D. L.; Braz-Filho, R.; Lopes, N. P.; Costa-Lotufo, L. V.; *J. Braz. Chem. Soc.* **2009**, *20*, 1455; Costa-Lotufo, L. V.; Carnevale-Neto, F.; Trindade-Silva, A. E.; Silva, R. R.; Silva, G. G. Z.; Wilke, D. V.; Pinto, F. C. L.; Sahm, B. D.; Jimenez, P. C.; Mendonça, J. N.; Lotufo, T. M. C.; Pessoa, O. D. L.; Lopes, N. P.; *Chem. Commun.* **2018**, *54*, 1952.
16. http://www.ncbi.nlm.nih.gov/, accessed in June 2019.
17. Miyamoto, M.; Kawamatsu, Y.; Kawashima, K.; Shinohara, M.; Tanaka, K.; Tatsuoka, S.; Nakanishi, K.; *Tetrahedron* **1967**, *23*, 421.
18. Toume, K.; Tsukahara, K.; Ito, H.; Arai, M. A.; Ishibashi, M.; *Mar. Drugs* **2014**, *12*, 3466.
19. Norio, S.; Eiji, H.; Takashi, S.; Mitsuko, A.; Kimiaki, M.; *Jpn. pat. 52102202* **1977**.
20. Oki, T.; Matsuzawa, Y.; Numata, K.; Takamatsu, A.; *J. Antibiot.* **1973**, *11*, 701.
21. Kawano, T.; Hidaka, T.; Furihata, K.; Mochizuki, J.; Nakayama, H.; Hayakawa, Y.; Seto, H.; *J. Antibiot.* **1990**, *43*, 110.
22. Garcia, G. D.; Gregoracci, G. B.; Santos, E. O.; Meirelles, P. M.; Silva, G. G. Z.; Edwards, R.; Sawabe, T.; Gotoh, K.; Nakamura, S.; Iida, T.; Moura, R. L.; Thompson, F. L.; *Microb. Ecol.* **2013**, *65*, 1076.

23. Heuer, H.; Krsek, M.; Baker, P.; Smalla, K.; Wellington, E. M. H.; *Appl. Environ. Microbiol.* **1997**, *63*, 3233.
24. Jiang, H.; Dong, H.; Zhang, G.; Yu, B.; Chapman, L. R.; Fields, M. W.; *Appl. Environ. Microbiol.* **2006**, *72*, 3832.
25. https://www.geneious.com, accessed in June 2019.
26. Katoh, K.; Misawa, K.; Kuma, K.; Miyata, T.; *Nucleic Acids Res.* **2002**, *30*, 3059.
27. Saitou, N.; Nei, M.; *Mol. Biol. Evol.* **1987**, *4*, 406.
28. Rambaut, A.; *FigTree*, version 1.4.2.; University of Edinburgh, UK, 2014. Available at http://tree.bio.ed.ac.uk/software/figtree/, accessed in June 2019.
29. Mosmann, T.; *J. Immunol. Methods* **1983**, *65*, 55.
30. *GraphPad Prism 6.1*; Intuitive Software for Science, San Diego, CA, 2015.

Submitted: February 13, 2019
Published online: June 25, 2019

This is an open-access article distributed under the terms of the Creative Commons Attribution License.

6. Chapter 2

Targeting the oncogenic TBX2 transcription factor with chromomycins.

frontiers in Chemistry

ORIGINAL RESEARCH
published: xx February 2020
doi: 10.3389/fchem.2020.00110

Targeting the Oncogenic TBX2 Transcription Factor With Chromomycins

*Bianca Del B. Sahm[1], Jade Peres[2], Paula Rezende-Teixeira[1], Evelyne A. Santos[2], Paola C. Branco[1], Anelize Bauermeister[1,3], Serah Kimani[4], Eduarda A. Moreira[3], Renata Bisi-Alves[2], Claire Bellis[2], Mihlali Mlaza[2], Paula C. Jimenez[5], Norberto P. Lopes[3], Glaucia M. Machado-Santelli[2], Sharon Prince[1,2] and Leticia V. Costa-Lotufo[1]**

[1] Department of Pharmacology, Institute of Biomedical Sciences, University of São Paulo, São Paulo, Brazil, [2] Division of Cell Biology, Department of Human Biology, University of Cape Town, Cape Town, South Africa, [3] Department of Cell and Developmental Biology, Institute of Biomedical Sciences, University of São Paulo, São Paulo, Brazil, [4] Department of Physics and Chemistry, School of Pharmaceutical Sciences, University of São Paulo, Ribeirao Preto, Brazil, [5] Department of Sea Sciences, Federal University of São Paulo, Santos, Brazil

The TBX2 transcription factor plays critical roles during embryonic development and it is overexpressed in several cancers, where it contributes to key oncogenic processes including the promotion of proliferation and bypass of senescence. Importantly, based on compelling biological evidences, TBX2 has been considered as a potential target for new anticancer therapies. There has therefore been a substantial interest to identify molecules with TBX2-modulatory activity, but no such substance has been found to date. Here, we adopt a targeted approach based on a reverse-affinity procedure to identify the ability of chromomycins A_5 (CA_5) and A_6 (CA_6) to interact with TBX2. Briefly, a TBX2-DNA-binding domain recombinant protein was N-terminally linked to a resin, which in turn, was incubated with either CA_5 or CA_6. After elution, bound material was analyzed by UPLC-MS and CA_5 was recovered from TBX2-loaded resins. To confirm and quantify the affinity (K_D) between the compounds and TBX2, microscale thermophoresis analysis was performed. CA_5 and CA_6 modified the thermophoretic behavior of TBX2, with a K_D in micromolar range. To begin to understand whether these compounds exerted their anti-cancer activity through binding TBX2, we next analyzed their cytotoxicity in TBX2 expressing breast carcinoma, melanoma and rhabdomyosarcoma cells. The results show that CA_5 was consistently more potent than CA_6 in all tested cell lines with IC_{50} values in the nM range. Of the cancer cell types tested, the melanoma cells were most sensitive. The knockdown of TBX2 in 501mel melanoma cells increased their sensitivity to CA_5 by up to 5 times. Furthermore, inducible expression of TBX2 in 501mel cells genetically engineered to express TBX2 in the presence of doxycycline, were less sensitive to CA_5 than the control cells. Together, the data presented in this study suggest that, in addition to its already recognized DNA-binding properties, CA_5 may be binding the transcription factor TBX2, and it can contribute to its cytotoxic activity.

Keywords: DNA-binding agents, T-box factors, reverse affinity, microscale thermophoresis

OPEN ACCESS

Edited by:
Enrica Calleri,
University of Pavia, Italy

Reviewed by:
Lingxin Chen,
Yantai Institute of Coastal Zone Research (CAS), China
Benjamin L. Oyler,
United States Food and Drug Administration, United States

****Correspondence:***
Leticia V. Costa-Lotufo
costalotufo@usp.br

Specialty section:
This article was submitted to Analytical Chemistry, a section of the journal Frontiers in Chemistry

Received: *22 September 2019*
Accepted: *05 February 2020*
Published: *xx February 2020*

Citation:
Sahm BDB, Peres J, Rezende-Teixeira P, Santos EA, Branco PC, Bauermeister A, Kimani S, Moreira EA, Bisi-Alves R, Bellis C, Mlaza M, Jimenez PC, Lopes NP, Machado-Santelli GM, Prince S and Costa-Lotufo LV (2020) Targeting the Oncogenic TBX2 Transcription Factor With Chromomycins. Front. Chem. 8:110. doi: 10.3389/fchem.2020.00110

INTRODUCTION

Traditionally, drug discovery and development (D&D) programs have made use of phenotypic approaches, which are characterized by observable changes in a disease model (animal or cellular). Advances in molecular biology and biochemistry, as well as the sequencing of the human genome, has enabled a more reductionist and rational approach to D&D. It has made possible the principle of targeting molecular drivers of diseases as well as increasing and improving approaches to targeting these molecules (Strausberg and Schreiber, 2003; Overington et al., 2006; Swinney and Anthony, 2011). In this context, designing targeted-based drug screening protocols with integrated strategies, is an attractive point to start drug discovery programs.

Affinity-based methods have gained attraction as innovative approaches to targeted oriented drug discovery. These involve the use of a molecular probe that is specifically designed to identify one or more target proteins from many others present in a complex cell lysate mixture. The identification and quantification of the isolated targets are ascertained by liquid-chromatography coupled to tandem mass spectrometry (LC-MS) (Rylova et al., 2015). Using the reverse of this approach, Lau et al. (2015) screened natural crude extracts for compounds with affinity for a specific biological protein that had previously been characterized and, hence, proposed as an important therapeutic target. Briefly, in this approach, the target protein was attached to an affinity resin, exposed to complex natural extracts and compounds that were bound to the protein were then detected by LC-MS.

The establishment of new targets in cancer therapy is a key step in the development of new effective therapies. In this realm, the transcription factor TBX2 overexpression has been directly linked to several cancers, including rhabdomyosarcoma (Zhu et al., 2016), breast (Jacobs et al., 2000; Redmond et al., 2010), melanoma (Vance et al., 2005; Peres et al., 2010), nasopharyngeal (Lv et al., 2017), and prostate cancers (Du et al., 2017). Indeed, TBX2 functions as a potent growth-promoting factor, in part due to its ability to bypass senescence and to repress key negative cell cycle regulators such as p14ARF, p21, and NDRG (Jacobs et al., 2000; Prince et al., 2004; Redmond et al., 2010). Furthermore, there is strong *in vitro* and *in vivo* biological evidence that TBX2 may be a novel target for anti-cancer drugs that can be administered on their own or in combination with other chemotherapies. Indeed, knocking down TBX2 in melanomas or in several metastatic breast cancer cell lines resulted, respectively, in induction of senescence or in a profound inhibition of proliferation, regardless of their receptor status (Peres et al., 2010; Wansleben et al., 2014). TBX2 also confers resistance to the widely used chemotherapeutic drug cisplatin by promoting p53 activity via Chk2, further leading to an S-phase arrest and DNA repair. Importantly, depleting TBX2 sensitizes cisplatin-resistant breast cancer and metastatic melanoma cells to this drug. These results suggest that TBX2 stimulates proliferation and inappropriate survival of cells with damaged DNA (Wansleben et al., 2013). Any drug that therefore impacts TBX2 expression or activity is likely to have a major impact on cancer progression and recurrence.

Natural products have provided an important source of bioactive molecules for clinical use. They are extensively used in the pharmaceutical industry as either drugs or in influencing the synthesis and semisynthesis of therapeutic molecules. Of particular importance, ∼60% of anti-cancer agents currently in the clinic are derived from natural products (Newman and Cragg, 2016). DNA-binding agents are the most common class of anticancer drugs. They function by interacting with DNA of dividing cells, resulting in DNA-damage and, thus, blocking transcription and replication that, ultimately, halts the cell cycle and/or activates cell death pathways. They can also inhibit enzymes that are important for the maintenance of DNA integrity such as topoisomerases. Chromomycins are tricyclic glycosylated polyketides belonging to the aureolic acid family, with promising anticancer activity and antiproliferative properties (Guimarães et al., 2014; Pettit et al., 2015; Pinto et al., 2019). These molecules bind to the DNA minor groove, causing DNA damage of treated cells, enhancing the expression of apoptosis related genes (Boer et al., 2009; Zihlif et al., 2010).

In this context, the present study employed a reverse affinity approach using the DNA-binding domain of the anticancer target TBX2 as bait to access the potential affinity of the marine chromomycins CA_5 and CA_6. Microscale thermophoresis was applied to quantify the binding affinities of the natural compounds, CA_5 and CA_6, to TBX2. Cytotoxicity of these compounds were determined in TBX2-driven breast carcinoma, melanoma, and rhabdomyosarcoma cell lines.

MATERIALS AND METHODS

Reagents

The isolation and characterization of chromomycins A_5 (CA_5) and A_6 (CA_6) was previously described by Pinto et al. (2019). The substances were resuspended in dimethyl sulfoxide (DMSO, Sigma Aldrich, USA). **Figure 1A** shows the chemical structure of CA_5 and CA_6.

Cell Culture

The human melanoma cells lines 501mel, MM200, and WM293a (kindly donated by Professor Dorothy Bennet, St George's University of London) were cultured in Roswell Park Memorial Institute Medium (RPMI)-1640 (Sigma Aldrich, USA). The human breast adenocarcinoma cell lines MCF-7 (ATCC® HTB-22) and T47D (ATCC® HTB-133) were cultured in Dulbecco's Modified Eagle medium:nutrient mixture F-12 (Ham) (DMEM/F-12) (Gibco by Thermo Fisher Scientific, USA). The human embryonal rhabdomyosarcoma cell line RD (ATCC® CCL-136) and the human alveolar rhabdomyosarcoma cell line RH30 (kindly provided by Professor Judith Davie, Southern Illinois University) were cultured in DMEM (Sigma Aldrich, USA). All culture medium was supplemented with 10% heat-inactivated fetal bovine serum (FBS), 100 U/mL penicillin and 100 µg/mL streptomycin. Cells were maintained at 37°C in a 5% CO_2 humidified incubator and medium was replaced every 2–3 days.

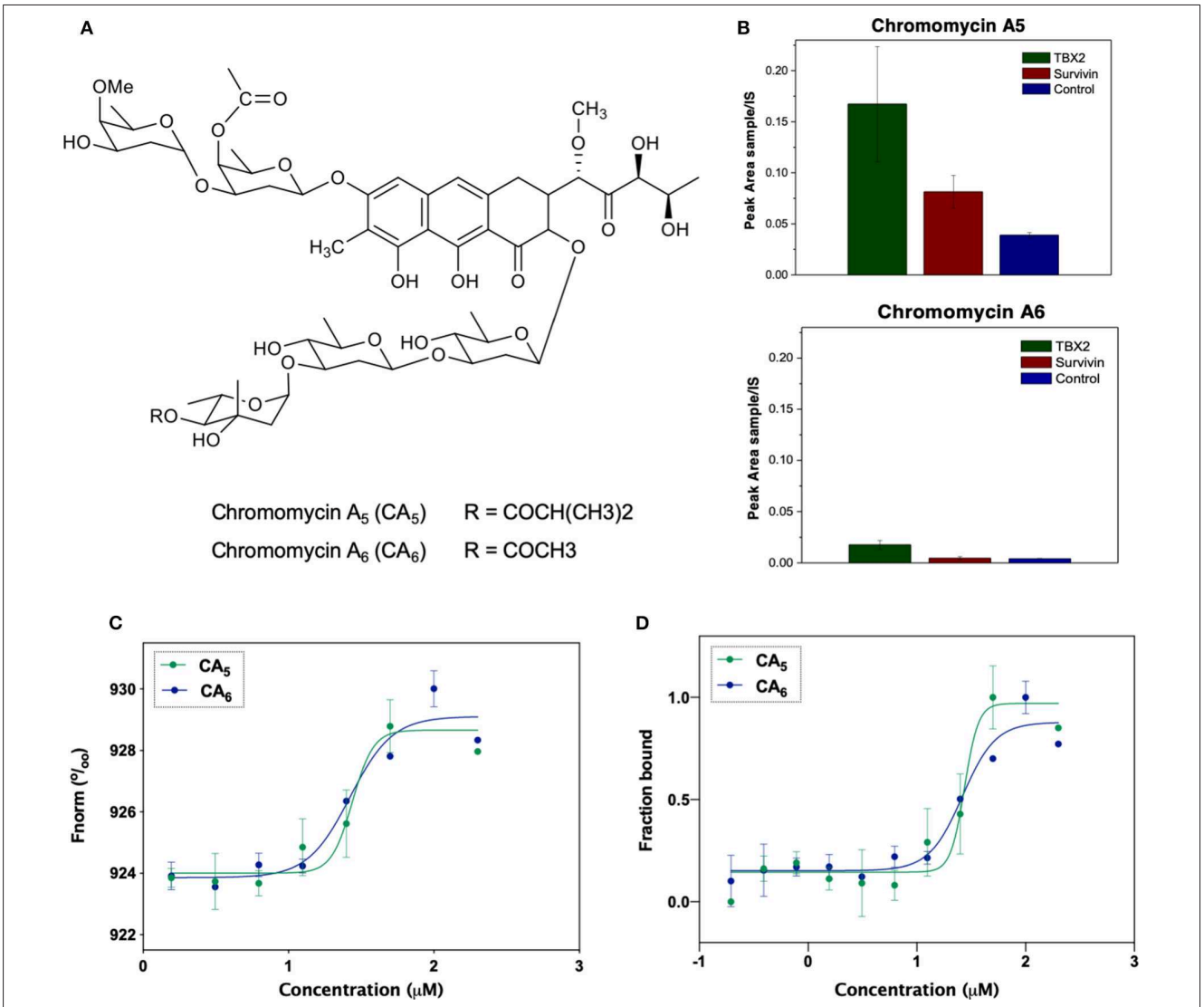


FIGURE 1 | (A) Chemical structures of the compounds used in the present study: chromomycin A_5 and chromomycin A_6. **(B)** Relative quantification of compounds chromomycin A_5 and chromomycin A_6 recovered from the bioaffinity chromatography technique using resins functionalized with TBX2 (green) or Survivin (red), or non-functionalized (control, blue) resin. The value of peak areas (triplicate) was used to construct the graphic. **(C)** Binding affinities of test compounds to TBX2 assessed through microscale thermophoresis. Normalized fluorescence of labeled TBX2 in the presence of serial concentrations of each of the test molecules. Data correspond to the mean values from two independent experiments. **(D)** Bound fraction of fluorescently labeled TBX2 with serial concentrations of each of the two chromomycins CA_5 and CA_6.

TBX2 Protein Expression and Purification

The coding region of the human TBX2 DNA binding domain (residues 94–287) was amplified by PCR and cloned into a pET28b vector between Nde1 and Xho1 restriction sites to generate an N-terminal His6-tagged sequence containing a thrombin cleavage site. The construct was verified by DNA sequencing. The pET28b-TBX294-287 plasmid was transformed into *Escherichia coli* strain BL21(DE3) and expression carried out at 37○C for 4 h, resulting in a 215-amino acid protein with a molecular weight of 24 kDa. The protein was purified by immobilized nickel affinity chromatography (GE Healthcare Life Sciences, USA); using HisTrap HP nickel affinity column (GE Healthcare Life Sciences, USA), with binding in a buffer containing 20 mM sodium phosphate buffer (pH 7.5), 500 mM NaCl and 50 mM imidazole and elution in the same buffer with a 50–300 mM imidazole gradient. The protein was further purified by size exclusion chromatography on a Superdex 200 column (GE Healthcare Life Sciences, USA) in a Reverse Affinity (RA) buffer containing 20 mM HEPES pH 7.4, 150 mM KCl, 1 mM $MgCl_2$, 2 mM β-mercaptoethanol (BME). Purity of the protein was verified by SDS-PAGE and protein concentration was determined using NANODROP 2000 system (Thermo Fisher Scientific, USA).

Survivin protein was included in the reverse-affinity chromatography assay as negative protein control. The survivin plasmid was obtained from Professor Eli Chapman (Department of Pharmacology and Toxicology, University of Arizona, USA), containing the full-length protein with an extra kanamycin-resistant histidine tail (His-tag). The plasmid was transformed into the *E. coli* strain BL21(DE3) and expression carried out at 16○C overnight. The survivin protein was purified as described for the TBX2 DNA binding domain. After removing the non-specific binders with wash buffer (lysis buffer + 2 mM BME) and complete astringent washing (50 mM Hepes pH 7.4, 1 M KCl, 5 mM $MgCl_2$, 2.5% glycerol in ddH_2O + 2 mM BME), elution buffer (50 mM Hepes pH 7.4, 150 mM KCl, 5 mM $MgCl_2$, 5% glycerol, 250 mM Imidazole in ddH_2O) was added. The protein was further purified overnight by dialysis using Spectra/Por dialysis membrane of 3.5 kD (Spectrum Labs Inc., USA) and dialysis buffer (20 mM Hepes pH 7.4, 150 mM KCl, 1 mM $MgCl_2$ in ddH_2O), then concentrated in Amicon Ultra-15 10 K (Merck-Millipore, USA) centrifuge filters at 4,000 rpm at 4○C. Purity of the protein was verified as described for TBX2 DNA binding domain.

Reverse Affinity Procedure

The samples obtained from the bioaffinity chromatography (triplicate) were solubilized with 0.5 mL of methanol containing 0.2 mg/mL of chlorogenic acid (3-caffeoylquinic acid) used as internal standard (IS). Samples were filtered in a small column (made in house on the tip of a Pasteur pipette) containing Sephadex LH-20 in order to remove the salt scraps from buffer. Filtered samples were analyzed by UPLC-MS/MS method on an Acquity TQD (WatersR Corporation, USA) instrument equipped with an ultra-performance liquid chromatography (UPLC) system coupled to a mass spectrometer fitted with an electrospray ionization source and a triple-quadrupole MS detector. Twenty microliter were injected into a Kinetex—Core-Shell Technology C18 column (100 A, 50 × 2.1 mm, 1.7 µm; Phenomenex, USA) kept at 40°C. The mobile phase consisted of deionized water (phase A) and methanol (phase B), both containing 0.2% of formic acid. The chromatographic condition applied was as follows: 5% phase B at 0 min, 100% phase B at 6 min, 100% phase B at 8 min, and 5% phase B at 10 min. The flow rate used was 0.2 mL/min. The ionization source conditions were as follows: 3.0 kV capillary voltage; 20 V cone voltage; 150°C source temperature; 300°C desolvation temperature; 500 L/h desolvation gas flow; 50 L/h cone gas flow. Data was acquired in positive ionization mode employing selected ion recording (SIR) mode. The peak area obtained for the compounds in each sample was normalized by the peak area of the IS in the same run, which allows the quantitative comparison between different sample (obtained from different proteins) for the same compound.

Microscale Thermophoresis

Binding affinities between target proteins and ligands were measured using microscale thermophoresis (MST) according to the NanoTemper technologies protocol in a Monolith NT.115 (Nanotemper Technologies, Germany) (Duhr and Braun, 2006). Proteins were fluorescently labeled using the Monolith Protein Labeling Kit RED-NHS 2nd Generation (Amine Reactive) (Nanotemper Technologies, Germany) according to the manufacturer's' instructions. The experiments were performed in three independent replicates using Monolith NT.115 Premium glass capillaries (Nanotemper Technologies, Germany) and driven in RA buffer with final concentration of 2% DMSO and 0.05% Tween 20. PCR microtubes were prepared with ligands and the target protein solutions. Ligand concentrations ranged from 10 nM to 400 µM while protein concentrations remained constant. After 5 min at room temperature, the samples were loaded into Premium glass capillaries and the experiments were performed using 20 and 40% MST power and between 20 and 80% LED power at 24°C. MST traces were recorded using the standard parameters: 5 s MST power off, 30 s MST power on and 5 s MST power off. The binding affinities of the compounds to the protein were determined according to with dissociation values (Kd) and the generated data were processed using MO. Control software (Nanotemper Technologies, Germany).

Western Blot Analyses

Rhabdomyosarcoma cells were lysed in whole cell lysis buffer (0.125 M Tris-HCl pH 6.8, 4% SDS, 0.2% glycerol, 0.1% BME, and a pinch of bromophenol blue) and boiled for 10 min and the remaining cell lines were lysed in RIPA buffer [50 mM Tris–HCl (pH 7.5), 150 mM NaCl, 0.1% NP-40, 0.5% sodium deoxycholate, 1 mM EDTA, and 2 mM EGTA] containing 1 mM sodium orthovanadate, 1 mM phenylmethylsulfonyl fluoride, 10 mg/ml leupeptin and 10 mg/ml aprotinin. Equal amounts of proteins were resolved by SDS-PAGE (12% gels) and transferred to Hybond ECL (Amersham Biosciences, UK) or nitrocellulose (Bio Rad Laboratories, USA) membranes. The membranes were incubated with goat polyclonal antibody to TBX2 (sc-17880) from Santa Cruz Biotechnology (USA) for rhabdomyosarcoma cells, or with rabbit polyclonal antibody to TBX2 (16930-1-AP) from Proteintech (USA) for melanoma and breast carcinoma cells. Mouse monoclonal antibody antiFlag M2 (F1804) from Sigma-Aldrich (USA) was used in the genetically engineered 501mel cells experiments. To control for loading, the rabbit polyclonal antibody to p38 MAPK (#9212) from Sigma-Aldrich (USA), or α-tubulin rabbit polyclonal antibody (#2144) or β-actin rabbit monoclonal antibody to (#4970) from Cell Signaling Technology (USA) were used. After incubation with primary antibodies, membranes were washed then incubated with HRP-conjugated secondary antibodies (#7074 Cell Signaling Technology, USA). Antibody reactive proteins were visualized by enhanced chemiluminescence using SuperSignal West Pico Chemiluminescent Substrate Kit (Thermo Fisher Scientific, USA) or WesternBright ECL HRP Substrate Kit (Advansta Company Inc., USA). Densitometry readings were obtained using UN-SCAN-IT gel 6.1 software (Silk Scientific, USA) and protein expression levels were represented as ratio signals for TBX2/respective loading control. All blots are representative of at least two independent repeats.

Cell Viability Assays

Cells were seeded in 96-well-plates and, in the following day, they were treated with a range of CA_5 and CA_6

concentrations or vehicle (1.0 µL DMSO) for 48 or 72 h. Cell viability was measured using the 3-(4,5-dimethylthiazol-2-yl)-2,5-diphenyl-trazolium bromide (MTT) assay (Invitrogen by Thermo Fisher Scientific, USA) (Mosmann, 1983). Mean cell viability was calculated as a percentage of the mean vehicle control. Three independent experiments were performed from which the half maximal inhibitory concentration (IC_{50}) and their respective 95% CI (confidence interval) were obtained by non-linear regression using GraphPad Prism version 8.0 (GraphPad Software, USA).

TBX2 Knockdown (shTBX2) 501mel Cells

To generate stably transfected cell lines in which TBX2 mRNA levels are knocked down (shTBX2), oligonucleotides targeting 5′-ACAGCTGAAGATCGACAACAA-3′ (TBX2 siRNA) of the human coding sequences was cloned into the pSuper.neo/GFP (Oligoengine) shRNA expression vector. The non-specific siRNA oligonucleotide (shControl) was directed against a 5′-ATTTCTCCGAACGTGTCACGT-3′ target sequence. 501mel cells were transfected with the pSuper.neo/GFP expression vector containing sequences targeted to TBX2 or the non-specific control using Transfectin® (BioRad, Hercules, CA). Four hundred microgram per milliliter of G418 disulfate salt (Sigma Aldrich, A1720) were used to maintain and select transfected cells (Webster and Dickson, 1983). Prior to experiments, cells were probed for TBX2 by Western blot to confirm protein knockdown relative to parental- and shControl-cell levels. Cytotoxicity of CA_5 was compared in these different 501mel cell models using the MTT assay following 72 h incubation. Therefore, three independent experiments were performed in duplicates from which the IC_{50} was obtained by non-linear regression using GraphPad Prism version 8.0 (GraphPad Software, USA).

FLAG-Tagged TBX2 (iTBX2) 501mel Cells—Rescue Experiments

501mel cells were genetically engineered to allow for inducible expression of 3XFLAG-tagged TBX2 (iTBX2) using a tetracycline-on (Tet-On) system (kindly provided by Professor Colin Goding, Ludwig Institute of Cancer, Oxford University, UK). TBX2 was induced using 60 ng/mL (135 nM) of doxycycline (Das et al., 2016). TBX2 was induced using 60 ng/mL (135 nM) of doxycycline either 12 h before, or 12 h following, drug treatments with CA_5. An iTBX2-empty cell line was used as an experimental control. Cells were exposed to serial concentrations of either drug, and the end point for both conditions was at 48 h after drug exposure. IC_{50} for cell models subjected to both experimental conditions and drug treatments were obtained using the MTT assay and calculated from three independent experiments performed in duplicates by non-linear regression using GraphPad Prism version 8.0 (GraphPad Software, USA).

RESULTS AND DISCUSSION

Chromomycins Directly Interact With the TBX2 DNA Binding Domain

Our group has been focused on screening and developing natural products with anticancer potential. In order to optimize and test new strategies in this field, we are currently applying the reverse affinity procedure as a tool to screen and guide the isolation of target-specific anticancer substances within crude bacterial

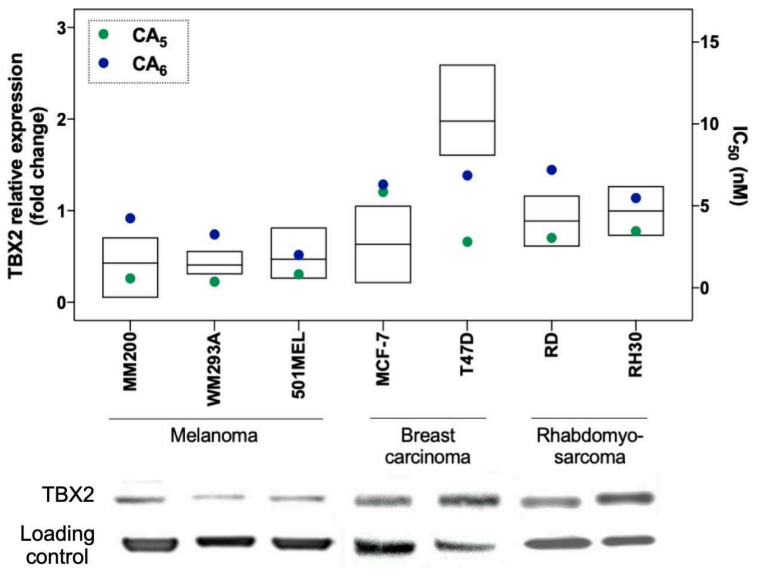


FIGURE 2 | Relative protein expression of TBX2 and cytotoxicity (IC_{50}) data in melanoma, breast cancer, and rhabdomyosarcoma cell lines. Protein expression levels are plotted in the left y axis as ratio signals for TBX2/respective loading control obtained from the densitometry readings using UN-SCAN-IT gel 6.1 software. Loading controls were obtained using α-tubulin for melanoma and breast carcinoma cells, and P-38 for sarcoma cells. IC_{50} values are represented in the right y axis and were obtained by the MTT assay cytotoxicity readings after 72 h exposure of drugs to the respective cell line and analyzed by non-linear regression using GraphPad Prism version 8.0 (GraphPad Software, USA) from three independent experiments performed in duplicate.

extracts. In this context, the oncogenic TBX2 transcription factor appears as an intriguing target due to its important pro-tumor roles and the fact that no known modulator was discovery so far. In fact, the DNA binding agent trabectedin (Yondelis®) was the first compound able to displace an oncogenic transcription factor from its target promoters with high specificity (D'Incalci et al., 2014). Moreover, a comparable cytotoxicity profile of trabectedin and chromomycin A_3, as assessed in the COMPARE analysis using data from NCI 60 cell line panel, point to a similar mechanism of action (Marco and Gago, 2005). Therefore, pondering on these evidences, we first attempted to verify whether the chromomycins A_5 and A_6–previously isolated by our group from a marine bacteria *Streptromyces* sp. BRA384—showed affinity to the TBX2 DNA binding domain.

The analyses of samples recovered from the reverse affinity procedure (**Figure 1B**) shows that both compounds displayed a residual binding to the resin itself and to either of the protein-loaded resins, however the recovery of CA_5 was increased by the presence of TBX2 linked to the resin. Although this technique has been described as a cost-effective procedure to identify binding compounds based on their affinity properties to a target protein (Lau et al., 2015), further analyses are necessary to validate the observed interactions. Actually, multiple unspecific interactions could be expected due to the ability of natural products to interact with proteins (Clardy and Walsh, 2004) and, moreover, binding to the target does not necessarily turn out in any biological modulation. Herein, we describe, for the first time, that this procedure can also be applied to screen modulators of transcription factors, such as the TBX2 DNA-binding domain as target.

In order to characterize the binding affinity between TBX2 and chromomycins, we used microscale thermophoresis (MST). This technique characterizes a ligand-binder interaction based on the movement of a given protein along a temperature gradient (thermophoresis), which, in turn, depends on its molecular size, charge and hydration shell. Once a ligand is bound to the protein, a distinct thermophoretic movement is expected due to a change in at least one of the above-mentioned parameters, and the information is compared between unbound and bound states (Wienken et al., 2010; Mueller et al., 2017). **Figure 1C** shows that CA_5 and CA_6 were able to change the thermophoretic movement of TBX2. The dissociation constants (K_D) for interactions were calculated for each chromomycin by measuring changes in the fluorescently labeled TBX2 by thermophoresis upon compound binding then normalizing and plotting this as a function of the ligand concentration (**Figure 1D**). The results suggest that CA_5 and CA_6 exhibit similar binding affinities to the TBX2 DNA-binding domain, with K_D of 31.3 ± 23.3 and 24.4 ± 13.6 μM, respectively.

Most of the available reports on this class of molecules regard the biological properties of CA_3 and, to a less extent, of CA_2. These chromomycins are, in turn, stereoisomers of CA_6 and CA_5, respectively, as demonstrated by Pinto et al. (2019) and Pettit et al. (2015). CA_3 binds to the minor groove of the DNA complex as a dimer in a process dependent on Mg^{+2}, in which a portion of the chromophore along with the D, E and F sugar moieties interact with residues of the minor groove, while the A and B sugar moieties and another portion

TABLE 1 | Cytotoxic activity of chromomycins A_5 (CA_5) and A_6 (CA_6) against different tumor cells.

Cell line	Compound IC_{50} (nM) 72 h (95% confidence interval)	
	CA_5	CA_6
MELANOMA		
501-mel	0.8 (0.6–1.0)	2.0 (1.6–2.4)
WM293A	0.3 (0.2–0.5)	3.2 (2.4–4.3)
MM200	0.5 (0.3–1.0)	4.2 (2.2–8.0)
BREAST CARCINOMA		
MCF-7	2.1 (1.8–2.5)	6.5 (5.0–8.4)
T47D	6.5 (5.1–8.9)	6.8 (2.8–16.3)
RHABDOMYOSARCOMA		
RD (Embryonal)	3.0 (2.8–3.3)	7.2 (5.6–8.8)
RH30 (Alveolar)	3.5 (3.3–3.6)	5.5 (3.6–7.3)

The compounds were incubated during 72 h, and cell viability was measured through the MTT assay. IC_{50} and the 95% confidence interval were obtained through non-linear regression using GraphPad Prism version 8.0.

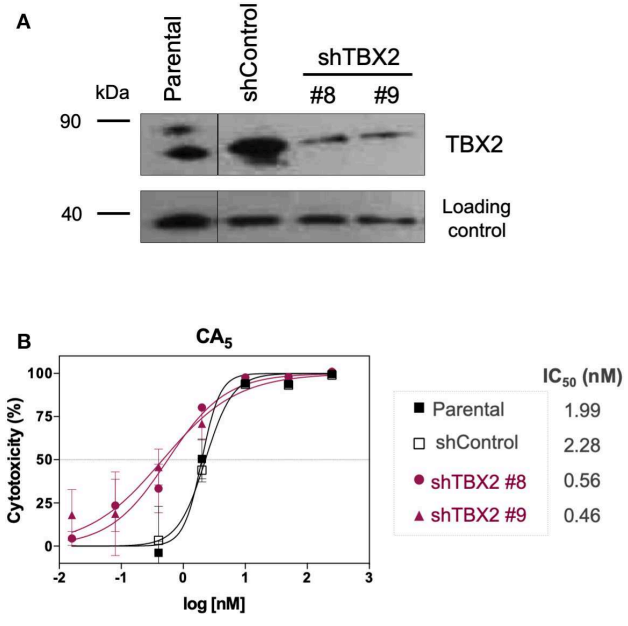


FIGURE 3 | Cytotoxicity of CA_5 on stably TBX2-knockdown cells (shTBX2). **(A)** TBX2 protein expression in parental, shControl and shTBX2 clones #8 and #9 501mel cell models, achieved by Western blot. **(B)** Cytotoxicity profiles of 501mel cell models exposed to CA_5. IC_{50} (nM) values for CA_5 in the 501mel cell models. Cytotoxicity curves and respective IC50 values we obtained by MTT assay, after cells were exposed to the respective drugs during 72 h and calculated by non-linear regression on GraphPad Prism 8.0 (GraphPad Software, USA) from three independent experiments performed in quadruplicate.

of the chromophore interact with the phosphate backbone (Gao and Patel, 1989; Boer et al., 2009). Moreover, studies on the interaction of CA_3 and DNA revealed an apparent affinity constant in the micromolar range (Behr et al., 1969; Aich et al., 1992). To the best of our knowledge, there is no data on the interaction of CA_5 and CA_6 with DNA. Nonetheless, the structural similarities among this class of compounds suggest that DNA-binding properties should be expected. Further studies are necessary to verify whether these molecules are directly binding to DNA and, furthermore, whether the interaction of TBX2 with DNA could be altered in the presence of chromomycins.

CA_5 Displays Potent Cytotoxicity Against Different TBX2-Driven Cancer Cell Lines

In order to characterize the anticancer activity of CA_5 and CA_6 in TBX2-driven cancers, we first assessed their cytotoxicity in melanoma, breast carcinoma and rhabdomyosarcoma cell lines. These cell lines were selected based on previous data showing that TBX2 plays an important role in their proliferation and survival (Peres et al., 2010; Wansleben et al., 2013; Zhu et al., 2016). Briefly, the cells were treated with a range of concentrations of CA_5 and CA_6, for 72 h followed by MTT assay. Regardless of the origin of the cancer, the IC_{50} values obtained for both compounds were in the nanomolar range but the IC_{50} values obtained for CA_5 were lower (**Figure 2** and **Table 1**). These results suggest that both chromomycins are highly cytotoxic and that CA_5 was more potent than CA_6 in this cell panel (**Table 1**). It is worth noting that, among the cell lines tested, those derived from melanomas were the most sensitive to both chromomycins. Indeed, the IC_{50} values obtained for the melanoma cell lines ranged from 0.3 to 0.8 nM for CA_5 and from 2.0 to 4.2 nM for CA_6. **Figure 2** shows data where the relative levels of basal TBX2 in all cell lines tested were plotted against IC_{50} values for CA_5 and CA_6. The results show that the T47D cells showed slightly higher levels of TBX2 and there is no significant correlation between IC_{50} values and TBX2 levels.

Other chromomycins were previously reported for their anticancer activities with similar potencies as those described here. Indeed, Toume et al. (2014) reported that CA_2 (a stereoisomer of CA_5) and CA_3 (a stereoisomer of CA_6) are cytotoxic against a human gastric adenocarcinoma cell line, with IC_{50} values ranging from 1.7 to 22.1 nM. Pettit et al. (2015) also assessed the cytotoxicity of CA_5 against a mini-panel of human cancer cell lines and found IC_{50} values ranging from 0.6 (MCF-7) to 3.4 nM (KM20L2, colon cancer cell). An earlier investigation from our group also evaluated the cytotoxicity of CA_2 against a panel of tumor cells from different origins, including colon, prostate, leukemia and melanoma. Consistent with the current study, we showed that the melanoma cells were among the most sensitive to CA_2. However, CA_2 had an IC_{50} of 18.8 nM in the metastatic melanoma cell line Malme-3M and was thus less cytotoxic than the CA_5 and CA_6 chromomycins tested in this study against melanoma cells (Guimarães et al., 2014). Furthermore, a recent study from our group compared the cytotoxicity of 4 different chromomycins in a 5 human tumor cell line panel and showed that CA_5 was the most potent, especially against the MM200 (IC_{50} of 0.2 nM) and 501Mel (IC_{50} of 0.8 nM) melanoma cells (Pinto et al., 2019).

To investigate whether CA_5 exerts its cytotoxicity, in part, through binding TBX2, we firstly tested the effect of

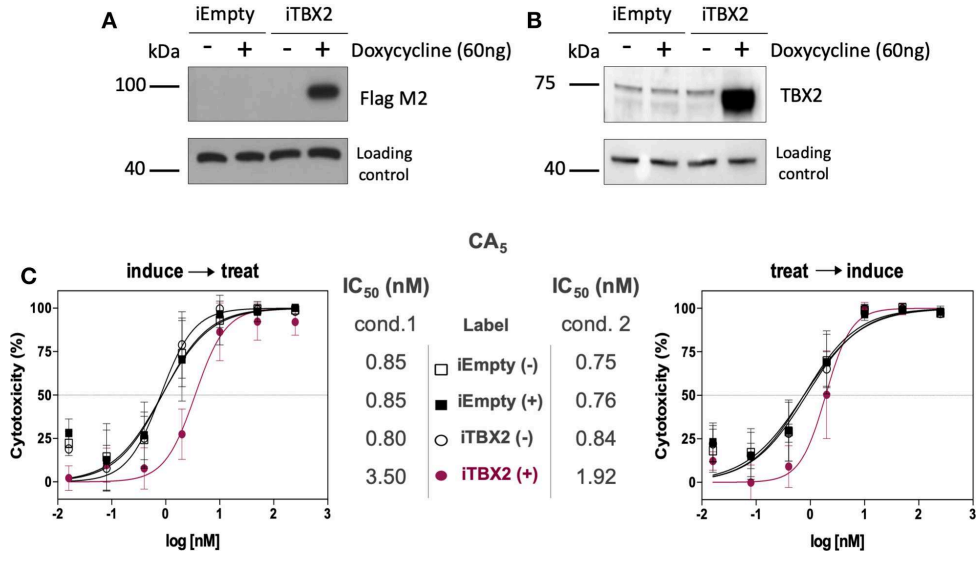


FIGURE 4 | Cell viability assay (MTT) of CA_5 in 501mel cells with induced and non-induced TBX2-overexpression. **(A,B)** Western blot membranes of samples from iEmpty and iTBX2 cells, without (–) and with (+) 60 ng/mL doxycycline, showing that only iTBX2 (+) is inducing TBX2 overexpression; A—probed for anti-Flag M2; B—probed for anti-TBX2. **(B)** CA_5 cytotoxicity profiles and respective IC_{50} (nM) values accessed under cond.1 and cond.2 after 48 h drug exposure. IC_{50} values were obtained by non-linear regression using GraphPad Prism version 8.0 (GraphPad Software, USA) from three independent experiments performed in duplicate. Cond.1, experiment setup where induction of TBX2 expression was done before drug treatment; Cond.2, experiment setup where drug treatment was done prior to TBX2 induction.

knocking down TBX2 on the sensitivity of 501mel cells to the chromomycin. Results from MTT assays show that depleting TBX2 reduced the IC_{50} of CA_5, by at least 4 times in 501mel cells (**Figure 3**).

Furthermore, when TBX2 expression was induced (iTBX2) in 501mel cells genetically engineered to express TBX2 in the presence of doxycycline for 12 h prior to CA_5 treatment for 48 h, the cells were more resistant to the drug (**Figure 4A**). When the same experiment was carried out but TBX2 was induced for the last 12 h of CA_5 treatment, the cells were also more resistant to CA_5 when compared to their iTBX2-empty counterparts (**Figure 4B**). Indeed, the IC_{50} values increased by 7 times (from 0.6 to 4.2 nM) when TBX2 was induced prior to CA_5 treatment and by 1.8 times (from 0.8 to 1.4 nM) when TBX2 was induced post CA_5 treatment (**Figure 4B**). The induction of TBX2 prior to exposure to CA_5 thus produced a greater resistance response in TBX2-expressing cells.

Taking together, the evidences herein suggest that TBX2 is indeed conferring resistance to these drugs, as observed to cisplatin (Davis et al., 2008; Wansleben et al., 2013). Although these findings point to a direct association between TBX2 levels and CA_5 cytotoxicity, the previously observed relation between TBX2 and DNA repair pathways (Wansleben et al., 2013) should also be taken in account to explain the increased toxicity observed in TBX2-knockdown cells.

In summary, CA_5 and CA_6 displayed high levels of cytotoxicity at relatively low concentrations against all TBX2-driven cancer cell lines tested. Taken together, the evidences generated in the present study through reverse affinity chromatography, and MST assays, then pondered with data from the literature, suggest that, beyond the already established DNA-damaging effects, chromomycins, and especially CA_5, bind TBX2 and its modulation may contribute to the observed cytotoxic properties of this group of molecules.

DATA AVAILABILITY STATEMENT

The datasets generated for this study are available on request to the corresponding author.

AUTHOR CONTRIBUTIONS

All authors listed have made a substantial, direct and intellectual contribution to the work, and approved it for publication.

FUNDING

This work was funded by Fundação de Amparo à Pesquisa do Estado de São Paulo (FAPESP) process # 2015/17177-6; 2018/08400-1; 2019/02008-5; 2018/24865-4; and 2017/09022-8; Conselho Nacional de Desenvolvimento Científico e Tecnológico (CNPq, LC-L and GM-S are CNPq researcher fellows); Coordenação de Aperfeiçoamento de Pessoal de Nível Superior (CAPES) and ArboControl Brasil Project (FNS/UnB TED74/2016 and TED42/2017).

ACKNOWLEDGMENTS

We are grateful to Dr. Otilia Pessoa for the supply of chromomycins A_5 and A_6 and, also, to Helori Vanny Domingos and Simone Aparecida Teixeira for technical assistance. We further thank the National Laboratory of Biosciences (LNBIO-CNPEM, Campinas, São Paulo) for making available their facilities, and finally, Dr. Daniel Maturana for valuable discussions.

REFERENCES

Aich, P., Sen, R., and Dasgupta, D. (1992). Role of magnesium ion in the interaction between chromomycin A3 and DNA: binding of chromomycin A3-Mg2+ complexes with DNA. *Biochemistry* 31, 2988–2997. doi: 10.1021/bi00126a021

Behr, W., Honikel, K., and Hartmann, G. (1969). Interaction of the RNA polymerase inhibitor chromomycin with DNA. *Eur. J. Biochem.* 9, 82–92. doi: 10.1111/j.1432-1033.1969.tb00579.x

Boer, D. R., Canals, A., and Coll, M. (2009). DNA-binding drugs caught in action: the latest 3D pictures of drug-DNA complexes. *Dalton. Trans.* 3, 399–414. doi: 10.1039/B809873P

Clardy, J., and Walsh, C. (2004). Lessons from natural molecules. *Nature* 432, 829–837. doi: 10.1038/nature03194

Das, A. T., Tenenbaum, L., and Berkhout, B. (2016). Tet-On Systems for doxycycline-inducible gene expression. *Curr. Gene. Ther.* 16, 156–167. doi: 10.2174/1566523216666160524144041

Davis, E., Teng, E., Bilican, B., Parker, M. I., Liu, B., Carriera, S., et al. (2008). Ectopic Tbx2 expression results in polyploidy and cisplatin resistance. *Oncogene* 27, 976–984. doi: 10.1038/sj.onc.1210701

D'Incalci, M., Badri, N., Galmarini, C. M., and Allavena, P. (2014). Trabectedin, a drug acting on both cancer cells and the tumor microenvironment. *Br. J. Cancer.* 111, 646–650. doi: 10.1038/bjc.2014.149

Du, W. L., Fang, Q., Chen, Y., Teng, J. W., Xiao, Y. S., Xie, P., et al. (2017). Effect of silencing the T Box transcription factor TBX2 in prostate cancer PC3 and LNCaP cells. *Mol. Med. Rep.* 16, 6050–6058. doi: 10.3892/mmr.2017.7361

Duhr, S., and Braun, D. (2006). Why molecules move along a temperature gradient. *Proc. Natl. Acad. Sci. U.S.A.* 103, 19678–19682. doi: 10.1073/pnas.0603873103

Gao, X., and Patel, D. J. (1989). Solution structure of the Chromomycin-DNA complex. *Biochemistry* 28, 751–762. doi: 10.1021/bi00428a051

Guimarães, L. A., Jimenez, P. C., Sousa, T. D. S., Freitas, H. P. S., Rocha, D. D., Wilke, D. V., et al. (2014). Chromomycin A2 induces autophagy in melanoma cells. *Mar. Drugs* 12, 5839–5855. doi: 10.3390/md12125839

Jacobs, J. J. L., Keblusek, P., Robanus-Maandag, E., Kristel, P., Lingbeek, M., Nederlof, P. M., et al. (2000). Senescence by-pass screen identifies TBX2, which represses Cdkn2a (p19ARF) and is amplified in a subset of human breast cancers. *Nat. Genet.* 26, 291–299. doi: 10.1038/81583

Lau, E. C., Mason, D. J., Eichhorst, N., Engelder, P., Mesa, C., Kithsiri-Wijeratne, E. M., et al. (2015). Functional chromatographic technique for natural product isolation. *Org. Biomol. Chem.* 13, 2255–2259. doi: 10.1039/c4ob02292k

Lv, Y., Si, M., Chen, N., Li, Y., Ma, X., Yang, H., et al. (2017). TBX2 over-expression promotes nasopharyngeal cancer cell proliferation and invasion. *Oncotarget* 8, 52699–52707. doi: 10.18632/oncotarget.17084

Marco, E., and Gago, F. (2005). DNA structural similarity in the 2:1 complexes of the antitumor drugs trabectedin (yondelis) and chromomycin A3 with an oligonucleotide sequence containing two adjacent TGG binding sites on opposing strands. *Mol. Pharm.* 68, 1559–1567. doi: 10.1124/mol.105.015685

Mueller, A. M., Breitsprecher, D., Stefan, D., Philipp, B., Schubert, T., and Längst, G. (2017). "Chapter 10 – MicroScale thermophoresis: a rapid and precise method to quantify protein-nucleic acid interactions in solution," in *Functional Genomics: Methos and Protocols, Methods in Molecular Biology, Vol. 1654,*

eds M. Kaufmann, et al. (Springer Science+Business Media, LLC), 151–164. doi: 10.1007/978-1-4939-7231-9_10

Newman, D. J., and Cragg, G. M. (2016). Natural products as sources of new drugs from 1981 to 2014. *J. Nat. Prod.* 79, 629–661. doi: 10.1021/acs.jnatprod.5b01055

Overington, J. P., Al-Lazikani, B., and Hopkins, A. L. (2006). How many drug targets are there? *Nat. Rev. Drug Discov.* 5, 993–996. doi: 10.1038/nrd2199

Peres, J., Davis, E., Mowla, S., Bennett, D. C., Li, J. A., Wansleben, S., et al. (2010). The highly homologous T-Box transcription factors, TBX2 and TBX3, have distinct roles in the oncogenic process. *Genes Cancer* 1, 272–282. doi: 10.1177/1947601910365160

Pettit, G. R., Tan, R., Pettit, R. K., Doubek, D. L., Chapuisa, J. C., and Webera, C. A. (2015). Antineoplastic agents 596. isolation and structure of chromomycin A5 from a Beaufort Sea microorganism. *RSC Adv* 5, 9116–9122. doi: 10.1039/C4RA16517A

Pinto, F. C. L., Silveira, E. R., Vasconcelos, A. C. L., Florêncio, K. G. D., Oliveira, F. A. S., Sahm, B. D. B., et al. (2019). Dextrorotatory chromomycins from the marine *Streptomyces* sp. associated to *Palythoa caribaeorum*. *J. Braz. Chem. Soc.* 31, 1–10. doi: 10.21577/0103-5053.20190144

Prince, S., Carreira, S., Vance, K. W., Abrahams, A., and Goding, C. R. (2004). Tbx2 directly represses the expression of the p21(WAF1) cyclin-dependent kinase inhibitor. *Cancer Res.* 64, 1669–1674. doi: 10.1158/0008-5472.can-03-3286

Redmond, K. L., Crawford, N. T., Farmer, H., D'Costa, Z. C., O'Brien, G. J., Buckley, N. E., et al. (2010). T-box 2 represses NDRG1 through an EGR1-dependent mechanism to drive the proliferation of breast cancer cells. *Oncogene* 29, 3252–3262. doi: 10.1038/onc.2010.84

Rylova, G., Ozdian, T., Varanasi, L., Soural, M., Hlavac, J., Holub, D., et al. (2015). Affinity-based methods in drug-target discovery. *Curr. Drug Targets.* 16, 60–76. doi: 10.2174/1389450115666141120110323

Strausberg, R. L., and Schreiber, S. L. (2003). From knowing to controlling: a path from genomics to drugs using small molecule prodes. *Science* 300, 294–295. doi: 10.1126/science.1083395

Swinney, D. C., and Anthony, J. (2011). How were new medicines discovered? *Nat. Rev. Drug Discov.* 10, 507–519. doi: 10.1038/nrd3480

Toume, K., Tsukahara, K., Ito, H., Arai, M. A., and Ishibashi, M. (2014). Chromomycins A2 and A3 from marine actinomycetes with TRAIL resistance-overcoming and Wnt signal inhibitory activities. *Mar. Drugs* 12, 3466–3476. doi: 10.3390/md12063466

Vance, K. W., Carreira, S., Brosch, G., and Goding, C. R. (2005). Tbx2 is overexpressed and plays an important role in maintaining proliferation and suppression of senescence in melanomas. *Cancer Res.* 65, 2260–2268. doi: 10.1158/0008-5472.CAN-04-3045

Wansleben, S., Davis, E., Peres, J., and Prince, S. (2013). A novel role for the anti-senescence factor TBX2 in DNA repair and cisplatin resistance. *Cell Death. Dis.* 4:e846. doi: 10.1038/cddis.2013.365

Wansleben, S., Peres, J., Hare, S., Goding, C. R., and Prince, S. (2014). T-box transcription factors in cancer biology. *Biochim. Biophys. Acta.* 1846, 380–391. doi: 10.1016/j.bbcan.2014.08.004

Webster, T. D., and Dickson, R. C. (1983). Direct selection of saccharomyces cerevisiae resistant to antibiotic G418 following transformation with a DNA vector carrying the kanamycin-resistance gene of Tn903. *Gene.* 26, 243–252. doi: 10.1016/0378-1119(83)90194-4

Wienken, C. J., Baaske, P., Rothbauer, U., Braun, D., and Duhr, S. (2010). Protein-binding assays in biological liquids using microscale thermophoresis. *Nat. Commun.* 1:100. doi: 10.1038/ncomms1093

Zhu, B., Zhang, M., Williams, E. M., Keller, C., Mansoor, A., and Davie, J. K. (2016). TBX2 represses PTEN in rhabdomyosarcoma and skeletal muscle. *Oncogene* 35, 4212–4224. doi: 10.1038/onc.2015.486

Zihlif, M., Catchpoole, D. R., Stewart, B. W., and Wakelin, L. P. G. (2010). Effects of DNA minor groove binding agents on global gene expression. *Cancer Genomics Proteomics* 7, 323–330.

Conflict of Interest: The authors declare that the research was conducted in the absence of any commercial or financial relationships that could be construed as a potential conflict of interest.

Copyright © 2020 Sahm, Peres, Rezende-Teixeira, Santos, Branco, Bauermeister, Kimani, Moreira, Bisi-Alves, Bellis, Mlaza, Jimenez, Lopes, Machado-Santelli, Prince and Costa-Lotufo. This is an open-access article distributed under the terms of the Creative Commons Attribution License (CC BY). The use, distribution or reproduction in other forums is permitted, provided the original author(s) and the copyright owner(s) are credited and that the original publication in this journal is cited, in accordance with accepted academic practice. No use, distribution or reproduction is permitted which does not comply with these terms.

7. Chapter 3

Antitumor characterization of chromomycin A_5 in TBX2-driven melanoma cells

Antitumor characterization of chromomycin A_5 in TBX2-driven melanoma cells

Bianca Del B. Sahm[1,2], Jade Peres[2], Francisco das Chagas L. Pinto[3], Otilia D.L. Pessoa[3], Paula C. Jimenez[1,4], Glaucia M. Machado-Santelli[5], Sharon Prince[1,2], Leticia V. Costa-Lotufo[1]

[1] Department of Pharmacology, Institute of Biomedical Sciences, University of São Paulo, São Paulo – SP, Brazil;
[2] Division of Cell Biology, Department of Human Biology, University of Cape Town, Cape Town, South Africa;
[3]Department of Organic and Inorganic Chemistry, Federal University of Ceara, Ceara, Brazil;
[4]Department of Sea Sciences, Federal University of São Paulo, Santos – SP, Brazil;
[5]Department of Developmental and Cellular Biology, Institute of Biomedical Sciences, University of São Paulo, São Paulo – SP, Brazil;.

Manuscript under preparation to be submitted for publication

Abstract

The TBX2 transcription factor have been described to play important oncogenic functions in several types of cancer, including melanoma. It is known that its expression in melanoma cells favor the proliferation and confers resistance to DNA-alkylating agents. Therefore, finding molecules with potential to inhibit TBX2 functions figures as a new anticancer strategy. We previously demonstrate that chromomycin A_5 (CA_5) was recovered from a reverse affinity procedure using the TBX2 recombinant protein as a magnet. Further studies reveal that CA_5 and TBX2 present binding affinities and that different levels of TBX2 in a melanoma cell line reveals different patterns in CA_5 cytotoxicity. In the present study, we go deeper in understanding the relationship between CA_5 cytotoxicity, damage DNA generation and its involvement in the TBX2 pathway on a TBX2-driven melanoma cell line. Studies were compared with the well know chemotherapy doxorubicin (DOX) and chromomycin A_6 (CA_6). The results found herein suggest that DNA damage is not the only mechanism of action played by CA_5, where repair-signaling pathways has been

activated in low concentrations. Moreover, we also found that low doses of CA_5, under specific conditions, up-regulates protein and mRNA levels of TBX2 target genes. Finally, we discuss some aspects of the mechanism of action described to DNA minor-groove binders' molecules and suggest that CA_5 has the potential to be playing its cytotoxicity effects due interferences in the TBX2 transcriptional activity.

Keywords: Chromomycins; T-box Factors; TBX2; melanoma; anticancer; target-therapy.

Introduction

TBX2 is a transcription factor belonging to T-box genes family which are importantly during embryonic development but do not have recognized functions in adult tissues (NAICHE et al, 2005; WOJAHN et al., 2019). In the last decades, the overexpression of TBX2 have been linked with several types of cancer, including melanomas (CARREIRA; LIU; GODING, 2000; VANCE et al., 2005; CHEN et al., 2016; BADAL et al., 2017). The roles that this transcription factor plays in cancer cells have been extensively studied. There is strong evidence to suggest that TBX2 is implicated in key carcinogenesis processes such as tumor cell immortality and proliferation, tumorigenesis, invasion and metastasis through inducing epithelial to mesenchymal (EMT) process, and resistance to anticancer chemotherapeutics (JACOBS et al., 2000; PRINCE et al 2004; DAVIS et al., 2008; ABRAHAMS et al., 2010; WANSLEBEN et al., 2013; CHANG et al., 2016). Such evidences characterize TBX2 as a new potential anticancer target.

In this direction, we have recently described a target-oriented screening procedure aiming the identification of natural small molecules with potential to interact with TBX2. We identified that molecules from the aureolic acid family, chromomycin A_5 (CA_5) and A_6 (CA_6), bound to TBX2 DNA-binding domain with KD in micromolar range (SAHM et al., 2020). Importantly, CA_5 is a rare chromomycin that have been poorly studied regarding its biological activity (PETTIT et al., 2015; PINTO et al., 2019) and was recovered in greater amounts from the TBX2-interaction screening. We thus tested CA_5 in a melanoma cell models with either TBX2 overexpression or depleted levels. We found that, in both cases, the level of TBX2 protein expression interfered in the cytotoxic activity of CA_5, but we could not

conclude whether CA_5 is operating its anticancer properties through interaction with TBX2 functions (SAHM et al., 2020).

Importantly, chromomycins are in general described as glycosylated DNA-binders where a dimer formed by two molecules interacting directly with residues in the DNA minor groove (BOER; CANALLS; COLL, 2009). Such interaction can cause severe DNA-damage and activates the DNA-repair cell system (NORBURY; HICKSON, 2001). The chemotherapeutic resistance function described to TBX2 is related to its participation in the ATM-TBX2-ChK2 cascade, which in turn is responsible for stopping the cell cycle after detected DNA damage and directing the cell to repair or death (WANSLEBEN et al., 2014; ZANNINI; DELIA; BUSCEMI, 2014). Therefore, the overexpression of TBX2 in cancer cells would be favoring the resistance against DNA alkylating agents (like chromomycins) through strengthening the DNA damage and repair signaling system.

In the present study, we intensified the investigation on CA_5 bioactivity in a metastatic melanoma cell line in which TBX2 is known as an important proliferative factor (PERES et al., 2010) and also conferring resistance to chemotherapeutic agents (WANSLEBEN et al., 2014). We lead our efforts to better characterize the extension of the DNA damage generated by CA_5 in these cells and additional experiments were developed aiming at a better understanding of the participation and possible modulation of TBX2 functions in the cytotoxicity properties played by this natural molecule.

Materials and Methods

Cell culture

Human 501mel metastatic melanoma cells and 501mel cells genetically engineered to inducible express 3XFLAG-tagged TBX2 using a tetracycline-on (Tet-On) system (kindly provided by Professor Colin Goding, Ludwig Institute of Cancer, Oxford University, UK) were maintained in Roswell Park Memorial Institute Medium (RPMI)-1640 (Sigma Aldrich, Missouri, USA) supplemented with 10% heat-inactivated fetal bovine serum (FBS), 100 U/ml penicillin and 100 µg/ml streptomycin (+ 400 µg/mL of G418 disulfate salt - Sigma Aldrich, Missouri, USA - catalogue no. A1720 - for vector selection in 3XFLAG-tagged cells). Culture medium were replaced every 3 days.

Cells were maintained at 37 °C in an atmosphere of 95% air/5% CO2, 65% humidity. Medium was replaced every 2 to 3 days and cells were routinely subjected to mycoplasma tests. Only mycoplasma free cells were used in experiments. Cell morphology was monitored using an Olympus CKX41 inverted microscope (MSAC Ltd, UK) and imaged with an EVOS™ XL AMEX1000 Core Imaging System (Thermo Fisher Scientific, Massachusetts, USA).

Generation of 501mel stable cell lines with TBX2 knockdown (shTBX2)

The generation of shTBX2 and shControl 501mel stable cell lines were performed as previously described (SAHM et al., 2020). Cells were maintained in RPMI culture medium supplemented with 10% FBS, 1% antibiotics and 400 µg/mL of G418 disulfate salt (Sigma Aldrich, Missouri, USA - catalogue no. A1720) for vector selection. Culture medium were replaced every 3 days.

Cell treatments

The isolation and characterisation of chromomycin A_5 (CA_5) and A_6 (CA_6) were previously described (Pinto et al., 2019). CA_5, CA_6 and Doxorubicin (DOX; Sigma-Aldrich, USA) were dissolved in dimethyl sulfoxide (DMSO, D8418, Sigma-Aldrich, USA) to give stocks of 50µM, 2 µM, 1 µM or 0.5 µM for C-A_5, 50 µM or 2 µM for C-A_6 and 2 mM or 200 µM for DOX. All stock solutions were stored at -20 °C. All drugs were diluted in cell culture medium to achieve the desired final concentration and a vehicle control (DMSO) of the same concentration was prepared simultaneously.

Cell viability assays

Cells were seeded in 96-well plates and treated the next day with a range of concentrations of CA_5 (0.016 nM – 250 nM), CA_6 (0.016 nM – 250 nM), DOX (2.8 nM - 45 µM) or with an equivalent volume of vehicle (DMSO) for 48 or 72 h. Cell viability was measured using the 3-(4,5-dimethylthiazol-2-yl)-2,5-diphenyl-trazolium bromide (MTT) assay (11465007001, Sigma-Aldrich, USA) according to the manufacturer's instructions. Mean cell viability was calculated as a percentage of the mean vehicle control. At least two independent experiments in duplicate were performed from which the half maximal inhibitory concentration (IC_{50}) was determined using GraphPad Prism version 6.0 (GraphPad Software, California, USA).

FLAG-Tagged TBX2 (iTBX2) 501mel cells – rescue experiments

Experiments with genetically engineered 501mel cell for inducible expression of 3XFLAG-tagged TBX2 (iTBX2) were performed as described before (SAHM et al., 2020). Condition 1 - 12 h pre-induction of iTBX2 followed by drug treatments with DOX. Condition 2 - 12 h drug treatments with DOX followed by induction od iTBX2. The end point for both conditions was at 48 h after drug exposure. IC50 obtained by MTT assay and calculated from three independent experiments performed in duplicates by non-linear regression using GraphPad Prism v.6.0 (GraphPad Software, USA).

TBX2 Protein Expression and Purification

The expression and purification of TBX2 and survivin recombinant proteins were performed as described before (SAHM et al., 2020).

Reverse affinity procedure

Samples from bioaffinity chromatography (reverse affinity procedure) were obtained and analysed as described before (SAHM et al., 2020).

Microscale thermophoresis

The binding affinity analysis of DOX and TBX2 recombinant protein was measured by microscale thermophoresis (MST) under conditions previously described (SAHM et al., 2020). For experiments carried with TBX2 double-strand DNA sequence, Cy5-labelled DNA sequence (5'-/5Cy5/GGCCAGCTGAGGTGTGAGCAGCTGCCG-3' - 3'-CCGGTCGACTCCACACTCGTCGACGGC-5') was obtained by IDT, Inc (Integrated DNA Technologies, USA, reference #: 193081841). Binding affinities between DNA and ligands (DOX and CA_5) were measured by MST according to NanoTemper technologies protocol in a Monolith NT.115 (Nanotemper Technologies, Germany). The experiments were performed in at least two independent replicates using NT.115 premium glass capillaries (Nanotemper Technologies, Germany) and driven in RA buffer containing 20 mM HEPES pH 7.4, 150 mM KCl, 1 mM $MgCl_2$ with final concentration of 2% DMSO and 0.05% Tween 20. Ligand concentrations ranged from 0.3 nM to 10 µM for CA_5 and from 0.3 nM to 100 µM for DOX while DNA concentration remained constant at 20 nM. Experiments were performed using 20%

and 40% MST power and between 20% and 60% LED power at 24 °C. MST traces were recorded using the standard parameters: 5 s MST power off, 30 s MST power on and 5 s MST power off. The binding affinities of the compounds to the protein were determined according to with dissociation values (Kd) and the generated data were processed using MO. Control software (Nanotemper Technologies, Germany) and analysed by GraphPad Prism v6.0 (GraphPad software, USA).

Western blot analyses

Cells were harvested after exposure to CA_5, CA_6, DOX or vehicle (DMSO) for 24 h, 48 h or 72 h. Cells were lysed at 4°C in whole cell lysis buffer (0.125M Tris-HCl pH 6.8, 4% SDS, 0.2% glycerol, 0.1% β-Mercaptoethanol and a pinch of bromophenol blue) and boiled for 10 min. Proteins were resolved by SDS-PAGE (8-15% gels) and transferred to Hybond ECL membranes (Amersham, UK). The membranes were incubated with primary antibodies: rabbit polyclonal antibodies to phospho-histone H2A.X (Ser139) (#2577), phospho-chk2 (Thr68) (#221), and mouse monoclonal antibody to E-cadherin (4A2) (#14472) from Cell Signaling Technology (Massachusetts, USA); rabbit polyclonal antibodies to p21 (C-19) (sc-397) and mouse monoclonal antibodies to β-actin (C4) (sc-47778) from Santa Cruz Biotechnology (Texas, USA) and mouse monoclonal antibody Flag M2 (F1804) from Sigma-Aldrich (USA). After primary antibody incubation, membranes were incubated with goat anti-rabbit or goat anti-mouse HRP-conjugated secondary antibodies (Bio-Rad Laboratories, California, USA). Antibody reactive proteins were visualized by enhanced chemiluminescence using SuperSignal West Pico Chemiluminescent Substrate Kit (Thermo Fisher Scientific) or WesternBright ECL HRP Substrate Kit (Advansta, California, USA). Densitometry readings were obtained using ImageJ v1.50i (SCHNEIDER; RASBAND; ELICEIRI, 2012) and protein expression levels were represented as a ratio of protein of interest/β-actin loading control normalized to the vehicle treated control sample where appropriate. All blots are representative of at least two independent repeats (unless otherwise stated).

Immunofluorescence

Cells were plated on glass coverslips and treated with ½ IC_{50} (0.5 nM), IC_{50} (1 nM) and 2x IC_{50} (2 nM) for CA_5 and compared with IC_{50} concentrations for DOX (200 nM) and CA_6 (2 nM) or vehicle. Cells were fixed with ice-cold 100% methanol at -20°C for

5 min followed by blocking and permeabilization with 0.2% Triton-X-100/5% BSA in phosphate buffered saline (PBS) for 30 min at RT. Slides were incubated with antibodies against phospho-histone H2A.X (#2577) (1:500) (Cell Signaling Technology) in blocking buffer overnight at 4 °C. After PBS washes coverslips were incubated with donkey anti-rabbit Cy3 conjugated secondary antibodies (Jackson ImmunoResearch Laboratories Inc, Pennsylvania, USA) diluted 1:1000 for 2 h in blocking buffer at RT. A secondary-antibody-only control was always included in these experiments. Cells were then counterstained with Hoechst (33342, Invitrogen, California, USA) for 10 min at RT in the dark, washed with PBS and then coverslips were mounted onto glass slides using Mowiol mounting medium. Cells were imaged with an LSM 510 confocal microscope (Carl Zeiss, Germany) using a Plan-Apochromat 63x/1.40 Oil DIC objective. Multiple z layers were acquired with 1µm step width. Images were processed using ZEN 2012 imaging software (Carl Zeiss) and maximum intensity projections were generated. For quantification, mean fluorescence was measured from at least 20 fields of view per treatment condition and pooled from three independent repeats.

Quantitative real time PCR (qRT-PCR)

Total RNA was extracted from cells using the High Pure RNA Isolation Kit (Roche, Switzerland) (catalogue no: 11828665001). The quality and concentration of RNA was determined by spectrophotometry using a NanoDrop® ND-1000 spectrophotometer (Thermo Fisher Scientific, MS, USA). Only samples exhibiting a A260/A280 ratio equal to or above 1.8 and an A260/A230 ratio close to 2.0 were selected and were either used immediately or stored at -80 °C. Reverse transcription of RNA (1 µg) was performed according to the manufacturer's instructions using the InProm-IITM reverse transcription system (A3800; Promega, Madison, WI, USA). Briefly, 1 µg of RNA was combined with 0.5 µg of Oligo (dT)15 primer in a 5 µL volume and denatured at 70 °C for 5 min, chilled on ice and combined with reverse transcription reaction mix (1X InProm-IITM reaction buffer, 3 mM $MgCl_2$, 0.5 mM dNTP mix, 20 units RNasin® ribonuclease inhibitor and 1 µL of ImProm-IITM reverse transcriptase) to a final volume of 20 µL. After a brief annealing step at 25 °C for 5 min, the reactions were incubated at 42 °C for 1 hr, followed by 15 min incubation at 70 °C to inactivate the reverse transcriptase prior to PCR. Quantitative real time PCR was conducted on a LightCycler Version 3 (Roche, Switzerland) using KAPA SYBR

FAST Master Mix (Kapa Biosystems, Sigma Aldrich), a final concentration of 0.4 µl of combined forward and reverse primers and 1µL of BSA (2 mg/mL), a 9 µL reaction were made up as a master mix and aliquoted into glass capillaries (Roche) (catalogue no: 04929292001), with 1 µL of cDNA added to give a final reaction volume of 10 µL. The capillaries were sealed, centrifuged at 2500 rpm for 30 sec prior to place into LightCycler. PCR cycle parameters were: denaturation for 15 min at 95 °C, combined annealing and extension for 35 cycles at 60 °C for 1 min. Each DNA sample was quantified in duplicate and a negative control without cDNA template was run with every assay to assess the overall specificity. Melting curve analysis was carried out to ensure product specificity. Relative mRNA expression levels were normalised to glucuronidase beta (GUSB) using the 2-ΔΔCt method. Primers used to amplify human TBX2 (catalogue no. QT00091266), human p21 (catalogue no. QT00060235), human E-cadherin (catalogue no. QT00060235) and human GUSB (catalogue no. QT00046046) were purchased from Qiagen.

Clonogenic assays

Cells were seeded in 60 mm dishes and treated the following day with ½ IC_{50} (0.5 nM), IC_{50} (1 nM) and 2x IC_{50} (2 nM) for CA_5 and compared with IC_{50} concentrations for DOX (200 nM) and CA_6 (2 nM) or vehicle. After 24 h, 1000 cells were seeded in 35 mm dishes (in duplicate for each treatment) in drug-free medium. Formation of colonies were monitored and after 7 days cells were fixed with 3:1 methanol: acetic acid and stained with 0.5% crystal violet (Sigma-Aldrich, USA) in 100% methanol. Colonies were imaged and percentage colony area was determined using ImageJ v1.50i (21) and the plugin ColonyArea (22). Colony area was determined for each drug concentration and expressed as a percentage of vehicle treated control.

Scratch Motility Assay

Cells were seeded in 60 mm dishes and treated as for clonogenic assays for 24 h. Cells were then collected, counted and replated to achieve 100% confluency in a 12-well plate in starvation medium (RPMI + 0.1% FBS). The following day a sterile 10 µl pipette tip was used to make a vertical scratch in the cell monolayer of each well and the cells were imaged at 0, 6, 12 and 24 h post-wound formation and ImageJ v1.50i (21) was used to calculate the area of the scratch. The total areas migrated were

determined by subtracting the area for a specific time point from the area measured at 0 h.

Statistical analyses

All data were obtained from at least three independent experiments (unless otherwise stated) with error bars representing standard error of the mean (SEM). Data were analysed using GraphPad Prism version 6.0 (GraphPad Software) and a parametric unpaired t-test was performed. Significance was accepted at *$p<0.05$, **$p<0.01$ and ***$p<0.001$.

Results

TBX2-driven advanced melanoma cells are 500x more sensitive to CA_5 cytotoxicity effects than doxorubicin

In order to compare the biological effects of CA_5 in the TBX2-driven advanced melanoma cell line 501mel, we used the well-established chemotherapy doxorubicin (DOX), and chromomycin A6 (CA_6), which is molecularly analogous to CA_5, as references controls. CA_5, DOX and CA_6 cytotoxicity were previously investigated in 501mel cell line, where their IC_{50} concentrations were estimated as 0.8, 400, and 2.3 nM respectively (PINTO et al., 2019) (Fig. 1A). The comparison between IC_{50} concentrations of DOX and CA_5 reveals that 501mel cell line is up to 500x more sensitive to CA_5 effects than doxorubicin (Fig. 1B). Light microscopy images of 501mel cells treated for 24, 48 and 72 h, with their respective IC_{50} concentrations, show the impacts of CA_5, CA_6 and DOX on cell viability and morphology, compared to vehicle (Fig. 1C). Interestingly, morphological differences between chromomycins and DOX after 72 h incubation in 501mel suggest that drugs are acting through different pathways in order to induce cell death (arrows, Fig. 1C).

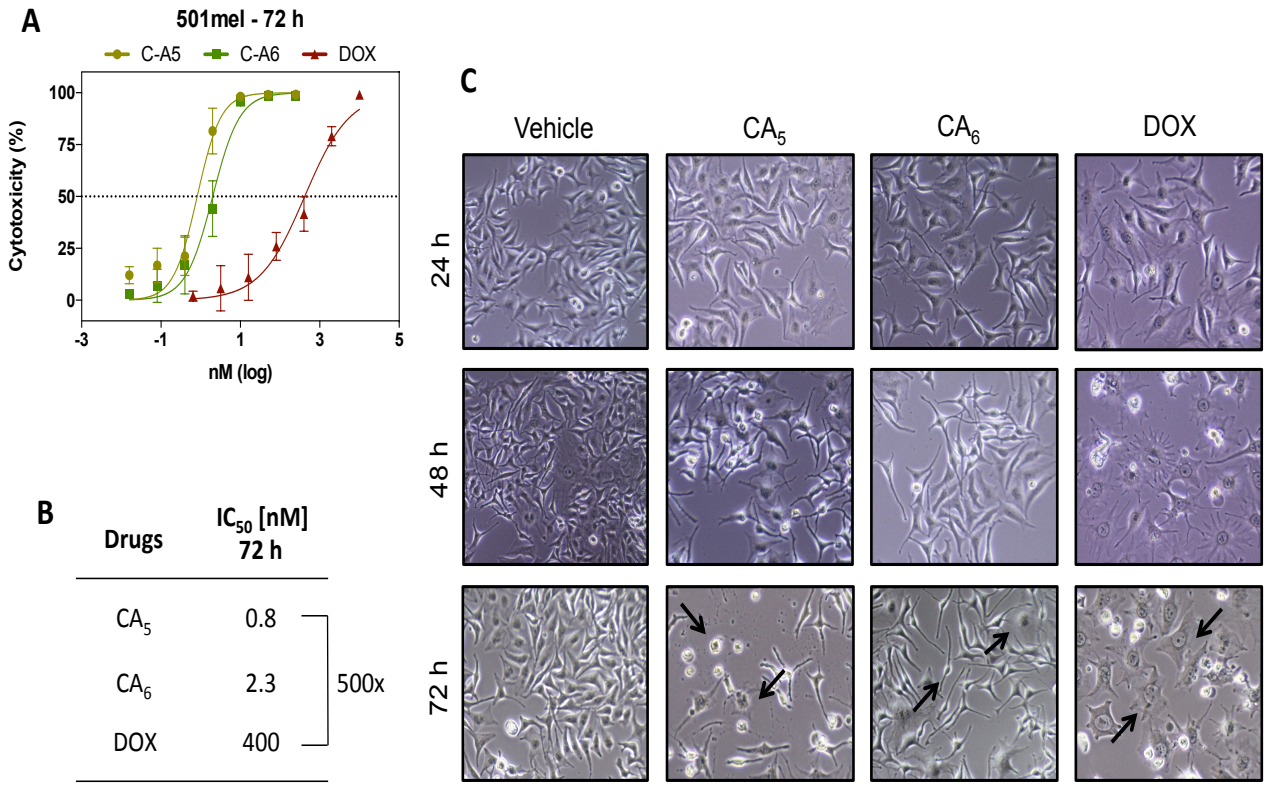


Figure 1. Cytotoxicity evaluation of CA_5, CA_6 and DOX in the TBX2 addicted 501mel advanced melanoma cells. A - MTT cell viability assays of 501mel cell line, treated with a range of CA_5 (0.016 nM – 250 nM), CA_6 (0.016 nM – 250 nM), DOX (2.8 nM - 45 µM) concentrations for 72 h. Graph show mean cell viability as a percentage of vehicle control ± SEM for each concentration of treatments determined from three independent experiments performed in duplicate. A curve was fitted using a non-linear regression to determine the IC_{50} concentration for each drug in 501mel cell line. Analysis were performed in GraphPad Prism v6.0 software. Data previously published in PINTO et al., 2019. **B** - IC_{50} concentrations in nM for CA_5 (0.8 nM), CA_6 (2.3 nM) and DOX (400 nM) determined as described in **A**. The differences between IC_{50} values of DOX and CA_5 was estimated in 500x. **C** - Representative light microscopy images (x200; EVOS XL AMEX1000 Core Imaging System) of 501mel cells treated with the respective IC_{50} concentration of CA_5, CA_6 and DOX for 24, 48 and 72 h. The arrows are indicating morphological differences between the treatments.

For all future biological experiments, concentrations corresponding to ½ IC_{50} (0.5 nM), IC_{50} (1 nM) and 2x IC_{50} (2 nM) for CA_5 was compared to IC_{50} values for DOX (400 nM) and CA_6 (2nM).

Doxorubicin baits but do not exhibit binding-affinity to TBX2 recombinant protein

Aiming to test DOX and CA_6 as reference controls to the anticancer characterization of CA_5 in TBX2-driven 501mel melanoma cell line, we first investigate the potential affinity of DOX (Fig 2A) and TBX2 recombinant protein, since such interaction was previously described for CA_5 and CA_6 (SAHM et al., 2020). Reverse affinity procedure and microscale thermophoresis (MST) were performed under the same conditions described in SAHM et al., 2020. We found that, similarly to CA_5, DOX displayed a residual binding to the resin itself and to the protein-loaded resins, where the presence of TBX2 linked to the resin increases the recovery of DOX (Fig 2B). The characterisation of the binding affinity between DOX and TBX2 was then analysed by MST. Figure 2C shows that DOX only slightly altered the thermophoretic movement of TBX2, when comparing to previous behaviour observed by CA_5 and CA_6(Fig. 2C), which suggest that DOX do not change the thermophoretic behaviour of TBX2, and it was not possible to measure its affinity to this protein. Furthermore, we measured the binding potential of CA_5 and DOX to a double strand DNA sequence that is recognized by TBX2 (Fig. 2D). The results show that CA_5 exhibit a very sensitive binding affinity to the sequence with a K_D of 65.7 nM, while DOX presented a much lower affinity to the DNA, with at least 3 order of magnitude lower affinity. It is also important to mention that DOX-binding to TBX2 DNA binding domain does not seem to have reached a maximum occupation of binding sites (plateau). However, we used the maximum observed binding as 100% to estimate the K_D value as 27.4 μM.

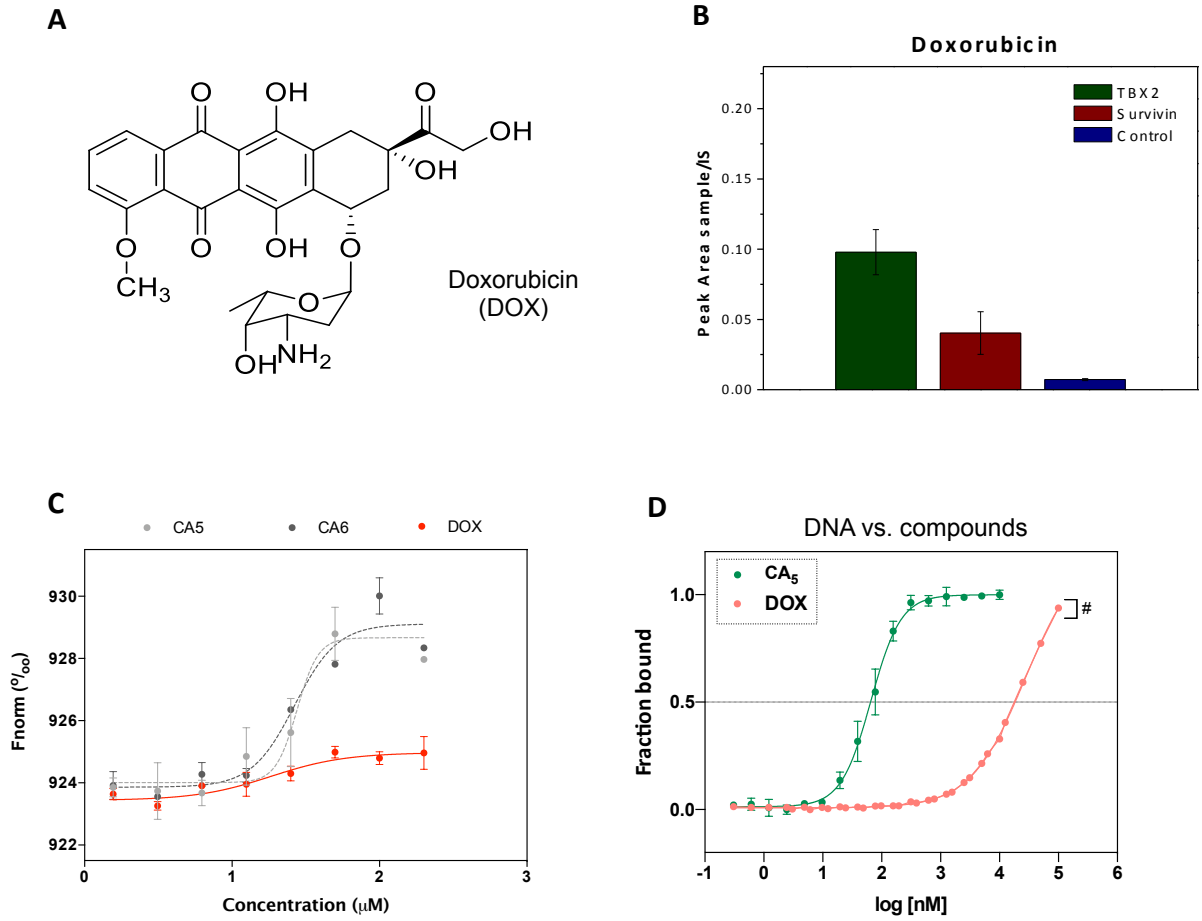


Figure 2. Potential affinity of DOX to TBX2 DNA-binding domain recombinant protein. A - Chemical structure of doxorubicin (DOX). **B** - Relative quantification of doxorubicin recovered from the bioaffinity chromatography technique using resins functionalized with TBX2 (green) or Survivin (red), or non-functionalized (control, blue) resin. The value of peak areas (triplicate) was used to construct the graphic. **C** - Comparative binding affinities of DOX, CA_5 and CA_6 to TBX2, assessed through microscale thermophoresis. Graph show the normalized fluorescence of labelled TBX2 in the presence of serial concentrations of each tested compounds, where DOX presented a different thermophoretic profile compared with chromomycins. Data correspond to the mean values from two independent experiments. Results for CA_5 and CA_6 were previously published by SAHM et al., 2020. **D** - Bound fraction of fluorescently Cy5-labelled double-strand DNA sequence that is recognized by TBX2 (IDT Inc, USA) with serial concentration of CA_5 and DOX accessed by microscale thermophoresis. The non-linear regression curves show the differences of fractions bounded between tested compounds and DNA. The dissociation constant (K_D) of compounds was estimated by M.O Affinity Analysis (Nanotemper Software, Germany). Graphics were generated by GraphPad Prism v6.0 (GraphPad Software, USA). Data correspond to the mean values from at least two independent experiments.

We next investigate the role of TBX2 in DOX activity using the TBX2 knocked down (Fig. 3A) and overexpressed (Fig. 3B) 501mel cells models, accessed by MTT assay. Results were similar to those observed for CA_5. TBX2 knockdown cells were more sensitive to DOX treatments after 72 h of drug incubation. Such behavior was more evidenced by DOX than by CA_5, where IC_{50} values of DOX in shTBX2 cells were reduced up to 187 times (Fig. 3C) comparing to CA_5 where the reduction varied by 4 to almost 5 times (SAHM et al., 2020). In contrast, overexpression of TBX2 leads to a more resistance to DOX cytotoxicity effects. The experiments were performed using genetically engineered 501mel cells where TBX2 expression was induced by doxycycline by either 12 h induction of iTBX2 followed by drug treatment (Fig. 3D); or 12 h drug treatment followed by induction of iTBX2 (Fig. 3E). For both setups, total drugs treatment time was 48 h. Once again, the results were similar to those found for CA_5 on both conditions (SAHM et al., 2020), where the induction of TBX2 prior to the 48-hours exposure to DOX produced a greater resistance response in TBX2-expressing cells, but, in this case, less prominent than CA_5.

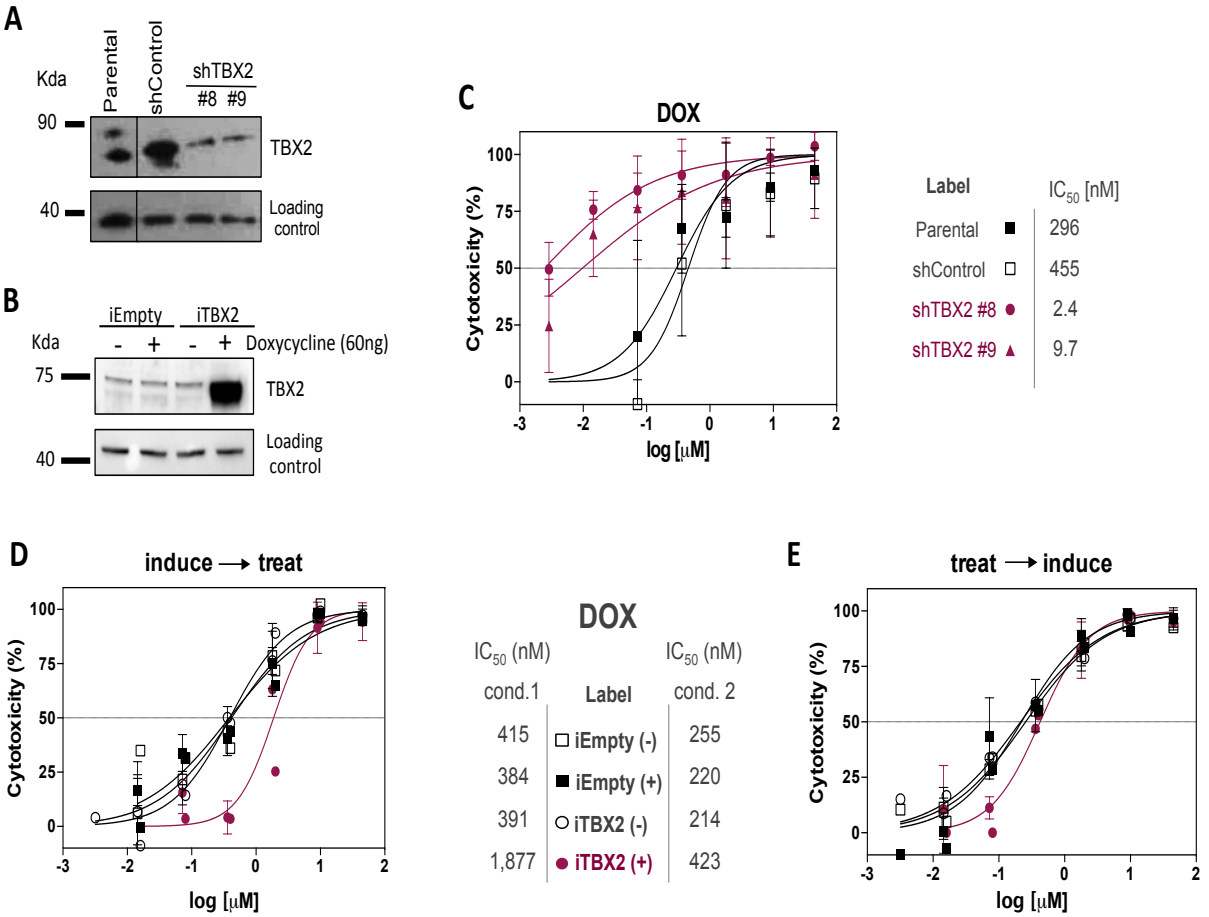


Figure 3. Cytotoxicity of DOX on stably TBX2-knockdown (shTBX2) and induced TBX2-overexpress 501mel cells. A - TBX2 protein expression in parental, shControl and shTBX2 clones #8 and #9 501mel cell models, achieved by western blot. **B** - TBX2 protein expression, achieved by western blot, of samples from iEmpty and iTBX2 cells, without (-) and with (+) 60 ng/mL doxycycline, showing that only iTBX2 (+) is inducing TBX2 overexpression. **C** - Cytotoxicity profiles of 501mel TBX2-knockdown models exposed to DOX. IC_{50} (nM) values for each labelled cell is found on the right. Cytotoxicity curves and respective IC_{50} values were obtained by MTT assay, after cells were exposed to the respective drugs during 72h. **D/E** - DOX cytotoxicity profiles and respective IC_{50} (nM) values accessed under cond.1 and cond.2 after 48 h drug exposure. Cond.1 = experiment setup where induction of TBX2 expression was done before drug treatment (**D**); Cond.2 = experiment setup where drug treatment was done prior to TBX2 induction (**E**). Cytotoxicity curves and respective IC_{50} values were obtained by MTT assay and analysed by non-linear regression using GraphPad Prism version 8.0 (GraphPad Software, USA) from two (C) or three (D-E) independent experiments performed in duplicate.

The effect of CA_5 on DNA-damage is concentration dependent and activates ChK2.

Chromomycins and DOX are known to exhibit their anticancer activity through their interaction with DNA (LOMBÓ et al., 2006; TACAR et al., 2013). Indeed, while DOX interacts with DNA by intercalation, chromomycins are minor groove binders and both interactions cause DNA-damage, which can lead to cell death (MIŠKOVIĆ et al., 2013; LEE et al., 2014). We therefore treated 501mel cells with drugs for 24 h and measured levels of the DNA-damage (double-strand breaks) marker γH2Ax by immunofluorescence (Fig. 4A) and western blot (Fig.4C). The results show that CA_5 induced γH2Ax levels in a dose-dependent manner and this was significant at its 2x IC_{50} concentration. Furthermore, DOX induced approximately two times more γH2Ax levels than 2x IC_{50} CA_5 and CA_6-treated cells had comparable levels of γH2Ax as vehicle-treated cells (Fig. 4B).

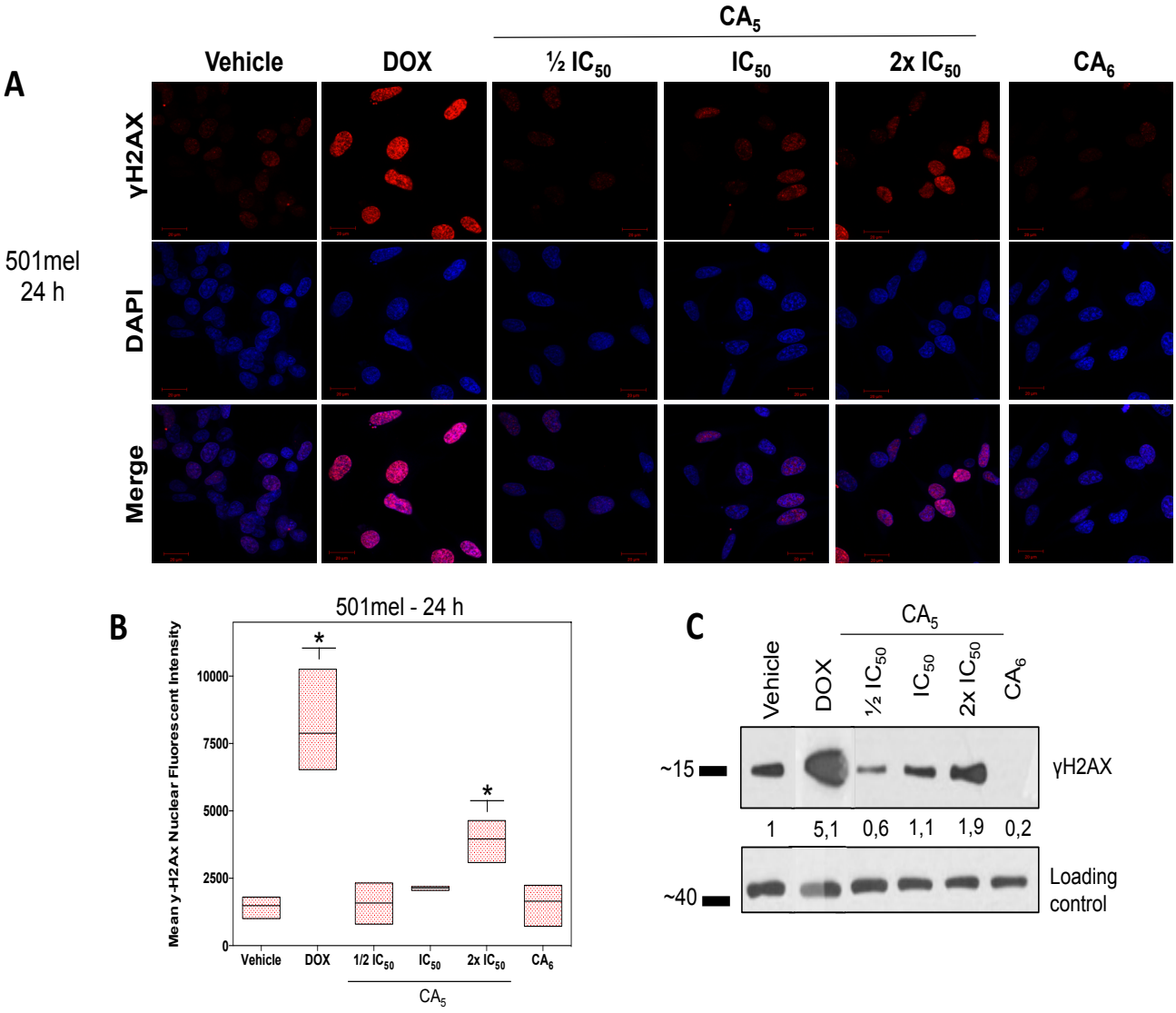


Figure 4. DNA-damaging effects of chromomycins and DOX in 501mel cell line. A - Representative confocal immunofluorescence maximum intensity projection images (x630; Carl Zeiss LSM 510) of 501mel cells treated with vehicle, DOX, CA_5 (½ IC_{50}, IC_{50}, 2xIC_{50} concentrations) or CA_6 for 24 h and γH2Ax detected with a fluorophore-conjugated Cy3 secondary antibody. Nuclei of cells were stained with DAPI. **B** - Graphic representing the quantification of γH2Ax levels per treatment condition as mean nuclear Cy3 fluorescence from 15 fields of view from three independent repeats. Data were analysed using GraphPad prism v6.0 (GraphPad Software, USA) and a parametric unpaired t-test was performed where *p < 0.05. **C** - γH2Ax protein levels detected by western blotting in 501mel cells following the treatment for DNA-Damage assay (A). β-actin was used as loading control. Densitometry reading were obtained using ImageJ (ImageJ Software, NIH, USA) and protein expression levels are represented as ratio of γH2Ax/β-actin normalized to vehicle control sample. Blots are representative of two independent repeats.

TBX2 is shown to have a role in the DNA-damage repair system. Wansleben et al (2013) demonstrated that TBX2 operates into the ATM-TBX2-ChK2 repair pathway, which confers resistance to DNA-damaging agents (WANSLEBEN et al., 2013). We therefore investigate the levels of γH2Ax, TBX2, ChK2 and p-ChK2 and p16 in 501mel cells treated with DOX, CA_5 and CA_6 for 24, 48 and 72 h by western blot (Fig. 5). Results demonstrate that TBX2 levels remains stable in all time points, with a slightly up-regulation at 72 h after the treatment with chromomycins. On the other hand, ChK2 appears drastically down regulated in DOX and 2X IC_{50} CA_5 treatment. This is inversely related to the results for γH2Ax, where DOX and 2x IC_{50} CA_5 presented the highest levels. However, activation of ChK2 (p-ChK2) occurs for all drug treatments but it is notable increased in the lowest concentrations of CA_5. Blottings also reveals that CA_5 DNA-damage in 501mel cells besides being concentration-dependent, it is also time-dependent. Finally, we probe samples for the cell senescence biomarker p16 and found that DOX and 2x IC_{50} CA_5 is up-regulating its levels, mostly after 72 h incubation.

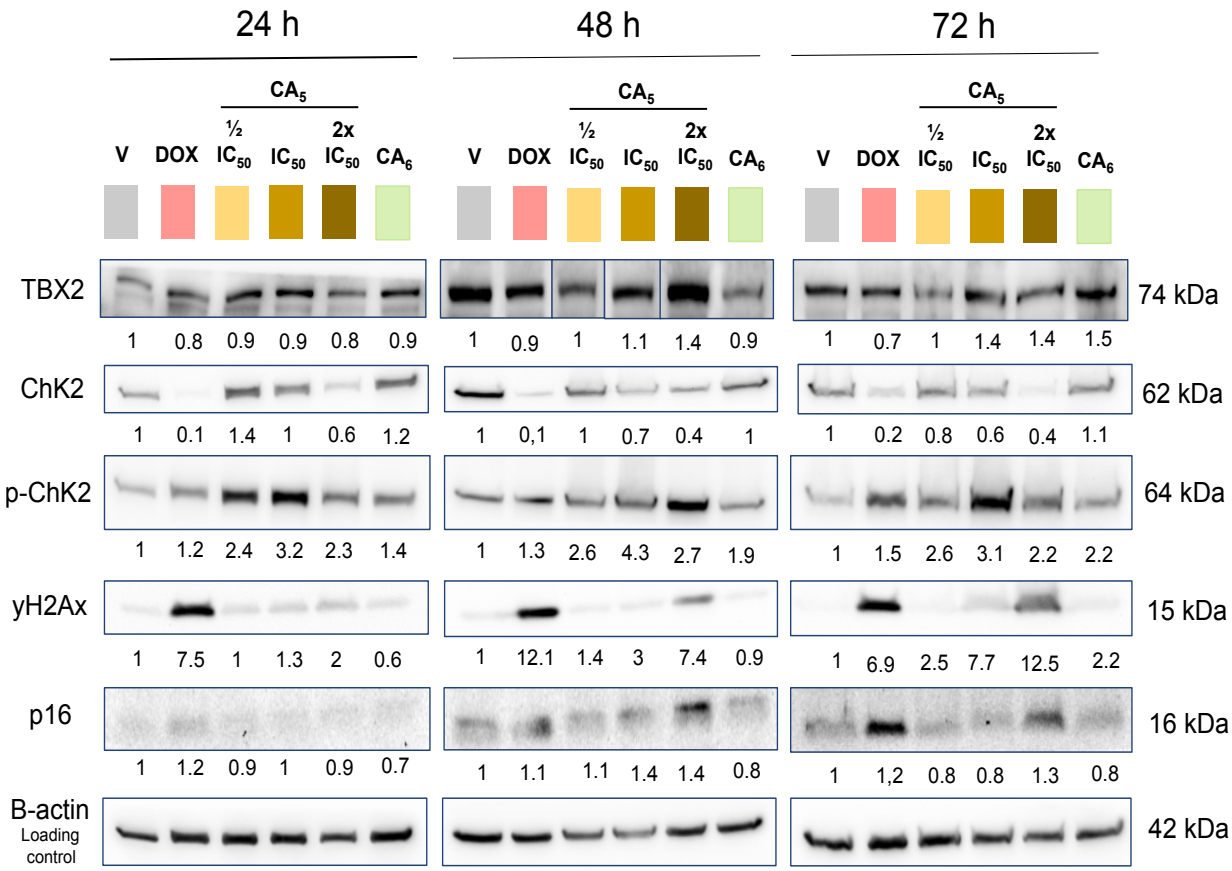


Figure 6. CA_5 activates ChK2 and upregulates p16 in 501mel cell line. Western blot analysis with antibodies to key DNA damage and stress signalling pathway proteins: TBX2, ChK2, p-ChK2, γH2Ax and p16. 501mel cells were treated with vehicle, DOX, CA_5 (½ IC_{50}, IC_{50}, 2xIC_{50} concentrations) or CA_6 for 24, 48 and 72 h. Densitometry reading were obtained using ImageJ (ImageJ Software, NIH, USA) and protein expression levels are represented as ratio of protein of interest/β-actin normalized to vehicle control sample. Blots are representative of three or two (p16) independent repeats.

CA_5 lowest concentrations increases protein and mRNA levels of TBX2 target genes in 501mel cells.

We have previously identified CA_5 in association with TBX2 protein in a reverse affinity procedure, which was aimed at identifying small molecules that potentially inhibit TBX2 oncogenic functions (SAHM et al., 2020). TBX2 was proven to favor the proliferation of melanoma cells by repressing the $p21^{WAF1}$ cyclin-dependent kinase inhibitor gene (PRINCE et al., 2004; VANCE et al, 2005).

Moreover, there are great evidences showing that TBX2 can promote several features of EMT in non-malignant cells, which includes the loss of expression of cell adhesion protein E-cadherin (WANG et al., 2012). We thus investigated the effect of treating 501mel cells with either DOX, CA_5, CA_6 or vehicle on their protein and mRNA levels of TBX2 and its target genes p21 and E-cadherin. Proteins expression were accessed by western blot where cells were pre-treated for 24 h followed by 48 h in drug free medium. Surprisingly, results revealed that both target genes appear up-regulated in IC_{50} and ½ IC_{50} CA_5 concentrations, in addition to CA_6 that also up-regulated p21 and 2x IC_{50} CA_5 that also regulated E-cadherin but at a lower intensity. In turn, TBX2 protein levels did not varied considerably with a slight increase for ½ IC_{50} and 2x IC_{50} CA_5. DOX did not affect the levels of the target proteins probed in this experiment (Fig. 6A).

Analysis of mRNA levels of TBX2 and its target genes in response to DOX, CA_5 and CA_6, were accessed by qRT-PCR. 501mel cells were pre-treated for 24 h followed by 24 h in drug-free medium. The results revealed that TBX2 mRNA was significantly up-regulated in cells treated with DOX, IC_{50} ($p < 0.001$) and 2x IC_{50} CA_5 ($p < 0.01$). No differences were identified in TBX2 mRNA levels in cells treated for ½ IC_{50} CA_5 and CA_6. All the drug treatments led to an increase in p21 mRNA levels, and E-cadherin were found significantly up-regulated in CA_5 lowest treatments, CA_6 and DOX as well. Among the target genes, p21 expression was the most significantly altered in the presence of DOX and 2x IC_{50} CA_5 presented the highest levels (9.4x and 35.9x, respectively). Alterations in E-cadherin expression were slightly less pronounced, yet still significant being 1.4x and 1.3x for CA_5 ½ IC_{50} and IC_{50} respectively, 1.5x for CA_6 and 3.7x to DOX (Fig. 6B).

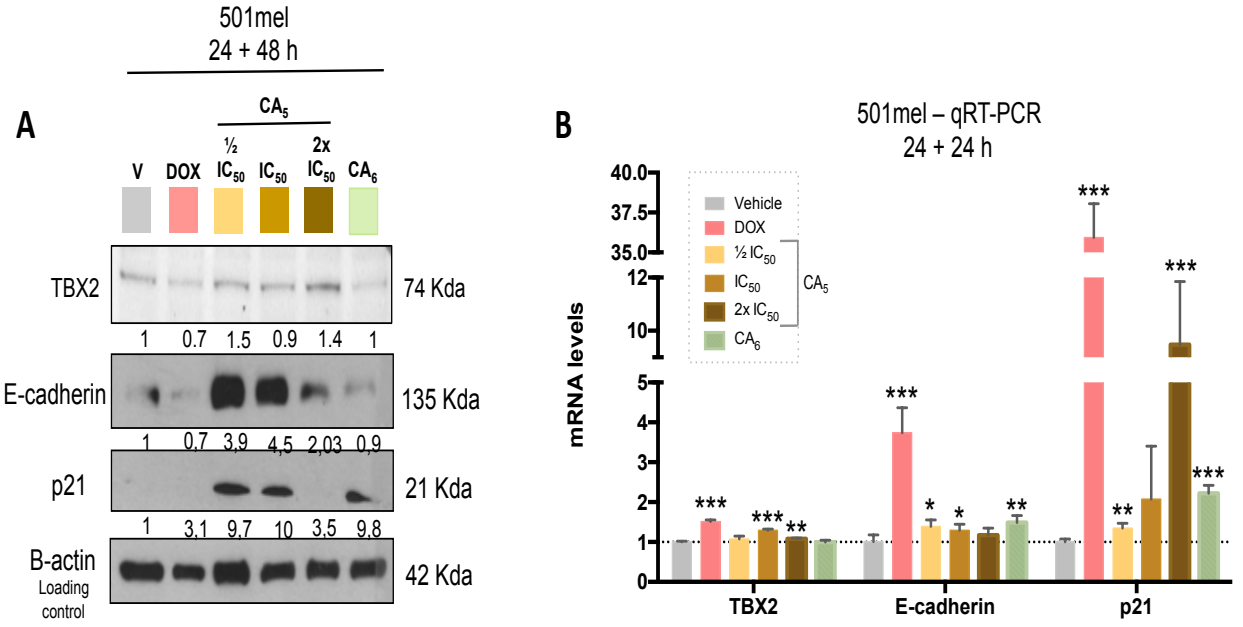


Figure 6. Low concentrations of CA_5 are able to alter TBX2 target genes protein and mRNA levels. A - Western blot analysis with antibodies to TBX2 and its target genes p21 and E-cadherin, which were compared to loading control β-actin, showing that CA_5 lowest concentration up-regulates protein levels of both TBX2 target genes. 501mel cells were pre-treated for 24 h with vehicle, DOX, CA_5 (½ IC_{50}, IC_{50}, 2xIC_{50} concentrations) or CA_6 followed by 48 h of incubation in drug-free medium. Densitometry reading were obtained using ImageJ (ImageJ Software, NIH, USA) and protein expression levels are represented as ratio of protein of interest/β-actin normalized to vehicle control samples. **B** - chromomycins and DOX increases relative mRNA levels of TBX2, p21 and E-cadherin in 501mel. Quantitative real-time PCR was performed in 501mel cells pre-treated with compounds for 24 h followed by 24 h incubation in drug-free medium. Graphic are representing the average of TBX2, p21 and E-cadherin relative mRNA levels + SD, of each treatment, normalized to GUSB. Data were analyzed using GraphPad Prism v6.0 (GraphPad Prism Software, USA) or Microsoft Excel 2011 (Microsoft corporation, USA) and parametric unpaired t-test were performed where *p < 0.05, **p < 0.01 and ***p < 0.001.The dotted line in the graph indicates normalized relative mRNA levels of vehicle as 1.

CA_5 inhibits 501mel survival and migration.

To better characterize the anticancer properties of CA_5 in 501mel cells, we next evaluated the effect of the drug on cell survival and migration using clonogenic and scratch motility assays respectively. Briefly, for the clonogenic assays 501mel cells were exposed to drug treatments for 24 h followed by 7 days in drug-free medium. DOX and CA_5 2xIC_{50} treatments significantly reduced the number of surviving colonies ($p<0.01$). The results show that CA_5 inhibited 501mel cell survival

in a dose-dependent manner, however, the treatment appears to have had an irreversible effect on cell survival only at the highest dosage tested - 2xIC_{50}. The survival rate for IC_{50} dose varied between 50 to 100%, which shows that cells are been effective in repair the cytotoxicity response of CA_5 within 24 h of drug exposure followed by drug-free medium incubation. Furthermore, the lower dose of CA_5 still seems to favor the proliferation of cells, since its growth was greater than the treatment with vehicle. Interestingly, when comparing the effects of CA_5, CA_6 and DOX, at their IC_{50} concentrations, the results reveal an interesting difference between DOX and chromomycins. Whereas DOX treatment was highly cytotoxic and resulted in only ~ 1% of cells surviving, CA_5 and CA_6 led to a survival rate around 85% (Fig. 2A-B). For the scratch motility assay the 501mel cells were pre-treated for 24 h with drugs and migration rates were measured at 0, 6, 12 and 24 h in drug- and serum-free medium. Similar to the results obtained for the clonogenic assay, CA_5-treated cells showed a dose-dependent decrease in migration rate with the IC_{50} and 2x IC_{50} doses having a significant effect at all time points tested. Cells treated with IC_{50} DOX had significantly lower ability to migrate ($p<0.001$), but these results are in part due to the cells not surviving the treatment. Furthermore, IC_{50} CA_6 had no effect on the migratory ability of the cells (Fig. 4C-D).

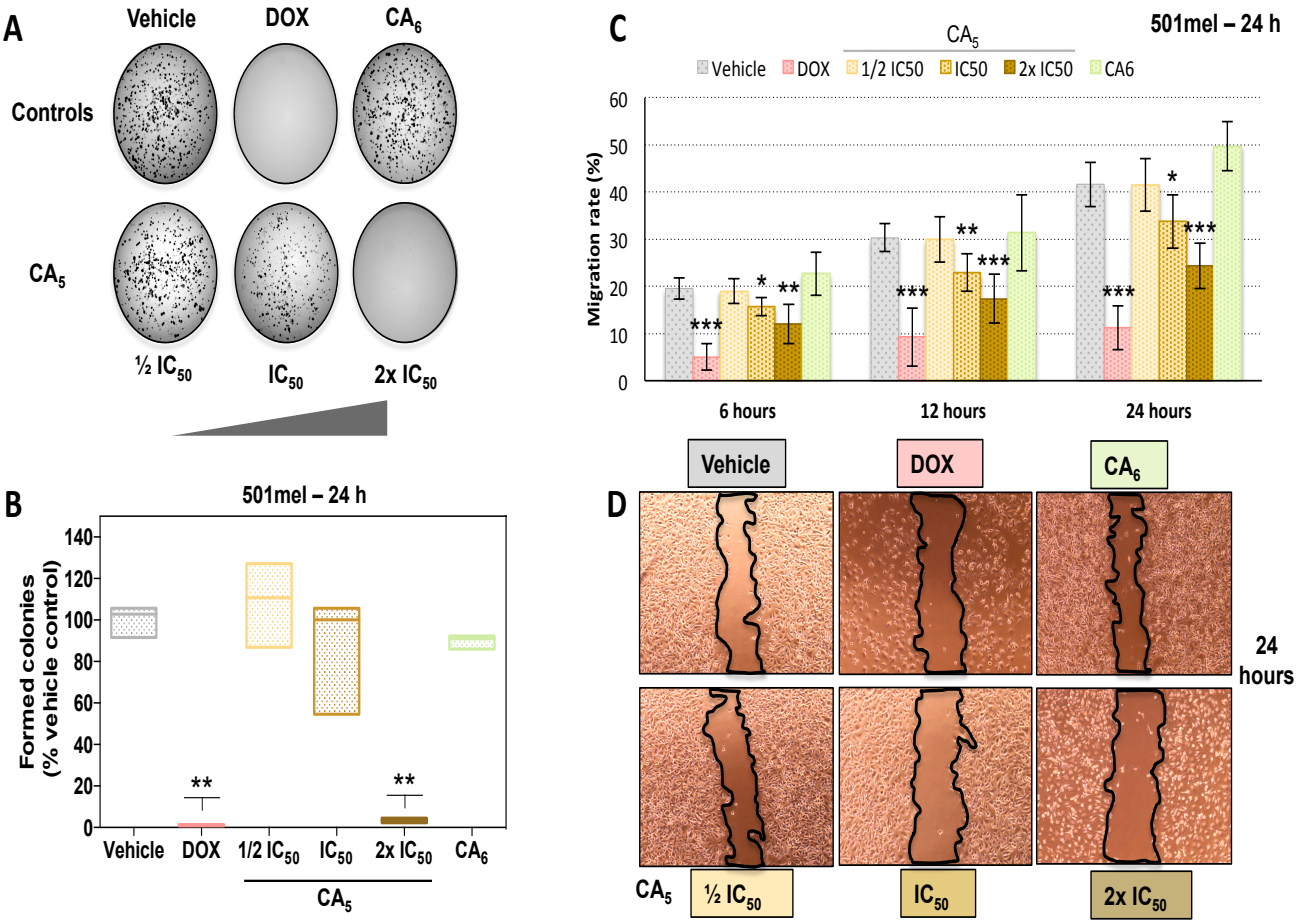


Figure 7. CA_5 effects on long-term survival and migration ability assays. A - Representative images of clonogenic assays in 501mel cells treated with vehicle, DOX, CA_5 (½ IC_{50}, IC_{50}, 2xIC_{50} concentrations) or CA_6 for 24 h and then replated at low densities in drug-free medium and left for 7 days for colonies to form. Colonies were stained with crystal violet. **B** - Quantification of images from three independent repeats using ImageJ plugin ColonyArea (ImageJ software, NIH, USA). The graph represents the mean number of formed colonies ± SD of each treatment as a percentage of the vehicle control. **C** - Quantification of scratch motility assays of 501mel cells pre-treated with vehicle, DOX, CA_5 (½ IC_{50}, IC_{50}, 2xIC_{50} concentrations) or CA_6 for 24 h and then replated at 100% confluence in drug- and serum-free medium. After cell adherence, a sterile 2 µl pipette tip was used to make a linear wound in the cell monolayer. Cells were imaged at 0, 6, 12 and 24 h post wound formation. Total area migrated was calculated by subtracting the wound area at each time point from the wound area at time 0 h, which is represented in the graph as mean area migrated (%) ± SD pooled from duplicates of one experiment. **D** - Representative images (×40; EVOS XL AMEX1000 Core Imaging System) of scratch motility assay from each treatment in 501mel cells at 24 h post wound formation time point. Data were analyzed using GraphPad Prism v6.0 (GraphPad Prism Software, USA) or Microsoft Excel 2011 (Microsoft corporation, USA) and parametric unpaired t-test were performed where *p < 0.05, **p < 0.01 and ***p < 0.001.

Discussion

The transcription factor TBX2 is considered a powerful proliferative factor in advanced 501mel melanoma cells and it confers cisplatin resistance on these cells (PERES et al., 2010; WANSLEBEN et al., 2013). We previously demonstrate that CA_5 exhibit a high cytotoxicity against the same cell line, where the IC_{50} concentration was estimated in 0.8 nM (PINTO et al., 2019). Later, we showed that CA_5 presented binding affinity to the TBX2 DNA-binding domain recombinant protein and that the overexpression and the lack of TBX2 in 501mel were sufficient to change the cytotoxicity profile of CA_5 (SAHM et al., 2020). We, therefore, turned our efforts in explore and characterize the anticancer activity of CA_5 in the TBX2 driven 501mel cell line, comparing its cytotoxicity profile with DOX and CA_6.

Firstly, we evidenced that DOX and chromomycins presented a very wide difference in cytotoxicity potency against 501mel, where CA_5 IC_{50} is up to 500x lower than that for DOX. Morphological observations also showed differences between the treatments, mainly evidenced after 72 h drug-incubations, where cells treated with chromomycins presented apoptotic phenotype (D'ARCY, 2019), while cells treated with DOX are morphologically similar to senescence-like phenotype mostly ending in death by mitotic catastrophe (EOM et al., 2005). Chromomycins and DOX are known to exhibit their anticancer activity through their interaction with DNA (LOMBÓ et al., 2006; TACAR et al., 2013). Indeed, while DOX interacts with DNA by intercalation, chromomycins are minor groove binders and both interactions cause DNA-damage which leads to cell death by different mechanisms (EOM et al., 2005; MIŠKOVIĆ et al., 2013; LEE et al., 2014).

We then speculate what would be the interaction between DOX and TXB2 recombinant protein. Although DOX was recovered from the reverse affinity procedure with TBX2 DNA-binding domain, the substance did not modify the thermophoretic behavior of the protein and it was not possible to measure affinity. As a transcription faction, TBX2 recognize specific DNA sequence to modulate its target genes transcription. Thus, we further consider the ability of both CA_5 and DOX to bind the DNA sequence recognized by TBX2, and although both compounds showed affinity to this specific DNA sequence, the observed K_D was three order of magnitude lower to CA_5, when compared to DOX. The components of the aureolic acid family, including chromomycins, are known to selective interact with DNA in regions with

high guanine-cytosine (GC) contents (LOMBÓ et al., 2005), which is in corroboration with our findings since approximately 85% of the DNA sequence used consists of such nitrogenize bases (CAMPBELL; CASEY; GOODRICH, 1998).

Further investigation on DOX activity against genetically engineering cell models, where TBX2 levels were depleted or overexpressed, revealed that the absence of TBX2 plays a more important role in the effects of DOX than CA_5, while overexpression of the factor had similar responses for both drugs. Chromomycins and DOX are described as DNA-damaged agents due its direct interaction with DNA structure into the cells. Despite binding differently and present different responses, both are able to generate genetic disorders (MIŠKOVIĆ et al., 2013). In the context of the experiment presented above, what it is also known is that TBX2 favors the DNA-repair system which configure resistance to DNA-binders chemotherapy in cancer cells that overexpress this factor (WANSLEBEN et al., 2013). Nevertheless, our findings suggest that cells lacking TBX2 are extremely more sensitive to DOX effects, showing that TBX2 is a very important factor for protecting these cells against DOX, whereas for CA_5 the absence of TBX2 sensitizes the cell but not as much as for DOX. These results suggest that the DNA-repair functions played by TBX2 seems to be less crucial for CA_5 treatments than it is for DOX.

In addition, the evaluation of DNA-damage generated by DOX and chromomycins in 501mel also revealed that this mechanism appears to be dominant in the cellular response for DOX treatment after 24 h, where equivalent level of the DNA-damage marker, γH2Ax, was only found at the highest dose for CA_5 (2x IC_{50}). This phenomenon was then proved to be maintained for 48 and 72 h as well where the intensity of the damage was enhanced over the time.

The serine/threonine kinase ChK2 is an important component in the cell response to DNA damage. Its activation can lead to diverse cellular responses, including cell cycle checkpoints activation, DNA repair, induction of apoptosis, senescence or tolerance of the damage (ZANNINI; DELIA; BUSCEMI, 2004). The way choose by ChK2 signaling is depending on the extent of damage where up to 20 proteins can be phosphorylated to induce the appropriate cellular response (ZANNINI; DELIA; BUSCEMI, 2004; OUCHI; OUCHI, 2014).

Analysis in the expression of p-ChK2 levels showed that treatments with both CA_5 and CA_6 are activating this signaling pathway, notably within the lowest concentrations of CA_5, whereas this phenomenon does not seem to be occurring with

such importance for the treatment with DOX. Moreover, levels of non-phosphorylated ChK2 protein revealed that its expression is knocked down in 501mel cells treated with DOX or CA_5 $2xIC_{50}$. This could be considered in agreement with the fact that ChK2 is known to be degraded in cells that overpass the DNA-damage response due severe damages (ZHANG et al., 2005), since the highest levels of γH2Ax were found for both samples. These results suggest that low concentrations of CA_5 is not causing a significant DNA-damage to account for the observed cytotoxicity, as repairing signaling seems to be activated, while DOX drives its cytotoxicity directly through un-repairable DNA damage. Moreover, the p16 up-regulation for DOX and $2xIC_{50}$ CA_5 also confirm that DNA-damage is leading to cell death or senescence in these treatments. We then propose that DNA-damage is not the central mechanism of action for CA_5 cellular toxicity, at least in low concentrations, in 501mel cells.

Indeed, the mechanism of action described for chromomycins, and others aureolic acids, is related with effects on RNA synthesis and blockage of gene expression through inhibition of DNA and RNA polymerase reactions at low concentrations (KAMIYAMA, 1967; LOMBÓ et al., 2005; NELSON; FERGUSON; DENNY, 2007). Turner and Denny (1996) reported that the effects on gene expression of minor groove binders *in vitro* is due the inhibition of sequence selective binding of various transcription factors to DNA, which may result in repression or expression of downstream genes (TURNER; DENNY, 1996). A comparison analysis in the global gene expression of DNA minor groove binding agents revealed that the treatment with high doses of chromomycin A_3 in a human leukemia cell line have negative impacts in genes related to important cellular functions while up-regulate apoptosis related genes (ZIHLIF et al., 2010).

Moreover, the specificity presented by these compounds to GC rich regions along the DNA demonstrates that chromomycins can prevent the binding of regulatory DNA proteins through inhibiting their specific promoter regions (LOMBÓ et al, 2005), which were recently reported for CA_3 suppression of Sp1-related anti-apoptotic proteins (SARANARUK et al., 2019). The up-regulation of TBX2 target genes protein and mRNA levels in 501mel cells treated with low doses of CA_5, plus the great binding affinity that this compound presents to the TBX2 DNA-binding sequence, is in complete agreement with the mechanism of action described above and suggest that modulation of TBX2 may be involved in the bioactivity that CA_5 is exerting on 501mel advanced melanoma cells. Although TBX2 protein and mRNA

levels were not found depleted, some investigators affirm that molecular targets can overcome the effect of an inhibitor by compensatory overexpression as an adaptive response to cellular homeostasis (DUNCAN et al., 2012; DANG et al., 2017). However, the results presented in this study are not sufficient to accurately confirm such conclusions.

Even more and despite being consistent, it is still not clear if the up-regulation of p21 and E-cadherin is due a direct inhibition of TBX2 functions. Both genes have been wide studied against its roles in carcinogenesis (KARIMIAN; AHMADI; YOUSEFI, 2016; KOURTIDIS et al., 2017). The cyclin-dependent kinase inhibitor p21 is known to promote cell cycle arrest in response to a variety of stimuli, and despite the report that TBX2 directly repress its gene in melanoma cells (PRINCE et al., 2004), this factor plays important functions in response to cell DNA-damage, such as transcriptional regulation and modulation or inhibition of apoptosis. Nevertheless, the role played by p21 in response to DNA-damage seems to be dependent on the factor that have critical roles in its expression than to its self-regulation (KARIMIAN; AHMADI; YOUSEFI, 2016). On the other hand, E-cadherin repression in melanoma is orchestrated by several signaling pathways involved in the epithelial to mesenchymal transitions and actually there is good evidences suggesting that TBX3, rather than TBX2, is the factor responsible for E-cadherin repression in melanoma cells (PERES; PRINCE, 2013; PERES et al., 2013; PERES; MOWLA; PRINCE, 2014; KOURTIDIS et al., 2017). Additional experiments are needed to better clarify whether up-regulation of p21 and E-cadherin are due TBX2 modulations in 501mel cell treated with CA_5.

Lastly, the characterization of the anticancer phenotypes of CA_5 in 501mel cells treated for 24 h showed that this natural substance potentially inhibits cell survival and migration ability in a dose-dependent manner. Nevertheless, cytotoxicity effects of CA_5 was not as efficient as DOX treatments on these cells following the same conditions, where only $2xIC_{50}$ CA_5 treatment reached significantly decreased survival rate and was comparable to DOX effects. On the other hand, CA_5 exhibited a greater anticancer property than its analogous CA_6 (Fig. 7). Anyway, we believe that low doses of CA_5 treatments still can be explored in order to sensitize tumor cells, against other agents, through interference in the repair machinery.

Trabectedin is a marine-derived anticancer drug (Yondelis®) approved for the treatment of unresectable or metastatic liposarcoma by the FDA in 2015 (BARONE

et al., 2017). Just like chromomycins, this compound exerts its anticancer functions through interaction with the DNA-minor groove. Beyond this, the binding of trabectedin with the DNA has been proven to result in several additional responses, which categorized its mechanisms of action as unique in the field of anticancer drugs (D'INCALCI; GALMARINI, 2010).

The binding of trabectedin in the DNA-minor groove leads to the inhibition of active transcription through disturbances of promoters in the major-groove (MINUZZO et al., 2005). It also promotes the RNA polymerase II degradation by the proteasome pathway due its direct enzyme blockage during DNA elongation (AUNE et al., 2008). Just like described to other minor groove binders, structural changes in the DNA induced by trabectedin seems to displace transcriptional factors from their target promoters. This was evidenced in a study reporting the interference of trabectedin in the binding of FUS-CHOP oncogene to its promoter which leaded to cell differentiation and diminished the expression of FUS-CHOP oncoproteins in a myxoid liposarcoma cell line (FORNI et al., 2009; DI GIANDOMENICO et al., 2014; ASSI et al., 2019). Moreover, the DNA adducts generated by trabectedin-DNA binding difficult the functions of NER (nucleotide excision repair) DNA repair system which results in double-strand breaks that trigger apoptosis cell death program (D'INCALCI et al., 2014). Trabectedin anticancer effects include cytotoxicity, anti-proliferation, inhibition of gene expression, and, more recently described, intercessions in the tumor microenvironment and sensitization in chemoresistant tumours (RAY-COQUARD, 2017; ASSI, 2019).

Such diverse and enthusiastic mechanism of action raised the question of whether other minor groove DNA-binders would have similar potential to act through the same way. Interestingly, after realizing that chromomycin A_3 and trabectedin presented a very correlated cytotoxicity response in a NCI 60-human tumor cell lines panel (carried out in the COMPARE analysis, NCI, USA), Marco and Gago (2005) investigated whether these two compounds would have similarities in their interaction with DNA. They found that a complex of 2:1 (chromomycin:trabectedin) presented DNA structural similarities in a binding site sequencing target by these two drugs. The structural similarities reported indicates that chromomycins would have the potential to cause the same structural changes as trabectedin do in the DNA. The authors suggest that comparison experiments on gene transcription expression and integrity of the NER system between these two drugs would address new insights

regarding similarities in their mechanism of action (MARCO; GAGO, 2005). Our data reinforce this hypothesis, since herein we showed that CA_5 is able to modulate the function of the transcription factor TBX2 by direct binding to both DNA and the protein itself, inducing high toxicity in TBX-driven melanoma cells. More studies are important to fully characterize the effects of CA_5 in other TBX2-driven cancer, and also its ability to interfere with other transcription factors.

Considering the role played by TBX2 in chemotherapy resistance against DNA-alkylating agents in cells that overexpress this factor, the identification of molecules with potential to modulate its functions and sensitizes cells to conventional treatments figure as an interesting approach in the treatment of resistant cancer cells. This approach seems to be achieved by trabectedin where its combination with PLD (pegylated liposomal doxorubicin) restores tumor sensitivity to first-line platinum-based chemotherapy due trabectedin interactions with components of the NER machinery (RAY-COQUARD, 2017).

Finally, the present study contributed to the understanding of the anticancer activity played by chromomycins in malignant melanoma cells, evidencing that the modulation of the T-box transcription factor, TBX2, may be involved in sensitizing cells to cytotoxicity effects of CA_5. In this context, we suggest that low doses of CA_5 can be explored as potential modulator of TBX2 proliferative and chemoresistance functions in malignant melanoma cells, which could open up to new possibilities in the treatment of this type of cancer.

8. FINAL CONSIDERATIONS

Although there are currently several anticancer therapeutic options in use, cancer remains one of the deadliest diseases in the world, which requires the development of new and more efficacious therapies. Melanoma is a type of cancer that has been increasing in its incidence rate. As it is a disease that mainly affects the elderly and has a carcinogenic relationship with UV radiation (UVR), the increase in the overall survival of the world population together with climate changes that enhance the incidence of UVR, new cases of melanoma tend to be more numerous and frequent in the next few years (BALATO et al., 2015). The relevance for developing new therapeutic strategies in the field of melanoma treatment is regarding to the lack of efficacy and cancer resistance to traditional and target-therapy (KOZAR et al., 2019).

The new biotechnological era has opened previously unimaginable doors for medical research. Advances in the development of efficient tools have enabled scientists to immerse themselves in understanding diseases and other biological processes. For example, The Cancer Genome Atlas (TCGA) program contributed significantly to uncover many drivers of tumorigenesis through progress in sequencing several cancer genomes (TOMCZAK; CZERWINKA; WIZNEROWICZ, 2015). The role played by transcription factors (TFs) in cancer has also reached great advances. TFs plays a pivotal role in regulating gene transcription and is found deregulated in many diseases, including cancer. It is estimated that around 20% of all oncogenes discovered so far are TFs (VAQUERIZAS et al., 2009; BRADNER; HNISZ; YOUNG, 2017).

The great interest in discovering approaches that modulate TFs functions in cancer is based on the fact that their deregulations occur specifically in cancer cells, which would result in the development of a specific therapeutic intervention with a reduction in adverse effects and patient-specific therapies (HAGENBUCHNER; AUSSERLECHNER, 2016). Even more, TFs are involved in diverse cellular process that ranges from replicative immortality to developing of resistance. The development of TFs target drugs figures as a great strategy in modulating many cancer properties at the same time, in contrast to the limited effects of various kinase inhibitors which are mainly regarding antiproliferative effect only (BUSHWELLER, 2019).

Nevertheless, for a long period, drug discovery researchers assumed that targeting transcription factors was impossible due its "undruggable" properties. In order to mediate TFs functions, interferences between protein-protein and protein-DNA interactions figured as the logical modulation of TFs. The challenges related to the "undruggable" features is due the fact that this factors present a large protein-protein interaction interfaces hardly occupied by a small molecule, lack of a deep protein pockets which difficult molecules accommodation, plus their intranuclear localization which in theory add further limits in accessing these targets (DALE et al., 2019; BUSHWELLER, 2019).

Yet, in cancer research, drugging an undruggable target is a key challenge that has been achieved before. It is important to highlight that many so-called undruggable targets were eventually developed as promising and successfully therapies. As examples, only a couple of decades ago tyrosine-kinases were considered difficult to target and nowadays inhibitors of this class of targets are widely used in personalized anti-cancer therapy (WU; NIELSEN; CLAUSEN, 2015). Moreover, it is now well proved that directly inhibition of TFs from BCL-2 family by small molecules are possible (ASHKENAZI et al., 2017; VAXMAN; SIDIQI; GERTZ, 2018), despite these factors possess all the "undruggable" features described to TFs above. Currently, many scientists believe that basic understanding of the biological and biochemical properties of TFs, using tools as X-ray crystallography and nuclear magnetic resonance, can make then druggable targets (DANG et al., 2017).

Actually, considerable progressions in modulating TFs functions for cancer therapy were achieved in the recent years (BHAGWAT; VAKOC, 2015; LAMBERT et al., 2018; BUSHWELLER, 2019). Most common approaches include targeting nuclear hormone receptor ligand binding domain; inhibition of TF-cofator protein-protein interactions; target chromatin remodeling/epigenetic readers protein in order to modulate expression of TF drivers; disrupting TF-DNA binding by directly binding TF's with small molecule or yet by compounds that binds to DNA preventing TFs recognition of its consensus sequence (HAGENBUCHNER; AUSSERLECHNER, 2016; BUSHWELLER, 2019).

Aiming at the development of new horizons for melanoma therapy, the present phD thesis starting point was the identification of marine natural compounds with binding affinity against the TF TBX2, previously known for their important oncogenic functions in melanomas (PRINCE et al., 2009; WANSLEBEN et al, 2013). Targeting

the TF DNA-binding domain directly by a small molecule, or other mimetic molecule, can changes its conformation or prevents its binding with DNA, thus cancelling its transcription functions. For these reasons, screening approaches use the TF DNA-binding domain as bait for identification of DNA-binding domain interacting compounds (HAGENBUCHNER; AUSSERLECHNER, 2016). Herein, we use a reverse affinity procedure where TBX2-DNA-binding domain recombinant protein was the bait. We found that the minor groove binder molecule, CA_5, has binding affinity to TBX2-DNA Binding domain and further investigations revealed that TBX2-driven melanoma cells are highly sensitive to these compound and up-regulation of TBX2 target genes, once repressed, were observed at low doses treatment.

Moreover, blockage of the interaction between protein/DNA-binding by compounds is an interesting approach for modulation of TFs functions, as mentioned above, and has proven to be efficient mechanism of action designated to DNA minor groove binders compounds. Identify compounds that compete with TF for their specific consensus sequence in the DNA, or molecules able to specific create conformational changes in the DNA that prevent the binding or recognition of TFs figures as good alternatives in inhibiting the activity plays by oncoTFs (HAGENBUCHNER; AUSSERLECHNER, 2016; BUSHWELLER, 2019). Notable, we also demonstrate that CA_5 have great binding affinity to the TBX2 DNA-target sequence, which configures this molecule as a potential modulator of the TBX2 functions in melanoma and other tumors that express this factor by either directly interaction with TBX2-DNA-binding domain or through blocking its specific binding sequence.

Still, the results found here represent the beginning of the investigation into the modulatory role that CA_5, or others minor groove binders, plays against TBX2. Several additional experiments still need to be performed in order to better clarify its mechanisms and further identifications of approaches for the development of a potential target-therapy. Moreover, the participation of TBX2 in the CA_5 cytotoxicity is currently being investigated in breast cancer and rhabdomyosarcomas cell lines as well, which will soon address new insights about the findings reported in the present study. In conclusion, we prove that marine natural products recovered from the Brazilian coast have the potential to produce interesting compounds with important biological activity. Also, we validate the reverse affinity procedure using the TBX2-

DNA-binding domain as bait, which open this approach for high throughput screenings in order to identify more molecules with potential binding to TBX2 TF.

9. REFERENCES

ABRAHAMS, A. et al. UV-mediated regulation of the anti-senescence factor Tbx2. **Journal of Biological Chemistry**, v. 283, n. 4, p. 2223–2230, 2008.

ABRAHAMS, A.; PARKER, M. I.; PRINCE, S. The T-box transcription factor Tbx2: Its role in development and possible implication in cancer. **IUBMB Life**, v. 62, n. 2, p. 92–102, 2010.

AGARWAL, A. et al. Use of in vitro bioassays for assessing botanicals. **Current Opinion in Biotechnology**, v. 25, p. 39–44, 2014.

AGULNIK, S. I. et al. Evolution of mouse T-box genes by tandem duplication and cluster dispersion. **Genetics**, v. 144, n. 1, p. 249–254, 1996.

ALONSO, S. R. et al. Progression in Cutaneous Malignant Melanoma Is Associated with Distinct Expression Profiles: A Tissue Microarray-based Study. **The American Journal of Pathology**, v. 164, n. 1, p. 193–203, 2004.

ANDTBACKA, R. H. I. et al. Talimogene laherparepvec improves durable response rate in patients with advanced melanoma. **Journal of Clinical Oncology**, v. 33, n. 25, p. 2780–2788, 2015.

ARRIETA, J. M.; ARNAUD-HAOND, S.; DUARTE, C. M. What lies underneath: Conserving the oceans' genetic resources. **Proceedings of the National Academy of Sciences**, v. 107, n. 43, p. 18318–18324, 2010.

ARTHAUD, I. D. B. et al. Studies on the secondary metabolites of a Pseudoalteromonas sp. isolated from sediments collected at the northeastern coast of Brazil. **Chemistry & biodiversity**, v. 9, p. 418–427, 2012.

ASHKENAZI, A. et al. From basic apoptosis discoveries to advanced selective BCL-2 family inhibitors. **Nature Reviews Drug Discovery**, v. 16, n. 4, p. 273–284, 2017.

ASNAGHI, L. et al. EMT-associated factors promote invasive properties of uveal melanoma cells. **Molecular Vision**, v. 21, n. April, p. 919–929, 2015.

ASSI, T. et al. A comprehensive review of the current evidence for trabectedin in advanced myxoid liposarcoma. **Cancer Treatment Reviews**, v. 72, n. November 2018, p. 37–44, 2019.

ATKINS, M. B. et al. High-dose recombinant interleukin 2 therapy for patients with metastatic melanoma: Analysis of 270 patients treated between 1985 and 1993. **Journal of Clinical Oncology**, v. 17, n. 7, p. 2105–2116, 1999.

AUNE, G. J. et al. Von hippel-lindau-coupled and transcription-coupled nucleotide excision repair-dependent degradation of RNA polymerase II in response to trabectedin. **Clinical Cancer Research**, v. 14, n. 20, p. 6449–6455, 2008.

BADAL, B. et al. Transcriptional dissection of melanoma identifies a high-risk subtype underlying TP53 family genes and epigenome deregulation. **JCI insight**, v. 2, n. 9, p. 1–15, 2017.

BAI, X. et al. MAPK pathway and TERT promoter gene mutation pattern and its prognostic value in melanoma patients: A retrospective study of 2,793 cases. **Clinical Cancer Research**, v. 23, n. 20, p. 6120–6128, 2017.

BALATO, N. et al. Effects of climate changes on skin diseases. **Expert Review of Anti-Infective Therapy**, v. 12, n. 2, p. 171–181, 2014.

BALLIF, B. C. et al. Identification of a Recurrent Microdeletion at 17q23.1q23.2 Flanked by Segmental Duplications Associated with Heart Defects and Limb Abnormalities. **American Journal of Human Genetics**, v. 86, n. 3, p. 454–461, 2010.

BARONE, A. et al. FDA approval summary: Trabectedin for unresectable or metastatic liposarcoma or leiomyosarcoma following an anthracycline-containing regimen. **Clinical Cancer Research**, v. 23, n. 24, p. 7448–7453, 2017.

BEN-PORATH, I. et al. An embryonic stem cell-like gene expression signature in poorly differentiated aggressive human tumors. **Nat Genet**, v. 40, n. 5, p. 499–507, 2008.

BERGMANN, W.; FEENEY, R. J. Contributions to the study of marine products. XXXII. the nucleosides of sponges. I. **Journal of Organic Chemistry**, v. 16, n. 6, p. 981–987, 1951.

BERWICK, M. et al. The Prevalence of CDKN2A Germ-Line Mutations and Relative Risk for Cutaneous Malignant Melanoma: An International Population-Based Study. **Cancer Epidemiology Biomarkers & Prevention**, v. 15, n. 8, p. 1520–1525, 2006.

BESCH, R.; BERKING, C. POU transcription factors in melanocytes and melanoma. **European Journal of Cell Biology**, v. 93, n. 1–2, p. 55–60, 2014.
BHAGWAT, A. S.; VAKOC, C. R. **Targeting Transcription Factors in CancerTrends in Cancer**, 2015.

BOER, D. R.; CANALS, A.; COLL, M. DNA-binding drugs caught in action: The latest 3D pictures of drug-DNA complexes. **Dalton Transactions**, n. 3, p. 399–414, 2009.

BORISSENKO, L.; GROLL, M. 20S proteasome and its inhibitors: Crystallographic knowledge for drug development. **Chemical Reviews**, v. 107, n. 3, p. 687–717, 2007.

BRADNER, J. E.; HNISZ, D.; YOUNG, R. A. Transcriptional Addiction in Cancer. **Cell**, v. 168, n. 4, p. 139-629–643, 2017.

BRIEGEL, K. J. Embryonic transcription factors in human breast cancer. **IUBMB life**, v. 58, p. 123–132, 2006.

BUSHWELLER, J. H. Targeting transcription factors in cancer — from undruggable to reality. **Nature Reviews Cancer**, v. 19, n. 11, p. 611–624, 2019.

CAMPBELL, C. E.; CASEY, G.; GOODRICH, K. Genomic structure of TBX2 indicates conservation with distantly related T-box genes. **Mammalian Genome**, v. 9, n. 1, p. 70–73, 1998.

CARLSON, E. E. Natural products as chemical probes. **ACS Chemical Biology**, v. 5, n. 7, p. 639–653, 2010.

CARREIRA, S.; LIU, B.; GODING, C. R. The Gene Encoding the T-box Factor Tbx2 Is a Target for the Microphthalmia-associated Transcription Factor in Melanocytes. **The Journal of biological chemistry**, v. 275, n. 29, p. 21920–21927, 2000.

CHANG, F. et al. The role of T-box genes in the tumorigenesis and progression of cancer (Review). **Oncology Letters**, v. 12, n. 6, 2016.

CHARYTONOWICZ, E. et al. PPARγ agonists enhance ET-743 - Induced adipogenic differentiation in a transgenic mouse model of myxoid round cell liposarcoma. **Journal of Clinical Investigation**, v. 122, n. 3, p. 886–898, 2012.

CHEN, Y. et al. The transcription factor TBX2 regulates melanogenesis in melanocytes by repressing Oca2. **Molecular and Cellular Biochemistry**, v. 415, n. 1–2, p. 103–109, 2016.

CHIAPPETTA, C. et al. BRAF and NRAS Mutations are Heterogeneous and Not Mutually Exclusive in Nodular Melanoma. **Appl Immunohistochem Mol Morphol**, v. 23, n. 3, p. 172–177, 2015.

CICHOREK, M. et al. Skin melanocytes: Biology and development. **Postepy Dermatologii i Alergologii**, v. 30, n. 1, p. 30–41, 2013.

CIRENAJWIS, H. et al. NF1-mutated melanoma tumors harbor distinct clinical and biological characteristics. **Molecular oncology**, v. 11, n. 4, p. 438–451, 2017.

COHEN-SOLAL, K. A.; KAUFMAN, H. L.; LASFAR, A. Transcription factors as critical players in melanoma invasiveness, drug resistance, and opportunities for therapeutic drug development. **Pigment Cell and Melanoma Research**, v. 31, n. 2, p. 241–252, 2018.

COSGAREA, I. et al. Update on the clinical use of kinase inhibitors in melanoma. **Journal of the German Society of Dermatology**, p. 887–893, 2017.

CRAGG, G. M.; NEWMAN, D. J. Natural products: a continuing source of novel drug leads. **Biochimica et biophysica acta**, v. 1830, n. 6, p. 3670–95, jun. 2013.

CUEVAS, C.; FRANCESCH, A. Development of Yondelis (trabectedin, ET-743). A semisynthetic process solves the supply problem. **Natural product reports**, v. 26, n. 3, p. 322–337, mar. 2009.

CURTIN, J. A et al. Distinct sets of genetic alterations in melanoma. **The New England journal of medicine**, v. 353, n. 20, p. 2135–2147, 2005.

D'ARCY, M. S. Cell death: a review of the major forms of apoptosis, necrosis and autophagy. **Cell Biology International**, v. 43, n. 6, p. 582–592, 2019.

D'INCALCI, M. et al. Trabectedin, a drug acting on both cancer cells and the tumour microenvironment. **British Journal of Cancer**, v. 111, n. 4, p. 646–650, 2014.

D'INCALCI, M.; GALMARINI, C. M. A Review of Trabectedin (ET-743): A Unique Mechanism of Action. **Molecular Cancer Therapeutics**, v. 9, n. 8, p. 2157–2163, 2010.

DAI, D. L.; MARTINKA, M.; LI, G. Prognostic Significance of Activated Akt Expression in Melanoma: A Clinicopathologic Study of 292 Cases. **Journal of Clinical Oncology**, v. 23, n. 7, p. 1473–1482, 2005.

DANG, C. V. et al. Drugging the "undruggable" cancer targets. **Nature Reviews Cancer**, v. 17, n. 8, p. 502–508, 2017.

DAVIES, H. et al. Mutations of the BRAF gene in human cancer. **Nature**, v. 417, n. 6892, p. 949–954, 2002.

DAVIS, E. et al. Ectopic Tbx2 expression results in polyploidy and cisplatin resistance. **Oncogene**, v. 27, p. 976–984, 2008.

DHAWAN, P. et al. Constitutive Activation of Akt / Protein Kinase B in Melanoma Leads to Up-Regulation of Nuclear Factor- κ B and Tumor Progression. **Cancer Research**, v. 62, p. 7335–7342, 2002.

DI GIANDOMENICO, S. et al. Mode of action of trabectedin in myxoid liposarcomas. **Oncogene**, v. 33, n. 44, p. 5201–5210, 2013.
DOUGLAS, N. C.; PAPAIOANNOU, V. E. The T-box transcription factors TBX2 and TBX3 in mammary gland development and breast cancer. **J Mammary Gland Biol Neoplasia**, v. 18, n. 2, p. 143–147, 2013.

DU, W. L. et al. Effect of silencing the T-Box transcription factor TBX2 in prostate cancer PC3 and LNCaP cells. **Molecular Medicine Reports**, v. 16, n. 5, 2017.

DUNCAN, J. S. et al. Dynamic reprogramming of the kinome in response to targeted MEK inhibition in triple-negative breast cancer. **Cell**, v. 149, n. 2, p. 307–321, 2012.

DUO, S. et al. Expression and clinical significance of Tbx2 in pancreatic cancer.

Asian Pacific Journal of Cancer Prevention, v. 10, n. 1, p. 119–122, 2009.

EOM, Y. W. et al. Two distinct modes of cell death induced by doxorubicin: Apoptosis and cell death through mitotic catastrophe accompanied by senescence-like phenotype. **Oncogene**, v. 24, n. 30, p. 4765–4777, 2005.

FENICAL, W. Marine Pharmaceuticals. **Oceanografy**, v. 19, n. 2, p. 110–119, 2006.

FENICAL, W. et al. Discovery and development of the anticancer agent salinosporamide A (NPI-0052). **Bioorganic & medicinal chemistry**, v. 17, n. 6, p. 2175–80, 15 mar. 2008.

FENICAL, W.; JENSEN, P. R. Developing a new resource for drug discovery: marine actinomycete bacteria. **Nature chemical biology**, v. 2, n. 12, p. 666–73, dez. 2006.

FERLAY, J. et al. Estimating the global cancer incidence and mortality in 2018: GLOBOCAN sources and methods. **International Journal of Cancer**, v. 144, n. 8, p. 1941–1953, 2019.

FERREIRA, E. G. et al. Guanidine alkaloids from Monanchora arbuscula: Chemistry and antitumor potential. **Chemistry and Biodiversity**, v. 8, n. 8, p. 1433–1445, 2011.

FORNI, C. et al. Trabectedin (ET-743) promotes differentiation in myxoid liposarcoma tumors. **Molecular Cancer Therapeutics**, v. 8, n. 2, p. 449–457, 2009.

FREDERICO, L. A.; SHAW, B. R.; KUNKEL, T. A. A Sensitive Genetic Assay for the Detection of Cytosine Deamination: Determination of Rate Constants and the Activation Energy. **Biochemistry**, v. 29, n. 10, p. 2532–2537, 1990.

GENG, F.; WENZEL, S.; TANSEY, W. P. Ubiquitin and Proteasomes in Transcription Fuqiang. **Bone**, v. Annu Rev B, n. 81, p. 177–201, 2012.

GHOSH, P.; GHOSH, D. Elucidating the Photoprotection Mechanism of Eumelanin Monomers. **Journal of Physical Chemistry B**, v. 121, n. 24, p. 5988–5994, 2017.

GILCHREST, B. A et al. The pathogenesis of melanoma induced by ultraviolet radiation. **New England journal of Medicine**, v. 340, p. 1341–1348, 1999.

GLASER, K. B.; MAYER, A. M. S. A renaissance in marine pharmacology: from preclinical curiosity to clinical reality. **Biochemical pharmacology**, v. 78, n. 5, p. 440–448, 1 set. 2009.

GORDON, E. M. et al. Trabectedin for Soft Tissue Sarcoma: Current Status and Future Perspectives. **Advances in Therapy**, v. 33, n. 7, p. 1055–1071, 2016.

GUIMARÃES, L. A. et al. Chromomycin A2 induces autophagy in melanoma cells. **Marine drugs**, v. 12, p. 5839–5855, 2014.

HA, L.; MERLINO, G.; SVIDERSKAYA, E. V. Melanomagenesis: Overcoming the

Barrier of Melanocyte Senescence. **Cell Cycle**, v. 7, n. 1, p. 1944–1948, 2008.

HAGENBUCHNER, J.; AUSSERLECHNER, M. J. Targeting transcription factors by small compounds - Current strategies and future implications. **Biochemical Pharmacology**, v. 107, p. 1–13, 2016.

HAN, Y. et al. Increased expression of TBX2 is a novel independent prognostic biomarker of a worse outcome in colorectal cancer patients after curative surgery and a potential therapeutic target. **Medical Oncology**, v. 30, n. 4, 2013.

HANAHAN, D.; WEINBERG, R. A. The Hallmarks of Cancer. **Cell**, v. 100, p. 57–70, 2000.

HANAHAN, D.; WEINBERG, R. A. Hallmarks of cancer: the next generation. **Cell**, v. 144, n. 5, p. 646–74, 4 mar. 2011.

HARLAND, M. et al. Prevalence and predictors of germline CDKN2A mutations for melanoma cases from Australia, Spain and the United Kingdom. **Hereditary cancer in clinical practice**, v. 12, n. 1, p. 20, 2014.

HARVEY, A. L. Natural products in drug discovery. **Drug discovery today**, v. 13, n. 19–20, p. 894–901, out. 2008.

HAUSCHILD, A. et al. Dabrafenib in BRAF-mutated metastatic melanoma: A multicentre, open-label, phase 3 randomised controlled trial. **The Lancet**, v. 380, n. 9839, p. 358–365, 2012.

HAYASHI, H. et al. Down-regulation of the PI3-kinase / Akt pathway by ERK MAP kinase in growth factor signaling. **Genes to Cells**, v. 13, p. 941–947, 2008.

HEIDENREICH, B.; KUMAR, R. TERT promoter mutations in telomere biology. **Mutation Research - Reviews in Mutation Research**, v. 771, p. 15–31, 2017.

HUGHES, J. P. et al. Principles of early drug discovery. **British Journal of Pharmacology**, v. 162, n. 6, p. 1239–1249, 2011.

ISMAIL, A.; BATEMAN, A. Expression of TBX2 promotes anchorage-independent growth and survival in the p53-negative SW13 adrenocortical carcinoma. **Cancer Letters**, v. 278, n. 2, p. 230–240, 2009.

JACKETT, L. A.; SCOLYER, R. A. A Review of Key Biological and Molecular Events Underpinning Transformation of Melanocytes to Primary and Metastatic Melanoma. **Cancers**, v. 11, n. 2041, p. 1–21, 2019.

JACOBS, J. J. et al. Senescence bypass screen identifies TBX2, which represses Cdkn2a (p19(ARF)) and is amplified in a subset of human breast cancers. **Nature genetics**, v. 26, n. 3, p. 291–299, 2000.

JIMENEZ, P. C. et al. Structure Elucidation and Anticancer Activity of 7-Oxostaurosporine Derivatives from the Brazilian Endemic Tunicate Eudistoma vannamei. **Marine Drugs**, v. 10, n. 5, p. 1092–1102, 2012.

JIMENEZ, P. C. et al. Enriching cancer pharmacology with drugs of marine origin. **British Journal of Pharmacology**, v. 177, n. 1, p. 3–27, 2020.

JIMENEZ, P.; WILKE, D.; COSTA-LOTUFO, L. Marine drugs for cancer: surfacing biotechnological innovations from the oceans. **Clinics**, v. 73, n. Suppl 1, p. 1–7, 2018.

JOHANNESSEN, C. M. et al. COT/MAP3K8 drives resistance to RAF inhibition through MAP kinase pathway reactivation. **Nature**, v. 468, n. 7326, p. 968–972, 2010.

JOHN, L.; COWEY, C. L. The Rapid Emergence of Novel Therapeutics in Advanced Malignant Melanoma. **Dermatology and Therapy**, v. 5, p. 151–169, 2015.

JORDAN, M. A. et al. The primary antimitotic mechanism of action of the synthetic halichondrin E7389 is suppression of microtubule growth. **Molecular Cancer Therapeutics**, v. 4, n. 7, p. 1086–1095, 2005.

KALLURI, R.; WEINBERG, R. A. The basics of epithelial-mesenchymal transition. **The journal of clinical investigation**, v. 119, n. 6, p. 1420–1428, 2009.

KAMATH, P. et al. A Review on Imiquimod Therapy and Discussion on Optimal Management of Basal Cell Carcinomas. **Clinical Drug Investigation**, v. 38, n. 10, p. 883–899, 2018.

KAMIYAMA, M. Mechanism of Action of Chromomycin A3. **The Journal of Biochemistry**, v. 63, n. 5, p. 566–572, 1968.

KARIMIAN, A.; AHMADI, Y.; YOUSEFI, B. Multiple functions of p21 in cell cycle, apoptosis and transcriptional regulation after DNA damage. **DNA Repair**, v. 42, p. 63–71, 2016.

KAROULIA, Z.; GAVATHIOTIS, E.; POULIKAKOS, P. I. New perspectives for targeting RAF knase in human cancer. **Nature reviews. Cancer**, p. 1–16, 2017.

KAVKA, A. I.; GREEN, J. B. A. Tales of tails: Brachyury and the T-box genes. **Biochimica et Biophysica Acta - Reviews on Cancer**, v. 1333, n. 2, p. 73–84, 1997.

KHAN, S. F. et al. The roles and regulation of TBX3 in development and disease. **Gene**, v. 726, n. May 2019, p. 144223, 2020.

KNACKSTEDT, T. et al. Malignant melanoma: Diagnostic and management update. **Plastic and Reconstructive Surgery**, v. 142, n. 2, p. 202E-216E, 2018.

KOURTIDIS, A. et al. A central role for cadherin signaling in cancer. **Experimental**

Cell Research, v. 358, n. 1, p. 78–85, 2017.

KOZAR, I. et al. Many ways to resistance: How melanoma cells evade targeted therapies. **Biochimica et Biophysica Acta - Reviews on Cancer**, v. 1871, n. 2, p. 313–322, 2019.

LADE-KELLER, J. et al. E- to N-cadherin switch in melanoma is associated with decreased expression of phosphatase and tensin homolog and cancer progression. **British Journal of Dermatology**, v. 169, n. 3, p. 618–628, 2013.

LAMBERT, M. et al. **Targeting transcription factors for cancer treatmentMolecules**, 2018.

LAMOUILLE, S.; XU, J.; DERYNCK, R. Fakultas Psikologi Dan Sosial Budaya Universitas Islam Indonesia Yogyakarta. **Nature Reviews Molecular Cell Biology**, v. 15, n. 3, p. 178–196, 2014.

LARSEN, A. K.; GALMARINI, C. M.; D'INCALCI, M. Unique features of trabectedin mechanism of action. **Cancer Chemotherapy and Pharmacology**, v. 77, n. 4, p. 663–671, 2016.

LAU, E. C. et al. Functional chromatographic technique for natural product isolation. **Org. Biomol. Chem.**, v. 13, n. 8, p. 2255–2259, 2015.
LAURELL, T. et al. Molecular and clinical delineation of the 17q22 microdeletion phenotype. **European Journal of Human Genetics**, v. 21, n. 10, p. 1085–1092, 2013.

LAVOIE, H.; THERRIEN, M. Regulation of RAF protein kinases in ERK signalling. **Nature Reviews Molecular Cell Biology**, v. 16, n. 5, p. 281–298, 2015.

LEACHMAN, S. A. et al. Selection criteria for genetic assessment of patients with familial melanoma. **Journal of Acad. Dermatol.**, v. 61, n. 4, p. 1–23, 2009.

LEE, J. A.; BERG, E. L. Neoclassic drug discovery: The case for lead generation using phenotypic and functional approaches. **Journal of Biomolecular Screening**, v. 18, n. 10, p. 1143–1155, 2013.

LEE, S. J. et al. DNA-damage-induced apoptosis. In: **Molecular oncology**. [s.l: s.n.]. p. 465–472.

LINGBEEK, M. E.; JACOBS, J. J. L.; VAN LOHUIZEN, M. The T-box repressors TBX2 and TBX3 specifically regulate the tumor suppressor gene p14ARF via a variant T-site in the initiator. **Journal of Biological Chemistry**, v. 277, n. 29, p. 26120–26127, 2002.

LIU, N. et al. Functional variants in TBX2 are associated with a syndromic cardiovascular and skeletal developmental disorder. **Human Molecular Genetics**, v. 27, n. 14, p. 2454–2465, 2018.

LIU, W.; SHARPLESS, N. Senescence-escape in melanoma. **Pigment cell &**

melanoma research, v. 25, n. 4, p. 408–409, 2012.

LOMBÓ, F. et al. The aureolic acid family of antitumor compounds: Structure, mode of action, biosynthesis, and novel derivatives. **Applied Microbiology and Biotechnology**, v. 73, n. 1, p. 1–14, 2006.

LU, J. et al. TBX2 and TBX3: The special value for anticancer drug targets. **Biochimica et Biophysica Acta - Reviews on Cancer**, v. 1806, n. 2, p. 268–274, 2010.

LV, Y. et al. TBX2 over-expression promotes nasopharyngeal cancer cell proliferation and invasion. **Oncotarget**, v. 8, n. 32, p. 52699–52707, 2017.

MAHUMUD, R. A. et al. Emerging cancer incidence, mortality, hospitalisation and associated burden among Australian cancer patients, 1982 - 2014: An incidence-based approach in terms of trends, determinants and inequality. **BMJ Open**, v. 9, n. 12, 2019.

MANIVASAGAN, P. et al. Pharmaceutically active secondary metabolites of marine actinobacteria. **Microbiological research**, p. 1–17, 16 ago. 2013.

MANOLA, J. et al. Prognostic factors in metastatic melanoma: a pooled analysis of Eastern Cooperative Oncology Group trials. **Journal of clinical oncology : official journal of the American Society of Clinical Oncology**, v. 18, n. 22, p. 3782–93, 2000.

MARCO, E.; GAGO, F. DNA structural similarity in the 2:1 complexes of the antitumor drugs trabectedin (Yondelis) and chromomycin A3 with an oligonucleotide sequence containing two adjacent TGG binding sites on opposing strands. **Molecular pharmacology**, v. 68, n. 6, p. 1559–67, dez. 2005.

MARTINS, A. et al. Marketed Marine Natural Products in the Pharmaceutical and Cosmeceutical Industries: Tips for Success. **Marine Drugs**, v. 12, n. 2, p. 1066–1101, 2014.

MCARTHUR, G. A. et al. Safety and efficacy of vemurafenib in BRAFV600E and BRAFV600K mutation-positive melanoma (BRIM-3): extended follow-up of a phase 3, randomised, open-label study. **Lancet Oncol.**, v. 15, n. 3, p. 323–332, 2014.

MELO, A. C. et al. Melanoma signature in Brazil: Epidemiology, incidence, mortality, and trend lessons from a continental mixed population country in the past 15 years. **Melanoma Research**, v. 28, n. 6, p. 629–636, 2018.

MENZIES, A. M.; LONG, G. V.; MURALI, R. Dabrafenib and its potential for the treatment of metastatic melanoma. **Drug Design, Development and Therapy**, v. 6, p. 391–405, 2012.

MILLER, A. J.; MIHN, M. C. Melanoma. **The New England journal of medicine**, v. 355, n. 1, p. 51–65, 2006.

MILLER, K. D. et al. Cancer Treatment and Survivorship Statistics , 2016. **CA: A Cancer Journal for Clinicians**, v. 66, n. 4, p. 271–289, 2016.

MINUZZO, M. Selective Effects of the Anticancer Drug Yondelis (ET-743) on Cell-Cycle Promoters. **Molecular Pharmacology**, v. 68, n. 5, p. 1496–1503, 2005.

MISHRA, H. et al. Melanoma treatment: from conventional to nanotechnology. **Journal of Cancer Research and Clinical Oncology**, v. 144, n. 12, p. 2283–2302, 2018.

MIŠKOVIĆ, K. et al. Antineoplastic DNA-binding compounds: Intercalating and minor groove binding drugs. **Arhiv za Higijenu Rada i Toksikologiju**, v. 64, n. 4, p. 593–602, 2013.

MOLINSKI, T. F. et al. Drug development from marine natural products. **Nature reviews. Drug discovery**, v. 8, n. 1, p. 69–85, jan. 2009.

MURPHY, T.; YEE, K. W. L. Cytarabine and daunorubicin for the treatment of acute myeloid leukemia. **Expert Opinion on Pharmacotherapy**, v. 18, n. 16, p. 1765–1780, 2017.

NAICHE, L. A et al. T-box genes in vertebrate development. **Annual review of genetics**, v. 39, p. 219–239, 2005.

NANDANA, S. et al. Bone metastasis of prostate cancer can be therapeutically targeted at the TBX2-WNT signaling axis. **Cancer Research**, v. 77, n. 6, p. 1331–1344, 2017.

NELSON, S. M.; FERGUSON, L. R.; DENNY, W. A. Non-covalent ligand/DNA interactions: Minor groove binding agents. **Mutation Research - Fundamental and Molecular Mechanisms of Mutagenesis**, v. 623, n. 1–2, p. 24–40, 2007.

NEWMAN, D. J.; CRAGG, G. M. Marine-sourced anti-cancer and cancer pain control agents in clinical and late preclinical development. **Marine Drugs**, v. 12, n. 1, p. 255–278, 2014.

NEWMAN, D. J.; CRAGG, G. M. Natural Products as Sources of New Drugs from 1981 to 2014. **Journal of Natural Products**, v. 79, n. 3, p. 629–661, 2016.

NIGG, E. A. Reviews and comment from the nature publishing group. **Nature Reviews Genetics**, v. 3, n. 10, p. 815–815, 2002.

NIMMAKAYALU, M. et al. Microdeletion of 17q22q23.2 encompassing TBX2 and TBX4 in a patient with congenital microcephaly, thyroid duct cyst, sensorineural hearing loss, and pulmonary hypertension. **American Journal of Medical Genetics, Part A**, v. 155, n. 2, p. 418–423, 2011.

NORBURY, C. J.; HICKSON, I. D. Cellular Responses to DNA Damage. In: **Ann. Rev. Pharmacol. Toxicol.** [s.l: s.n.]. v. 41p. 367–401.

NORBURY, C. J.; ZHIVOTOVSKY, B. DNA-damage-induced apoptosis. **Oncogene**, v. 23, p. 2797–2808, 2004.

OLSEN, C. M. et al. Trends in Melanoma Incidence Rates in Eight Susceptible Populations through 2015. **Journal of Investigative Dermatology**, v. 139, n. 6, p. 1392–1395, 2019.

ORTONNE, J. Photoprotective Properties of Skin Melanin_Ortonne. **British Journal of Dermatology**, v. 146, n. 61, p. 7–10, 2002.

OUCHI, M.; OUCHI, T. Distinct DNA damage determines differential phosphorylation of Chk2. **Cancer Biology and Therapy**, v. 15, n. 12, p. 1700–1704, 2014.

PALMIERI, G. et al. Molecular Pathways in Melanomagenesis: What We Learned from Next-Generation Sequencing Approaches. **Current Oncology Reports**, v. 20, n. 11, 2018.

PAPAIOANNOU, V. E. The t-box gene family: Emerging roles in development, Stem cells and cancer. **Development (Cambridge)**, v. 141, n. 20, p. 3819–3833, 2014.

PATTON, E. E. et al. BRAF Mutations Are Sufficient to Promote Nevi Formation and Cooperate with p53 in the Genesis of Melanoma. **Current Biology**, v. 15, p. 249–254, 2005.

PAXTON, C. et al. Murine Tbx2 contains domains that activate and repress gene transcription. **Gene**, v. 283, n. 1–2, p. 117–124, 2002.

PERES, J. et al. The Highly Homologous T-Box Transcription Factors, TBX2 and TBX3, Have Distinct Roles in the Oncogenic Process. **Genes & cancer**, v. 1, n. 3, p. 272–282, 2010.

PERES, J.; MOWLA, S.; PRINCE, S. The T-box transcription factor, TBX3, is a key substrate of AKT3 in melanomagenesis. **Oncotarget**, v. 6, n. 3, p. 1821–1833, 2014.

PERES, J.; PRINCE, S. The T-box transcription factor, TBX3, is sufficient to promote melanoma formation and invasion. **Molecular cancer**, v. 12, n. 1, p. 117, 2013.

PETTIT, G. R. et al. Antineoplastic agents 596. Isolation and structure of chromomycin A5 from a Beaufort Sea microorganism. **RSC Advances**, v. 5, n. 12, p. 9116–9122, 2015.

PHILPOTT, C. et al. The NF1 somatic mutational landscape in sporadic human cancers. **Human Genomics**, v. 11, n. 1, p. 1–19, 2017.

PINTO, F. DAS C. L. et al. Dextrorotatory Chromomycins from the Marine Streptomyces sp. Associated to Palythoa caribaeorum. **Journal os Brazilian Chemical Society**, v. 00, n. 00, p. 1–10, 2019.

PITT, J. M. et al. Resistance Mechanisms to Immune-Checkpoint Blockade in Cancer: Tumor-Intrinsic and -Extrinsic Factors. **Immunity**, v. 44, n. 6, p. 1255–1269, 2016.

POTTS, B. C. et al. **Marizomib, a proteasome inhibitor for all seasons: preclinical profile and a framework for clinical trials.** [s.l: s.n.]. v. 11

PRADO, G.; SVOBODA, R. M.; RIGEL, D. S. What's New in Melanoma. **Dermatologic Clinics**, v. 37, n. 2, p. 159–168, 2019.

PRINCE, S. et al. Tbx2 Directly Represses the Expression of the p21 WAF1 Cyclin-Dependent Kinase Inhibitor. **Cancer research**, v. 64, n. 5, p. 1669–1674, 2004.

RAMIREZ-LLODRA, E. et al. Deep, diverse and definitely different: Unique attributes of the world's largest ecosystem. **Biogeosciences**, v. 7, n. 9, p. 2851–2899, 2010.

RAY-COQUARD, I. Trabectedin mechanism of action and platinum resistance: Molecular rationale. **Future Oncology**, v. 13, n. 23S, p. 17–21, 2017.

REDMOND, K. L. et al. T-box 2 represses NDRG1 through an EGR1-dependent mechanism to drive the proliferation of breast cancer cells. **Oncogene**, v. 29, n. 22, p. 3252–3262, 2010.

RODRIGUES, B. S. F. et al. Bioprospection of cytotoxic compounds in fungal strains recovered from sediments of the Brazilian coast. **Chemistry & biodiversity**, v. 12, p. 432–442, 2015.

RODRÍGUEZ-CERDEIRA, C. et al. Advances in Immunotherapy for Melanoma : A Comprehensive Review. **Mediators of Inflammation**, v. 2017, p. 1–14, 2017.

SACCHETTO, L. et al. Trends in incidence of thick, thin and in situ melanoma in Europe. **European Journal of Cancer**, v. 92, p. 108–118, 2018.

SAHM, B. D. B. **Prospecção de substâncias com potencial anticâncer em microrganismos associados ao zoantídeo Protopalythoa variabilis (CNIDARIA, ANTHOZOA).** [s.l.] Universidade Federal do Ceará (UFC), 2014.

SAHM, B. D. B. et al. Targeting the oncogene TBX2 transcription factor with chromomycins. **Frontiers in chemistry.** v. 8, n. 110, p, 1-9, 2020.

SAKABE, M. et al. Ectopic retinoic acid signaling affects outflow tract cushion development through suppression of the myocardial Tbx2-Tgfβ2 pathway. **Development**, v. 139, n. 2, p. 385–395, 2012.

SANTOS, C. A. DOS; SOUZA, D. L. B. Melanoma mortality in Brazil: Trends and projections (1998-2032). **Ciencia e Saude Coletiva**, v. 24, n. 4, p. 1551–1561, 2019.

SARANARUK, P. et al. Chromomycin A3 suppresses cholangiocarcinoma growth by

induction of S phase cell cycle arrest and suppression of Sp1-related anti-apoptotic proteins. **International Journal of Molecular Medicine**, p. 1–12, 2019.

SCHNEIDER, C. A.; RASBAND, W. S.; ELICEIRE, K. W. NIH Image to ImageJ: 25 years of Image Analysis. **Nat. Methods.**, v. 9, n. 7, p. 671–675, 2012.
SEBÉ-PEDRÓS, A.; RUIZ-TRILLO, I. Evolution and Classification of the T-Box Transcription Factor Family. **Current Topics in Developmental Biology**, v. 122, p. 1–26, 2017.

SEBERG, H. E.; VAN OTTERLOO, E.; CORNELL, R. A. Beyond MITF: Multiple transcription factors directly regulate the cellular phenotype in melanocytes and melanoma. **Pigment Cell and Melanoma Research**, v. 30, n. 5, p. 454–466, 2017.

SENFT, D.; QI, J.; RONAI, Z. A. Ubiquitin ligases in oncogenic transformation and cancer therapy. **Physiology & behavior**, v. Nat Rev Ca, n. 18, p. 69–88, 2016.

SENTER, P. D.; SIEVERS, E. L. The discovery and development of brentuximab vedotin for use in relapsed Hodgkin lymphoma and systemic anaplastic large cell lymphoma. **Nature Biotechnology**, v. 30, n. 7, p. 631–637, 2012.

SHAIN, A. H. et al. The genetic evolution of melanoma from precursor lesions. **New England Journal of Medicine**, v. 373, n. 20, p. 1926–1936, 2015.

SHARMA, P.; ALLISON, J. P. Immune Checkpoint Targeting in Cancer Therapy : Toward Combination Strategies with Curative Potential. **Cell**, v. 161, n. 2, p. 205–214, 2015.

SHEEBA, C. J.; LOGAN, M. P. O. **The Roles of T-Box Genes in Vertebrate Limb Development**. 1. ed. [s.l.] Elsevier Inc., 2017. v. 122

SHINDE, P.; BANERJEE, P.; MANDHARE, A. **Marine natural products as source of new drugs: a patent review (2015–2018)Expert Opinion on Therapeutic Patents**, 2019.

SIEGEL, R. L.; MILLER, K. D.; JEMAL, A. Cancer statistics, 2019. **CA: A Cancer Journal for Clinicians**, v. 69, n. 1, p. 7–34, 2019.

SOUSA, T. D. S. et al. Anthracyclinones from Micromonospora sp. **Journal of Natural Products**, v. 75, n. 3, p. 489–493, 2012.

SPITZ, F.; FURLONG, E. E. M. Transcription factors: From enhancer binding to developmental control. **Nature Reviews Genetics**, v. 13, n. 9, p. 613–626, 2012.

STAHL, J. M. et al. Deregulated Akt3 activity promotes development of malignant melanoma. **Cancer research**, v. 64, n. 19, p. 7002–10, 2004.

SULLIVAN, R. J.; FLAHERTY, K. T. Resistance to BRAF-targeted therapy in melanoma. **European Journal of Cancer**, v. 49, n. 6, p. 1297–1304, 2013.

SUN, T. et al. SIRT1 induces epithelial-mesenchymal transition by promoting autophagic degradation of E-cadherin in melanoma cells article. **Cell Death and Disease**, v. 9, n. 2, 2018.

SVEJSTRUP, J. Q. Contending with transcriptional arrest during RNAPII transcript elongation. **Trends in Biochemical Sciences**, v. 32, n. 4, p. 165–171, 2007.

TACAR, O.; SRIAMORNSAK, P.; DASS, C. R. Doxorubicin: An update on anticancer molecular action, toxicity and novel drug delivery systems. **Journal of Pharmacy and Pharmacology**, v. 65, n. 2, p. 157–170, 2013.

TAKEARA, R. et al. Antileukemic effects of Didemnum psammatodes (Tunicata: Ascidiacea) constituents. **Comparative biochemistry and physiology. Part A, Molecular & integrative physiology**, v. 151, p. 363–369, 2008.

TASAKA, R. et al. TBX2 expression is associated with platinum-sensitivity of ovarian serous carcinoma. **Oncology Letters**, v. 15, n. 3, p. 3085–3090, 2018.

TCGA, T. C. G. A. R. N. Genomic Classification of Cutaneous Melanoma. **Cell.**, v. 161, n. 7, p. 1–23, 2015.

TERZI, M. Y.; IZMIRLI, M.; GOGEBAKAN, B. The cell fate: senescence or quiescence. **Molecular Biology Reports**, v. 43, n. 11, p. 1213–1220, 2016.

THIERY, J. P.; SLEEMAN, J. P. Complex networks orchestrate epithelial-mesenchymal transitions. **Nature Reviews Molecular Cell Biology**, v. 7, n. 2, p. 131–142, 2006.

TOMCZAK, K.; CZERWIŃSKA, P.; WIZNEROWICZ, M. The Cancer Genome Atlas (TCGA): An immeasurable source of knowledge. **Wspolczesna Onkologia**, v. 1A, p. A68–A77, 2015.

TRZOSS, L. et al. Seriniquinone, a selective anticancer agent, induces cell death by autophagocytosis, targeting the cancer-protective protein dermcidin. **Proceedings of the National Academy of Sciences**, v. 111, n. 41, p. 14687–14692, 2014.

TSAO, H. et al. Melanoma: From mutations to medicine. **Genes and Development**, v. 26, n. 11, p. 1131–1155, 2012.

TURNER, P. R.; DENNY, W. A. The mutagenic properties of DNA minor-groove binding ligands. **Mutation Research - Fundamental and Molecular Mechanisms of Mutagenesis**, v. 355, n. 1–2, p. 141–169, 1996.

VANCE, K. W. et al. Tbx2 is overexpressed and plays an important role in maintaining proliferation and suppression of senescence in melanomas. **Cancer Research**, v. 65, n. 6, p. 2260–2268, 2005.
VANCE, K. W. et al. The retinoblastoma protein modulates Tbx2 functional specificity. **Molecular biology of the cell**, v. 21, p. 2770–2779, 2010.

VAQUERIZAS, J. M. et al. A census of human transcription factors: Function, expression and evolution. **Nature Reviews Genetics**, v. 10, n. 4, p. 252–263, 2009.

VAXMAN, I.; SIDIQI, M. H.; GERTZ, M. Venetoclax for the treatment of multiple myeloma. **Expert Review of Hematology**, v. 11, n. 12, p. 915–920, 2018.

VREDEVELD, L. C. W. et al. Abrogation of BRAF V600E -induced senescence by PI3K pathway activation contributes to melanomagenesis. **Genes & Development**, v. 26, p. 1055–1069, 2012.

WAKKER, V. et al. Generation of mice with a conditional null allele for Tbx2. **Genesis**, v. 48, n. 3, p. 195–199, 2010.

WANG, B. et al. The T box transcription factor TBX2 promotes epithelial-mesenchymal transition and invasion of normal and malignant breast epithelial cells. **PLoS ONE**, v. 7, n. 7, 2012.

WANG, E. et al. Melanoma-restricted genes. **Journal of translational medicine**, v. 2, n. 34, p. 1–14, 2004.

WANSLEBEN, S. et al. A novel role for the anti-senescence factor TBX2 in DNA repair and cisplatin resistance. **Cell Death and Disease**, v. 4, n. 10, p. e846, 2013.

WANSLEBEN, S. et al. T-box transcription factors in cancer biology. **Biochimica et biophysica acta**, v. 1846, n. 2, p. 380–391, 2014.

WELSH, S. J. et al. Resistance to combination BRAF and MEK inhibition in metastatic melanoma: Where to next? **European Journal of Cancer**, v. 62, p. 76–85, 2016.

WILKE, D. V. et al. Cytotoxic Lipidic α -amino Acids from the Zoanthid. **J. Braz. Chem. Soc**, v. 20, n. 8, p. 1455–1459, 2009.

WILKE, D. V. et al. Pro-apoptotic activity of lipidic α-amino acids isolated from Protopalythoa variabilis. **Bioorganic & medicinal chemistry**, v. 18, n. 22, p. 7997–8004, 15 nov. 2010.

WOJAHN, I. et al. TBX2-positive cells represent a multi-potent mesenchymal progenitor pool in the developing lung. **Respiratory Research**, v. 20, n. 1, p. 1–14, 2019.

WORLD HEALTH ORGANIZATION. **STATUS OF THE HEALTH-RELATED SDGs**. [s.l: s.n.].

WU, P.; NIELSEN, T. E.; CLAUSEN, M. H. FDA-approved small-molecule kinase inhibitors. **Trends in Pharmacological Sciences**, v. 36, n. 7, p. 422–439, 2015.

YADAV, V. et al. Co-targeting BRAF and cyclin dependent kinases 4/6 for BRAF mutant cancers. **Pharmacology and Therapeutics**, v. 149, p. 139–149, 2015.

YOUNG, R. J. et al. Loss of CDKN2A expression is a frequent event in primary invasive melanoma and correlates with sensitivity to the CDK4/6 inhibitor PD0332991 in melanoma cell lines. **Pigment Cell and Melanoma Research**, v. 27, n. 4, p. 590–600, 2014.

YU, H. et al. T-box 2 expression predicts poor prognosis in gastric cancer. **Oncology Letters**, v. 10, n. 3, p. 1689–1693, 2015.

ZANNINI, L.; DELIA, D.; BUSCEMI, G. CHK2 kinase in the DNA damage response and beyond. **Journal of Molecular Cell Biology**, v. 6, n. 6, p. 442–457, 2014.

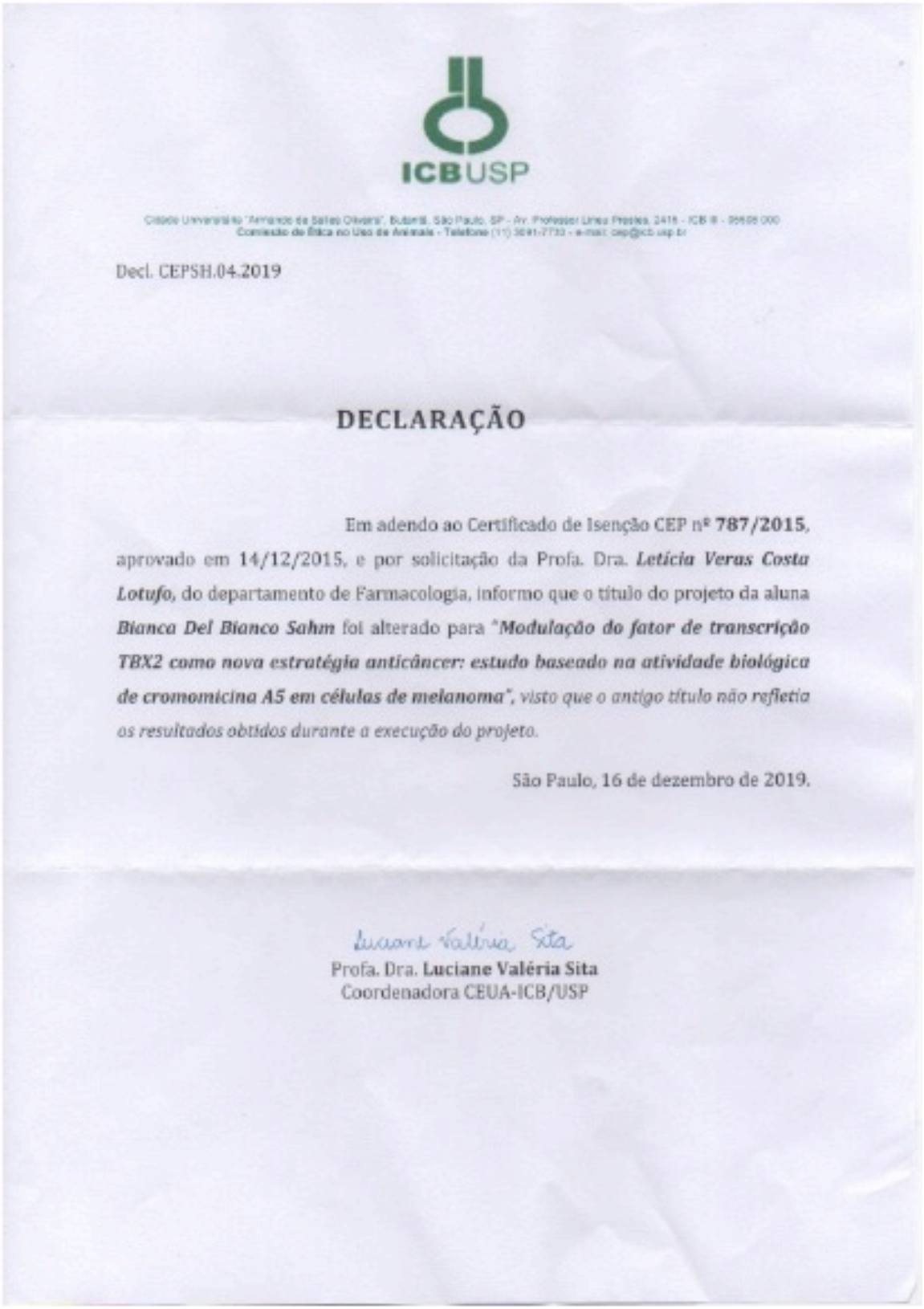
ZHANG, H. Molecular signaling and genetic pathways of senescence: Its role in tumorigenesis and aging. **Journal of cellular physiology**, v. 207, n. 1, p. 567–574, 2007.

ZHANG, P. et al. Inducible degradation of checkpoint kinase 2 links to cisplatin-induced resistance in ovarian cancer cells. **Biochemical and Biophysical Research Communications**, v. 328, n. 2, p. 567–572, 2005.

ZHU, B. et al. TBX2 represses PTEN in rhabdomyosarcoma and skeletal muscle. **Oncogene**, v. 35, n. 32, p. 4212–4224, 2016.

ZIHLIF, M. et al. Effects of DNA minor groove binding agents on global gene expression. **Cancer genomics & proteomics**, v. 7, n. 6, p. 323–30, 2010.

Attachment I - Ethics commiitee exempition certificate



ICB USP

Cidade Universitária "Armando de Salles Oliveira", Butantã, São Paulo, SP - Av. Professor Lineu Prestes, 2415 - ICB II - 05508-000
Comissão de Ética no Uso de Animais - Telefone (11) 3091-7733 - e-mail: cep@icb.usp.br

Decl. CEPSH.04.2019

DECLARAÇÃO

Em adendo ao Certificado de Isenção CEP nº **787/2015**, aprovado em 14/12/2015, e por solicitação da Profa. Dra. ***Letícia Veras Costa Lotufo***, do departamento de Farmacologia, informo que o título do projeto da aluna ***Bianca Del Bianco Sahm*** foi alterado para "***Modulação do fator de transcrição TBX2 como nova estratégia anticâncer: estudo baseado na atividade biológica de cromomicina A5 em células de melanoma***", *visto que o antigo título não refletia os resultados obtidos durante a execução do projeto.*

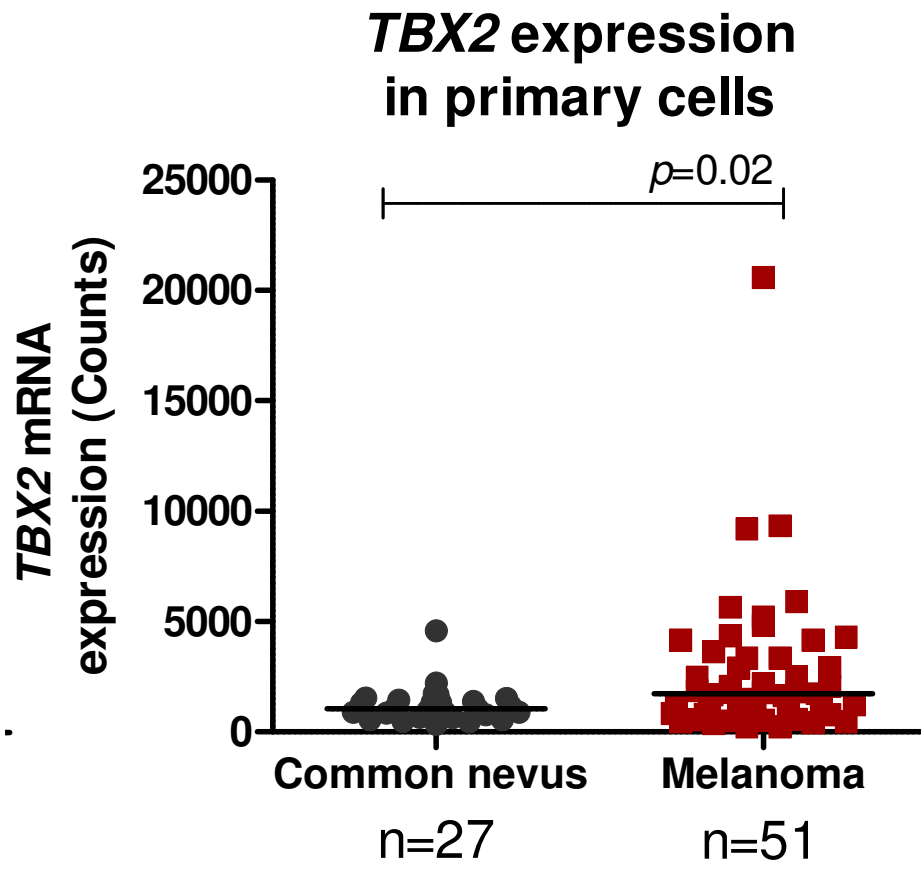
São Paulo, 16 de dezembro de 2019.

Luciane Valéria Sita

Profa. Dra. **Luciane Valéria Sita**
Coordenadora CEUA-ICB/USP

Supplementary figure S1

Figure S1 - TBX2 expression in primary melanoma samples.



TBX2 mRNA expression data from common acquired nevus (n=27) and primary malignant melanoma (n=51) generated by Illumina HiSeq 2500 plataform and deposited by Badal et al. (PMID 28469092) (GEO accession: GSE98394) was obtained from Gene Expression Omnibus (https://www.ncbi.nlm.nih.gov/geo/). Data sets were cross-referenced using tumor-specific identification numbers. For comparison, Mann-Whitney test was used, and a p value < 0.05 was considered statistically significant. Analysis performed by Prof. João Agostinho Machado Neto.